

HYDRODYNAMIC, AXIAL MIXING AND MASS TRANSFER STUDIES ON A MOBILE BED CONTACTOR WITH LOW DENSITY PARTICLES

A Thesis Submitted
In Partial Fulfilment of the Requirements
for the Degree of
DOCTOR OF PHILOSOPHY

by

OM PRAKASH RAMA

to the

DEPARTMENT OF CHEMICAL ENGINEERING
INDIAN INSTITUTE OF TECHNOLOGY KANPUR
JANUARY, 1984

CHE-1984-D-RAM-HYD

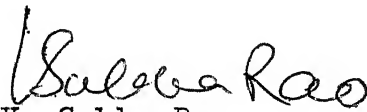
14 JUL 1985

LIBRARY
875011

Submitted on 12/11/81
8-77157

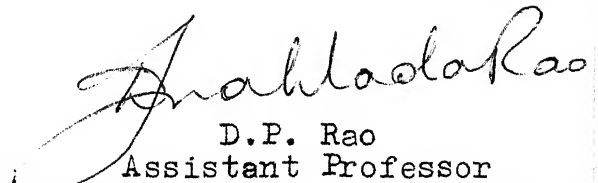
CERTIFICATE

This is to certify that the work presented in this thesis entitled, "HYDRODYNAMIC, AXIAL MIXING AND MASS TRANSFER STUDIES ON A MOBILE BED CONTACTOR WITH LOW DENSITY PARTICLES" has been carried out by Mr. O.P. Rama under our supervision and the same has not been submitted elsewhere for a degree.



V. Subba Rao
Ex-Professor

Department of Chemical Engg.
Indian Institute of Technology
Kanpur - 208016, INDIA



D.P. Rao
Assistant Professor
Department of Chemical Engg.
Indian Institute of Technology
Kanpur - 208016, INDIA

ACKNOWLEDGEMENTS

I am extremely grateful to Professor V. Subba Rao. Without his constant help, alround guidance and encouragement this would have not been possible for me to complete this work. Dr. D.P. Rao has provided me immense opportunity to work not only on the problems related to this thesis, but on many other interesting projects on solar energy, supervised by him, which have diversified my knowledge and helped in developing an aptitude for applied research work. I appreciate and consider that my association with these two esteemed professors has been the most enlightening phase of my academic career.

I must thank the Director and administration of I.I.T. Kanpur for providing excellent and ideal facilities and environment for the research work.

Professors J.K. Gehlawat, L.P. Singh, R.N. Sharma and K.S. Gandhi deserve many thanks for their continued interest in the progress of this work and particularly for their moral support in times of need.

I am indebted to many individuals who contributed either directly or indirectly to the fabrication of the pilot-plant type experimental set-up and in its smooth functioning. I would like to mention some of them by name; Messers L.S. Rao, D.B.

Chakarvorty, N.P. Singh, Ayodhya Singh, Kalicharan, Ram Chandra Ram and R.P. Yadav of the department of Chemical Engineering; Messers P.C. Mehta, Ichhadutt, A.R. Samson and R.S. Mishra of the Central Workshop; Messers J.N. Sharma, Piya Singh and Narsihman of the Glass-Blowing section. The help rendered by all these people in hours of need is deeply appreciated.

Mr. K.M.S. Prasad deserves special mention as he acquainted me with the details of data acquisition system and desktop computer and was always ready to help me for solving any trouble with the electronic equipment.

This work was carried out as a part of a project sponsored by the Council of Scientific and Industrial Research, New Delhi. The consistent financial help provided by the organisation is gratefully acknowledged.

I take this opportunity to express my obligation to the Director of H.B.T.I. Kanpur who kindly permitted me to register as a part-time scholar at I.I.T. Kanpur for the completion of this work. I also feel obliged to the Head and my other senior colleagues of the department of Chemical Engineering of HBTI, Kanpur for their cooperation and encouragement.

I appreciate the invaluable help rendered by my friends and colleagues, Drs. B. Roy and Prem Chand, Messers Murali Krishna, K.B.K. Rao, Ratan Mohan and Ram Prasad in the final preparation of this thesis. With Mr. Murali Krishna I have shared a long period of unforgetful moments of unpredictable experimental uncertainties. I am also thankful to Mr. V.V.S. Raju and Mr. S. Islam for helping me tirelessly in the analysis of gas and liquid samples.

I offer my warmest thanks to Mr. M.M. Beg for typing this thesis neatly, Mr. Hari Ram for his tireless efforts in cyclostyling, Messers D.S. Panesar, R.K. Bajpai, D.B. Chakravorty and Raj Kumar for the preparation of tables and figures.

On behalf of my family, I am grateful to the families of Drs. D.P. Rao, Prem Chand, B. Roy, Professor L.P. Singh and Mr. K.M.S. Prasad. Their pleasant company and helping attitude has been a source of great comfort for us during our stay at I.I.T. Campus.

Words would not profound to express my indebtedness to my parents. Their deep affection and silent words of inspiration have always guided me towards success and have helped me in facing bravely the ups and downs of life. I take this opportunity to thank sincerely my sisters and brother who shared

their joys and sorrows stoically and have encouraged me always for my all endeavour.

Last, but by no means the least, I appreciate the immense sense of tolerance and compromising attitude shown by my wife, Chitrlekha and daughter, Munmun, especially in the concluding phase of this work which kept me almost isolated from them over a couple of months.

OM PRAKASH RAMA

TABLE OF CONTENTS

		Page
	LIST OF FIGURES	(i)
	LIST OF TABLES	(vi)
	NOMENCLATURE	(viii)
	SYNOPSIS	(xiii)
CHAPTER		
1	INTRODUCTION	1
2	LITERATURE REVIEW	4
	2.1 HYDRODYNAMICS	4
	2.1.1 Pressure Drop and Liquid Holdup	4
	2.1.2 Bed Expansion	16
	2.1.3 Congregation Below the upper grid	17
	2.1.4 Minimum Fluidization Velocity	17
	2.2 AXIAL MIXING	19
	2.3 MASS TRANSFER	24
	2.3.1 Overall Mass-transfer Coefficients	28
	2.3.2 Individual Mass-transfer Co- efficients and Interfacial Area	35
3	EXPERIMENTAL SET-UP AND MEASUREMENT TECHNIQUES	43
	3.1 EXPERIMENTAL SET-UP	43
	3.1.1 Mobile Bed Contactor	43

	Page
3.1.2 Tracer Injection System	49
3.1.3 Tracer Monitoring System	50
3.1.4 Modifications for Mass Transfer studies	52
3.2 PACKING PARTICLES	53
3.3 EXPERIMENTAL PROCEDURE	56
3.3.1 Tracer Monitoring Technique	56
3.3.2 Determination of Delay time of Tracer Injection	59
3.3.3 Bed Expansion, Pressure Drop and Minimum Fluidization Velocity	61
3.3.4 Breakthrough Curves	61
3.3.5 Range of Variables Covered in Hydrodynamic and Axial Mixing Studies	64
3.3.6 Mass Transfer Measurements	64
3.3.7 Methods of Analysis	66
3.3.8 Range of Variables Covered in Mass Transfer Studies	66
4 RESULTS AND DISCUSSION	67
4.1 HYDRODYNAMICS	67
4.1.1 Bed-Behaviour-Visual Observations	67
4.1.2 Liquid Holdup and Pressure Drop	70

	Page
4.1.3 Correlations for h_1 and $\Delta P'_{1B}$	78
4.1.4 Bed Expansion	81
4.1.5 Minimum Fluidization Velocity	83
4.2 AXIAL MIXING	85
4.2.1 Interpretation of Breakthrough Curves	85
4.2.2 Peclet Number of the Liquid Phase	89
4.2.3 Axial Dispersion Coefficient	102
4.2.4 Correlations for Pe and D_L	107
4.3 MASS TRANSFER	114
4.3.1 Variations of Compositions and Temperatures of Gas and Liquid Streams During a Run	114
4.3.2 Evaluation of Interfacial Area and Surface-renewal Rate	115
4.3.3 Interfacial Area and Surface- renewal Rate	122
5 CONCLUSIONS	134
REFERENCES	139
Appendix A	146
Appendix B	150

LIST OF FIGURES

Figure		Page
3.1	Schematic diagram of the experimental set-up.	44
3.2	Sketch of the liquid distributor.	47
3.3	Cross-sectional drawing of the conductivity cell.	51
3.4	Sketches of a irregular and a cork particle.	54
3.5	A typical plot of Concentration of NaCl in tap water versus emf recorded by data acquisition system.	57
3.6	Average residence time of the liquid flow with respect to height through empty column (without gas flow).	60
3.7	A typical plot of emf versus time for the cork particles.	63
4.1	Maps depicting the regions of congregation at the wall.	69
4.2	h_1 versus U_g for $H_s/D = 0.78$.	72
4.3	h_1 versus U_g for $H_s/D = 1.6$.	73
4.4	h_1 versus U_g for $H_s/D = 2.4$.	74
4.5	h_1 versus U_g for $H_s/D = 3.2$.	75

Figure		Page
4.6	Typical plots of ΔP versus U_g .	76
4.7	Comparison of data of h_1 with Kito - Tabei - Murata correlation.	79
4.8	Comparison of data $\Delta P'_{1B}$ with Kito - Tabei - Murata correlation.	80
4.9	Typical plots showing the comparison of the data of H/H_s with other correlations.	82
4.10	Comparison of the observed values of U_{mf} with those calculated from Equations (4.4) and (4.5) and other correlation.	84
4.11	Comparison of an experimental breakthrough curve with the theoretical curve for spherical particles.	90
4.12	Comparison of an experimental breakthrough curve with the theoretical curve for irregular particles.	91
4.13	Comparison of an experimental breakthrough curve with the theoretical curve for cork particles.	92
4.14	Comparison of an experimental breakthrough curve with the theoretical curve in the case of congregation of irregular particles at the wall.	93

Figure		Page
4.15	Pe versus U_g for $H_s/D = 0.78$.	96
4.16	Pe versus U_g for $H_s/D = 1.6$.	97
4.17	Pe versus U_g for $H_s/D = 2.4$.	98
4.18	Pe versus U_g for $H_s/D = 3.2$ in the case of spherical particles.	99
4.19	Pe versus U_g for $H_s/D = 3.2$ in the case of irregular particles.	100
4.20	D_L versus U_g for the spherical particles.	103
4.21	D_L versus U_g for the irregular particles.	104
4.22	D_L versus U_g for the cork particles.	105
4.23	D_L versus U_g for the data of Chen and Douglas (1969) and Koval et al.(1975b).	106
4.24	Comparison of observed values of Pe with the values estimated using Equation (4.19).	109
4.25	Comparison of observed values of Pe with the values estimated using Equation (4.20).	110
4.26	Comparison of observed values of D_L with the values estimated using Equation (4.21).	111

Figure		Page
4.27	Comparison of observed values of Pe with the values estimated using Equation (4.19) for the data of Chen and Douglas (1969) and Koval et al. (1975b).	113
4.28	Variations of liquid and gas compositions and temperature with time during a mass-transfer run with lighter spherical particles.	116
4.29	Danckwerts' plot for the run depicted in Figure 4.28.	117
4.30	Variations of liquid and gas compositions and temperature with time during a mass-transfer run with heavier spherical particles.	118
4.31	Danckwerts' plot for the run depicted in Figure 4.30.	119
4.32	Interfacial area per unit cross-sectional area of the contactor versus gas velocity for lighter and heavier spherical particles.	125
4.33	Interfacial area per unit volume of the expanded bed versus gas velocity for lighter spherical particles.	127

Figure		Page
4.34	Interfacial area per unit volume of the expanded bed versus gas velocity for heavier spherical particles.	128
A-1	Schematic diagram of the Orsat-type carbon dioxide analyzer.	147

LIST OF TABLES

Table		Page
2.1	Summary of hydrodynamics studies on the mobile bed contactor.	5
2.2	Summary of correlations of pressure drop, liquid holdup, bed expansion and minimum fluidization velocity for mobile bed contactor.	8
2.3	Experimental details of liquid phase axial mixing studies on mobile bed contactor.	21
2.4	Summary of mass transfer studies on mobile bed contactor.	25
3.1	Liquid flow distribution pattern through nozzles of distributor.	48
3.2	Characteristics of particles.	58
3.3	Relations employed for the evaluation of average residence time, liquid holdup, Peclet number and axial dispersion coefficient from experimental breakthrough curves.	65
4.1	Two typical sets of Peclet numbers at low and high gas velocities in the case of spherical particles.	95

Table		Page
4.2	Summary of mass transfer results with lighter spherical particles	123
4.3	Summary of mass transfer results with heavier spherical particles	124
4.4	Summary of ranges of interfacial area reported in literature	130

NOMENCLATURE

A	= cross-sectional area of the contactor, m^2
A'	= interfacial area per unit cross-sectional area of the contactor, $m^2 m^{-2}$
a	= surface area of the packing particles per unit volume of the static bed, $m^2 m^{-3}$
a_B	= interfacial area per unit volume of the expanded bed, $m^2 m^{-3}$
a_p	= interfacial area per unit surface area of the packing particles, $m^2 m^{-2}$
a_{st}	= interfacial area per unit volume of the static bed, $m^2 m^{-3}$
a_T	= total area of interface, m^2
C	= tracer concentration at time t , $kgmol m^{-3}$
C_0	= initial tracer concentration, $kgmol m^{-3}$
$C_{CO_2}^*$	= $P_{CO_2} H_{CO_2}$ = concentration of dissolved carbon dioxide at interface, in equilibrium with gas at interface, $kgmol m^{-3}$
C_{fs}	= coefficient of friction in dry packed bed
C_{OH}	= concentration of sodium hydroxide in bulk of liquid, $kgmol m^{-3}$
D	= internal diameter of the contactor, m
D_{CO_2}	= diffusivity of dissolved carbon dioxide, $m^2 s^{-1}$
D_L	= axial dispersion coefficient, $m^2 s^{-1}$

- d = equivalent diameter of the free opening of the grid, m
- d_p = diameter of particle; defined as the diameter of a sphere having the volume of the particle, m
- Eu = Euler number, $\Delta P / (\rho_g u_g^2)$
- Fr = Froude number, $u_g / (g d_p \phi_s)^{0.5}$, $u_l / (g d_p \phi_s)^{0.5}$
- f = fraction of free open area of the bottom supporting grid
- Ga = Galileo number, $g(d_p \phi_s)^3 \rho_p^2 / \mu_l^2$
- g = acceleration due to gravity, 9.807 m s^{-2}
- g_c = Newton's law proportionality factor, $1 \text{ kg m N}^{-1} \text{ s}^{-2}$
- H = expanded bed height, m
- H_{CO_2} = solubility of carbon dioxide in sodium hydroxide solution, $\text{kgmol m}^{-3} \text{ Pa}^{-1}$
- H_{og} = overall gas-phase height of a transfer unit, m
- H_s = static bed height, m
- H_T = distance between lower and upper grids, m
- h_l = liquid volume held in the bed per unit cross-sectional area of the contactor, m
- h_{lG} = liquid volume held on the grid per unit cross-sectional area of the contactor, m
- K_g = overall mass-transfer coefficient based on partial pressure in the gas phase, $\text{kgmol s}^{-1} \text{ m}^{-2} \text{ Pa}^{-1}$
- K_l = overall mass-transfer coefficient based on concentration in the liquid phase, m s^{-1}

- k_2 = second-order rate-constant for the reaction of carbon dioxide into sodium hydroxide solution,
 $\text{m}^3 \text{kgmol}^{-1} \text{s}^{-1}$
- k_g = gas phase mass-transfer coefficient, $\text{kgmol m}^{-2} \text{s}^{-1} \text{Pa}^{-1}$
- k_l = liquid-phase mass-transfer coefficient in absence of reaction, m s^{-1}
- n_B = number of stages
- n_p = approximate number of particles to fill a 0.15 m ID and 0.12 m long cylindrical column
- P_{CO_2} = partial pressure of carbon dioxide in bulk of gas, Pa
- Pe = Peclet number, defined as $\bar{U}H/D_L$
- Pe' = liquid-phase Peclet number in the mobile bed, defined as $\bar{U} d_p/D_L$
- Pe_o = liquid-phase Peclet number in the fixed bed, defined as $\bar{U} d_p/D_L$
- ΔP = total pressure drop across the mobile bed column, Pa
- ΔP_f = pressure drop of the (dry) empty column with the grid, Pa
- ΔP_{1B} = pressure drop due to the liquid holdup in the bed, Pa
- $\Delta P'_{1B}$ = ΔP_{1B} expressed in terms of height of water, m
- ΔP_{1G} = pressure drop due to the liquid held on the grid, Pa
- ΔP_p = $(g/g_c)(1-\epsilon_{sp})(\rho_p - \rho_g)H_s$ = pressure drop due to fluidization of dry packing, Pa
- $\Delta P'_{OG}$ = pressure drop to overcome the interfacial tension at the grid, Pa

R	= average rate of absorption of carbon dioxide per unit area of interface, $\text{kgmol m}^{-2} \text{s}^{-1}$
Re	= Reynolds number, $(d_p \phi_s) u_g \rho_g / \mu_g$, $(d_p \phi_s) u_l \rho_l / \mu_l$
\bar{Re}_1	= Reynolds number, defined as $(d_p \phi_s) \bar{u} \rho_l / \mu_l$
s	= fractional rate of surface-renewal, s^{-1}
t	= time measured from the introduction of tracer, s
\bar{U}	= average interstitial velocity of the liquid phase, defined as H/θ , m s^{-1}
U_g	= superficial gas velocity, m s^{-1}
U_l	= superficial liquid velocity, m s^{-1}
U_{mf}	= minimum fluidization gas velocity of the irrigated particles, m s^{-1}
U_{mfo}	= minimum fluidization gas velocity of the dry particles, m s^{-1}
U_{gF}	= superficial gas velocity at which the particles start to congregate below the top grid, m s^{-1}
We	= Weber number, $(d_p \phi_s) u_g^2 \rho_l / \sigma$, $(d_p \phi_s) u_l^2 \rho_l / \sigma$
z	= number of moles of sodium hydroxide reacting with each mole of carbon dioxide

Greek letters

ϵ_g	= gas holdup, $\text{m}^3 \text{m}^{-3}$
ϵ_{gmf}	= gas holdup at minimum fluidization, $\text{m}^3 \text{m}^{-3}$
ϵ_{lmf}	= liquid holdup at minimum fluidization, $\text{m}^3 \text{m}^{-3}$

ϵ_{sl}	= liquid holdup defined as h_l/H_s
ϵ'_{sl}	= defined as $\Delta p'_{lB}/H_s$
ϵ_{sp}	= void fraction in the dry static bed
\bar{e}	= average residence-time of liquid in mobile bed, s
μ	= viscosity, $\text{kg m}^{-1} \text{s}^{-1}$
ξ_B	= coefficient which is dependent upon the characteristics of the grid and the packing
ξ_f	= coefficient which is dependent upon the characteristics of the grid
ξ_G	= hydraulic resistance coefficient of the grid
ρ	= density, kg m^{-3}
σ	= surface tension, N m^{-1}
ϕ_s	= sphericity of the particle; defined as the ratio of the surface area of a sphere having the same volume of the particle to the surface area of the particle

Subscripts

B	= bed
G	= grid
g	= gas
l	= liquid
mf	= minimum fluidization
p	= particle

SYNOPSIS

of the
Ph.D. Dissertation
on
HYDRODYNAMIC, AXIAL MIXING AND MASS TRANSFER STUDIES
ON A MOBILE BED CONTACTOR WITH LOW DENSITY PARTICLES
by

OM PRAKASH RAMA
Department of Chemical Engineering
Indian Institute of Technology Kanpur
Kanpur 208016(INDIA)

Mobile bed contactor, which is also referred to as Turbulent Bed Absorber, Turbulent Contact Absorber, Fluidized Bed Contactor etc., is a three-phase fluidized bed in which relatively large and low density particles are fluidized by the upward flow of gas and irrigated by the downward flow of liquid. It is increasingly finding application as an alternative to conventional packed bed in absorption, distillation, pollution control etc., because it permits higher throughputs, promotes higher heat and mass transfer rates, and processes dusty gas streams and slurries without clogging.

In the mobile bed contactor, the particles are presumed to generate turbulence and thus enhance the interphase heat and mass transfer rates. The pressure drop and hence the power required to keep the particles in a fluidized condition depends to a greater extent on the density and shape of the

particles. These should be such that the enhancement in heat and mass transfer rates per unit power expended in the bed is maximum. To achieve this objective, an understanding of the hydrodynamics, axial mixing of phases and mass transfer over a range of densities and different shapes and sizes is required. Studies on hydrodynamics and mass transfer with spherical particles of densities ranging from 150 to 1280 kg m⁻³ have been reported in literature. Only three studies have been reported for liquid-phase axial mixing. In this work hydrodynamic and axial mixing studies have been carried out and reported for a mobile bed contactor of 0.15 m ID, with spherical, cork and 'irregular' shaped particles of densities 53 kg m⁻³, 183 kg m⁻³ and 112 kg m⁻³, respectively, and for four static bed heights (0.12 m, 0.24 m, 0.36 m and 0.48 m). Mass transfer studies, with 0.038 m diameter spherical particles of densities 53 kg m⁻³ and 148 kg m⁻³ and for static bed height of 0.24 m, were also conducted using the absorption of CO₂ in NaOH solution to obtain interfacial area and liquid-phase mass-transfer coefficient.

To determine liquid holdup and axial mixing, breakthrough curves were obtained employing the step-input response technique using NaCl solution as a tracer.

It was observed that for higher static bed heights and at lower gas velocities, the particles congregated at the wall leaving a particle-free core. The congregation was more pronounced with the cork and irregular particles. Maps depicting the regions of congregation are presented. In literature, it has been reported that the liquid holdup is fully supported by the upward flow of gas. But, it was found that only a part of the liquid holdup is supported for these low density particles. The Kito-Tabei-Murata correlation has been adapted to fit the data of the liquid holdup and pressure drop. Correlations for the bed expansion and minimum fluidization velocity have been proposed.

It was found that axial mixing in the liquid phase was in between perfectly-mixed and plug flow conditions. The Peclet number increased with the static bed height and, in general, decreased with the gas velocity. Correlations for the Peclet number and axial dispersion coefficient have been proposed. The results indicate that near plug flow of liquid phase could be achieved with higher static bed heights if the congregation could be avoided.

In the mass-transfer studies, recycling arrangements for the solution and the gas were employed in order to conserve the reagents and to achieve saturation of inlet air with water

vapor. The composition of CO_2 in the gas stream, NaOH in the solution and temperatures of inlet and outlet gas and liquid streams were monitored. From this data, Danckwerts' plot for each run was made to evaluate the interfacial area and the surface-renewal rate.

It was found that interfacial area in the bed with lighter spherical particles was higher than with the heavier particles. Further, the surface-renewal rate was about an order magnitude smaller than the pseudo-first order reaction rate constant in the case of lighter particles, whereas it was almost negligible for heavier particles. Thus the contention of Strumillo and Kudra (1977), that the interfacial area as well as the surface renewal rate in this contactor has to be evaluated, appears to be justified.

The interesting finding, that the higher interfacial area and higher mass transfer coefficient resulted with lighter particles and that only a part of the liquid holdup is supported, were explained making use of the hypothesis advanced by O'Neill et al. (1972) with regard to the nature of fluidization with density of the particles.

Comparing with the values of interfacial area reported in literature it was shown that relatively low density particles will yield higher interfacial area and liquid phase mass-transfer coefficient per unit power required in fluidizing the particles in mobile bed contactors.

CHAPTER 1

INTRODUCTION

Mobile bed contactor is a three-phase fluidized bed in which relatively large and low density particles, placed between two retaining grids in a vertical column, are fluidized by the upward flow of gas and irrigated by downward flow of liquid. In literature this contactor has been referred as Turbulent Bed Contactor, Turbulent Contact Absorber, Floating Bed Scrubber, Fluidized Bed Contactor etc. Reference to the mobile bed contactor first appeared in literature in 1959 as a means for efficient removal of the particulate matter from dusty gas streams (Anon., 1959). The pilot plant studies revealed that the violently agitated particles bring about intimate contact between gas and liquid, promote heat and mass transfer rates, and allow higher throughputs at lower pressure drop; and this led to the installation of a number of large scale units (Douglas et al., 1963; Anon., 1964; Strumillo et al., 1976; Ramm and Gildenblat, 1970). The contactor is increasingly finding application as an alternative to conventional packed bed in absorption, distillation, cooling and humidification and pollution control (Gel'perin et al., 1966; Barile and Meyer, 1971; Strumillo et al., 1974).

Several studies on pressure drop, minimum fluidization velocity, expanded bed height and liquid holdup in the mobile bed contactor have been reported. Some of the mass transfer studies revealed that the sectionalization of the bed improves the mass transfer performance indicating that the mixing of the phases need to be accounted. Only three studies have been reported on the axial mixing of the liquid phase. Several studies on mass transfer have been reported. But, most of these studies are concerned with the overall mass-transfer coefficients and only few aimed at the evaluation of gas-and liquid-phase mass-transfer coefficients and interfacial area. Hence, most of studies appear to be applicable only to the specific systems studied and that too within the range of variables covered. In all the studies reported so far mainly the spherical particles of densities ranging from 150 to 1280 kg m^{-3} have been used.

In mobile bed contactor, the particles are presumed to generate turbulence and thus enhance the rates of interphase heat and mass transfer. But the pressure drop and hence the power required to keep the particles in a fluidized condition depends to a greater extent on the shape and density of the particles. The shape and density of the particles should be such that the enhancement in the interfacial rate of heat or mass transfer per unit power expended in the bed is maximum.

To achieve this objective, an understanding of the hydrodynamics, axial mixing and mass transfer over a range of densities and different shapes of particles is warranted.

The present work was undertaken to study these aspects with relatively low density spherical and non-spherical particles. The range of densities between 53 to 183 kg m^{-3} was used. The liquid holdup and liquid phase axial mixing were measured using the step-input response technique with air-water system. The breakthrough curves were analyzed using the single-parameter axial dispersion model. The mass transfer studies were conducted using the absorption of CO_2 from air into NaOH solution and the interfacial area was determined using the Danckwerts' plot.

A review of the literature on hydrodynamics, axial mixing and mass transfer has been presented in Chapter 2. The details of the experimental setup and measurement techniques are described in Chapter 3. Results and discussion are given in Chapter 4. Conclusions are presented in Chapter 5.

CHAPTER 2

LITERATURE REVIEW

A review of the literature concerning hydrodynamics, axial mixing and mass transfer studies on mobile bed contactor has been presented in this chapter.

2.1 HYDRODYNAMICS

A comprehensive survey of the literature upto 1974 on hydrodynamics of the mobile bed contactor has been presented by Strumillo et al.(1974). Some of the earlier studies have been also reviewed by Blyakher et al.(1967). The details of the contactor used, the range of variables covered and the nature of studies conducted by various investigators are summarized in Table 2.1. A list of correlations proposed by various investigators for pressure drop, liquid holdup, bed expansion and minimum fluidization velocity is presented in Table 2.2. Since some of these correlations are not in dimensionless form, they have been converted and reported here in the SI units. The results of these studies are discussed in the following sections.

2.1.1 Pressure Drop and Liquid Holdup

In general, the total pressure drop, ΔP , across the mobile bed (including the bottom supporting grid)

TABLE 21
SUMMARY OF HYDRODYNAMIC STUDIES ON THE MOBILE BED CONTACTOR

Reference	Details of the contactor				Range of variables								Nature of studies			
	D	H _T	f	n _B	d _p (10 ²)	ρ _p	H _s	H _s /D	H/H _s	U ₁ (10 ²)	U _g		Bed expansion	Minimum fluidization	Pressure drop	Liquid holdup
	m	m	%		m	kg m ⁻³	m	max.	m s ⁻¹	m s ⁻¹						
1	2	3	4	5	6	7	8	9	10	11	12		13	14	15	16
Douglas et al.(1963)	0.305 (Square)	3.05	?	1	3.8	160	0.127 to 1.5	0.4 to 5.15	2-24	0-2.66	0-10		✓	-	✓	-
Gelperin et al. (1966;1968a)	0.096	1.50	34.5	1	1.6 1.6	160 320	0.045 to 0.175	0.47 to 1.82	α	0-1.1	0.5-5		✓	✓	✓	?
Groeneveld (1967)	0.450	2.00	70	1	3.73	736	0.12 0.25 0.35 0.44	0.27 0.56 0.78 0.98	α	0-0.2	2-7		-	-	✓	✓
Blyakher (1967)	0.200 0.350	1.80 2.80	19 30 41	1-3	3.8 3.8	90 180	0.2 to 0.8	1-4	α	0-0.556	0-5		✓	✓	✓	-
Krainev et al.(1968) Levsh et al.(1968a)	0.178	1.20	?	1	rings	1083	0.07 0.14 0.21	0.39 0.79 1.18	α	0.28-1.71	0.5-4.5		✓	-	✓	-
Levsh et al.(1968c)	0.178	1.20	28.6 36.4 40.0 50.0	1	No packing	-	-	-	-	0-1.71	1-4.5		-	-	✓	-

TABLE 2.1(Continued)

1	2	3	4	5	6	7	8	9	10	11	12	13	14	15	16
Chen and Douglas (1968)	0.305	0.61	70	1	1.3 2.5 3.8	156 170 158	0.305	1.0	a	0.26-152	0-3.22	✓	✓	-	✓
Balabekov et al. (1969 a, 1969 b, 1971)	0.175	1.20	30 40 42 50 60 40	1	0.6 0.6 1.1 1.2 1.6 1.6 1.6 1.6	2600 1036 856 944 356 600 850 1010	0.038 0.075 0.110 0.150 0.225 0.300	0.22 0.43 0.63 0.86 1.29 1.71	a	0-3.4.	0-8	✓ d	✓	✓	✓
Barile and Meyer (1971)	0.286	1.63	82	1	1.90 3.80	160 109	0.152 0.178 0.356 0.533	0.53 0.62 1.24 1.86	a	1.4-4.0	0-5	-	-	✓	-
Tichy et al. (1972) Tichy and Douglas (1972)	0.140	0.3 to 1.4	78	1	1.27 1.9 1.9 1.9	155 155 234 458	0.14 0.21 0.28 0.35	1.0 1.5 2.0 2.5	a	0-32	0-4.6	✓	✓	✓	-
Tichy and Douglas (1973)	0.292	?	80	1	1.27 1.91	160 160	0.146 0.292	0.5 1.0	a	0-0.765	15-5.5	✓	-	✓	-
Wozniak and Ostergaard (1972, 1973)	0.100	1.0	?	1	0.97	388	0.22	2.2	3	2-7	0.2-1.4	✓	-	✓	-
Strumillo et al. (1974)	0.085 0.105 0.200	0.5 0.8 1.0	65b	1	1.00 1.50	1050 470	0.08 0.105	1	a	0.28-3.33	1-7	✓	✓	✓	-
Strumillo et al. (1976)	0.105 0.200 0.500	0.8 1.0 1.5	35 to 78	1	1.00 1.50 2.00 3.00	1030 470 470 470	-	0.22 to 1.5	a	0.5-3.33	0-7	✓	✓	✓	-

TABLE 2.1(Continued)

1	2	3	4	5	6	7	8	9	10	11	12	13	14	15	16
Vukovic et al. (1974)	0.194	1.0	60° Conical	1	1.00	320	0.243	1.25	3.1	0.188 0.563 0.938	0-2	✓	✓	✓	✓
Wozniak (1977)	0.200	?	60	2	1.96	266	0.2 to 0.5	1-2	a	0.5-2.7	1.7-3.1	-	-	✓	✓
Kito et al. (1976b, 1976c)	0.10	?	70.5 71.2 84.0	1	1.16 1.95 1.95 1.95 2.85 2.85	760 170 540 1160 290 590	0.05 0.10 0.20	0.5	a	0-35	0-37	✓	✓	✓	-
Kito et al. (1977)	0.104	1.20	70.5 84.5	3	1.55 1.95 2.85	1060 170 290	?	?	a	0-3.0	0-2.6	✓	✓	✓	✓
Uchida et al. (1977)	?	?	?	3	?	?	?	?	a	0.9-2.5	0-4.5	✓	✓	✓	-
Kito et al. (1978)	0.10	?	70.5 71.2 84.0	1	0.97 0.98 1.16 1.95 1.95 2.85 2.85	1250 1250 760 170 540 290 590	0.10 0.20 0.30	1 2 3	a	0-3.5 c Liquids used: (1) Water (2) 25% glycerol solution (3) 65% glycerol solution (4) ethanol	0-3.7	✓	✓	✓	✓
Uchida et al. (1980)	0.160	0.90	72.4	1	3.8 3.8 3.0	173 83.4 156	?	?	a	?	?	✓	-	-	-

a-the study was carried out upto the point of congregation below the upper grid. b-slotted tray; in rest of the cases perforated or wire meshes were used. c- in rest of the studies water-air system has been used. d-presented explicit correlation for the point of congregation below the upper grid.

TABLE 2.2

SUMMARY OF CORRELATIONS OF PRESSURE DROP, LIQUID HOLDUP, BED EXPANSION AND MINIMUM FLUIDIZATION VELOCITY FOR MOBILE BED CONTACTOR

Reference	Pressure drop, ΔP	Liquid holdup, h_L	Bed expansion, U/H_s	Minimum fluidization velocity, U_{mf}
Douglas et al. (1963)	Graphical (ΔP vs U_g)	—	—	—
Groeneveld (1967)	Graphical (ΔP vs U_g)	Graphical (h_L vs U_g)	—	—
Blyakher et al. (1967)	$\Delta P = \Delta P_G + \Delta P_{IG} + \Delta P_{IB}$ where $\Delta P_G = \Sigma G U_g^2 \frac{\rho_g}{g}$ $\Delta P_{IG} = \Sigma U_g^{1.75} U_l^{0.5}$ $\Delta P_{IB} = \Sigma U_l H_s$	—	$1.17 \cdot (0.65 + 24.63 U_l^{0.75}) \times U_g - U_{mf}^{1.25}$	$U_{mfo} + \frac{1587.35 U_{mf} U_l^{0.9}}{37.5 + 1587.35 U_l^{0.9}}$ where $U_{mfo} = 0.0366 d_p^{0.75} (\rho_p - \rho_g)^{0.572}$ $\mu_g^{0.143} \rho_g^{0.429}$
Levsh et al. (1968a)	$\Delta P = \Delta P_G + \Delta P_{IG} + \Delta P_{IB} + \Delta P_{GG}$ where $\Delta P_G = 18.63 \left(\frac{U_g}{t} \right)^2 \frac{\rho_g}{2g}$ $\Delta P_{GG} = 4.6/d$ $\Delta P_{IG} + \Delta P_{IB} = 37.35 U_l^{0.55} U_g (14.3 H_s)^m$ $m = 1$ for $0.8 \times 10^{-2} \leq U_l \leq 1.71 \times 10^{-2}$ $m = 0.75$ — 0.8 for $U_l < 0.8 \times 10^{-2}$	—	$0.13 (3600 U_l)^n U_g^2$ $n = 0.43$ for $U_l = 0.77 \times 10^{-2}; U_g < 2.5$ $n = 0.35$ for $U_l = 0.77 \times 10^{-2}; U_g > 2.5$	—
Levsh et al. (1968c)	$\Delta P = \Delta P_G + \Delta P_{IG} + \Delta P_{IB} + \Delta P_{GG}$ where $\Delta P_G = 18.63 (U_l/t)^2 (\rho_g/2g)$ $\Delta P_{GG} = 4.6/d$ $\Delta P_{IG} = 0.9807 h_G \rho_l \left[\frac{9}{m^2} \frac{1}{(\mu/\rho)^{0.5}} \cdot 1.2 m^{0.5} \right]$ $h_{IG} = U_l (1-t)$ $m = U_g/h_{IG}$	—	—	—

Reference	Pressure drop, ΔP	Liquid holdup, h_l	Bed expansion, H/H_s	Minimum fluidization velocity, U_{mf}
Chen and Douglas (1968)	$(\Delta P_p + \Delta P_g) \left[1 + C \left(\frac{U_l}{U_g} \right)^2 \left(\frac{\rho_l}{\rho_g} \right)^{k+1} \right]$ where C and k are constants.	$\epsilon_{sl} = 26.17 U_l^{0.6} d_p^{-0.05} + 0.02$ Graphical (h_A vs U_g)	Graphical (H/H_s vs U_g) $(1 - \epsilon_{g0} + \epsilon_{sl}) / (1 - \epsilon_g)$	$17.95 d_p^{1.15} \times 10^{-36.9 U_l}$ $\sqrt{\left[\frac{(89/\alpha)(\rho_l/\rho_g)(\rho_p/\rho_l)^{0.64} + 1.5}{4(U_l/U_g)^{0.25}(\rho_g/\rho_l)^{0.125}} \right]}$ x exp
Balabekov et al. (1969a, 1969b, 1971)				
Barile and Meyer (1971)	$\Delta P_p + \Delta P_{lg} = \Delta P_p + \epsilon_{sl}' H_s \rho_l$ where $\epsilon_{sl}' = 1160 (Fr)_l^{-0.51} (H_s/d_p)^{-0.36}$	—	—	—
Tichy et al. (1972)	$\log \left[2Eu(D/H_s) (1/(1.CQ_l)) \right] = 4.003 - 2.24 Q_g + 0.84 Q_g^2 - 0.127 Q_g^3$ for $0.4 < Q_g < 2.5$ where constant $C = 0.1083, 0.0816$ and 0.0780 $kg^{-1} m^{-2} s$ for $H_s/D = 1, 1.5$ and 2 respectively. Q_g are mass flow rate, $kg m^{-2} s^{-1}$	—	—	—
Tichy and Douglas (1972)	—	—	$0.8849 + 0.3166 \frac{U_g}{d_p} - 18.33 \frac{d_p}{U_g^{0.5}}$ $0.5852 (U_l \rho_l)^{0.6} d_p$	U_{mf} can be evaluated by substituting H/H_s in the correlation of H/H_s .
Wozniak and Østergaard (1972, 1973)	Graphical (ΔP vs U_l)	—	Graphical (H/H_s vs U_g)	—
Strumillo et al. (1974)	Graphical (ΔP vs U_g)	—	Graphical (H/H_s vs U_g)	$(13.3 D + 2.24) \exp - (3.6 U_l / D^{0.04})$
Strumillo et al. (1976)	?	—	?	$4.6 \frac{39.6 U_l}{d_p} - 4 + 0.7 D^{0.65} (H_s/D)$

TABLE 2.2 (Continued)

Reference	Pressure drop, ΔP	Liquid holdup, h_l	Bed expansion, H/H_s	Minimum fluidization velocity, U_{mf}
Vukovic et al. (1974)	Graphical (ΔP vs U_g)	Graphical (h_l vs U_g)	Graphical (H/H_s vs U_g)	—
Wozniak (1977)	$Eu = 4.672 \times 10^5 (H_s/D)^{0.4515} \times (Re)_g^{-1.798} (Re)_l^{0.8261}$ for $10 \leq H_s/d_p \leq 21$; $2200 \leq (Re)_g \leq 4100$ and $100 \leq (Re)_l \leq 520$.	Graphical (h_l vs U_l)	—	—
Kito et al. (1976b)	Graphical (ΔP vs U_g)	—	—	$0.598 U_{mf0} (fd/D)^{0.48} U_l^{-0.36}$ for $(fd/D) \leq 0.05$ $0.1486 U_{mf0} U_l^{-0.36}$ for $(fd/D) > 0.05$ where U_{mf0} is to be estimated from the Ergun equation.
Kito et al. (1976c)	$\Delta P_p + \Delta P_B = \Delta P_p + 9.807 \times 10^3 H_s \epsilon_{sl}'$ where $\epsilon_{sl}' = 0.06 + 0.0302 (fd/D)^{-0.84} d_p^{-0.84} \times \rho_p^{0.18} \mu_s^{0.4} U_l$	—	$(1 - \epsilon_{sp} + \epsilon_{sl}') / (1 - \epsilon_g)$ where $\epsilon_g = 0.417 U_g^{0.44}$	—
Uchida et al. (1977)	$\Delta P_p + \Delta P_B$ where $\Delta P_B = 9.38 \times 10^8 \times \mu_l^{2.3} f^{-0.42} (d/D)^{0.84} \times \frac{d_p}{0.84} \rho_p^{0.18} H_s U_l$	—	—	$0.0678 \times U_{mf0} \times U_l^{-0.36}$ where U_{mf0} is to be estimated from the Ergun equation.
Kito et al. (1978)	—	$\epsilon_{sl} = 12.8 (H_s/d_p)^{-0.4} (fd/D)^{-0.58} (Gao)^{0.09} (Fr)_l^{1.56} (Re)_l^{0.34} (We)_l^{-0.34}$	$(1 - \epsilon_{sp} + \epsilon_{sl}') / (1 - \epsilon_g)$ where $\epsilon_g = 0.19 (We)_g^{0.11} (Fr)_g^{0.22}$	—

TABLE 22(Continued)

Reference	Pressure drop, ΔP	Liquid holdup, η_l	Bed expansion, H/H_s	Minimum fluidization velocity, U_{mf}
Kuroda and Tabei(1981)	—	—	—	<p>Theoretical expression :- $C_{fi} \frac{U_{mf}^2}{dp} = \frac{(\rho_s - \rho)g}{\epsilon_{gm} w_p}$ where $C_{fi} = C_{fs} (1 + 800 \epsilon_{li}^2)$ $\epsilon_{li} = (1 - \epsilon_{sp}) / (1 + \epsilon_{li} - \epsilon_{sp})$ $P = \frac{\rho_s + \epsilon}{\rho_{sl}} \frac{P}{(1 - \epsilon_{sp})}$</p>

may be represented as a sum of various individual pressure drops:

$$\Delta P = \Delta P_p + \Delta P_{1B} + \Delta P_{1G} + \Delta P_f + \Delta P_{fG} \quad (2.1)$$

The analysis of the pressure drop data indicates that all the terms in Equation (2.1) may have to be considered if the free open area of the bottom supporting grid, f , is less than 65 % (Balabekov et al. 1969a, 1969b; Blyakher et al., 1967; Gel'perin et al., 1966, 1968a; Krainev et al., 1968; Levsh et al., 1968a, 1968c; Strumillo et al., 1974, 1976; Wozniak, 1977). In the case of, f , being greater than 65 %, only ΔP_p and ΔP_{1B} need to be considered (Barile and Meyer, 1971; Groeneveld, 1967; Kito et al., 1976b, 1976c; Tichy and Douglas, 1972, 1973; Uchida et al., 1977). The correlations obtained by various investigators for the different terms of Equation (2.1) are given in Table 2.2.

The variation of ΔP with gas velocity, U_g , at constant liquid velocity, U_l , is affected by the free open area of the grid, the ratio of the static bed height to the diameter of the contactor, H_s/D , and the density of the packing particles, ρ_p . It is observed that for $f \leq 65$ %, ΔP increased with increase in U_g , whereas it remained independent of U_g for $f > 65$ %.

Even the type of the supporting grid seems to influence the hydrodynamics of the mobile bed (Balabekov et al., 1969a, 1969b; Strumillo et al., 1974, 1976). For instance, the data obtained by Wozniak (1977) with perforated grid having $f = 60\%$ reveal only a marginal increase in ΔP with U_g , while that of Strumillo et al. (1974) with slotted grid having $f = 65\%$ show significant increase in ΔP with U_g . It may be pointed out that most of the investigators have used perforated plates or wire meshes as grids.

Kito and co-workers (Kito et al., 1976b, 1976c, 1977, 1978; Kuroda* and Tabei, 1981) studied the effect of several parameters including the physical properties of the liquid on hydrodynamics of the mobile bed. A wide range of different variables was covered in their studies. Uchida et al. (1977), who analysed the data obtained by Epstein et al. (1975) on large sized three-stage mobile bed contactors, have proposed correlation for ΔP by modifying the one proposed by Kito et al., (1976c). Kito and co-workers (Kito et al., 1976c; Kuroda and Tabei, 1981), Tichy and Douglas (1972, 1973), Uchida et al. (1977) represented the total pressure drop

* Kuroda was formerly known as Kito.

ΔP as the sum of ΔP_p and ΔP_{1B} . Since ΔP has been found to be independent of U_g for $f > 65\%$, it is expected that the variation of ΔP_{1B} with U_g will also remain constant.

The liquid holdup in mobile bed contactor has been measured employing either the direct method using quick acting valves (Balabekov et al., 1969a; Kito et al., 1978; Wozniak, 1977) or, the indirect method using the tracer technique of residence-time measurement (Chen and Douglas, 1968; Groeneveld, 1967). Chen and Douglas (1968) and Kito et al. (1978) have shown the liquid holdup, h_1 , to be independent of U_g . They used grids with $f > 70\%$, H_s/D ranging from 1 to 3 and ρ_p ranging from 150 to 1250 kg m⁻³. But Groeneveld (1967), who experimented with beds consisting of ping-pong balls of $\rho_p = 70$ kg m⁻³, $f > 70\%$ and $H_s/D < 1$, has found that while ΔP remained independent of U_g , h_1 increased with U_g ; whereas the data of Wozniak (1977) indicate a marginal increase in h_1 with U_g under the conditions with $f = 60\%$, $H_s/D = 1$ and $\rho_p = 263$ kg m⁻³.

Tichy et al. (1972) found that while ΔP was constant with U_g for $H_s/D = 1$ and $\rho_p = 155$ kg m⁻³, it decreased with U_g for H_s/D equal to 1.5 and 2.0. This decrease in ΔP was attributed to the congregation of the particles

in the form of a mono-static layer along the wall, which they termed as the 'wall effect'. It appears that they are the lone investigators to report such a phenomenon occurring in a mobile bed contactor. They measured also the variation of the static pressure along the height of the mobile bed and found it to be linear. They correlated their pressure drop data using an equation obtained by treating the mobile bed to be consisting of a number of gas channels, in a manner similar to the analysis of the pressure drop in fixed beds. Considering that the liquid holdup in the bed is located over the particles in the form of a film covering their entire surface, Kuroda and Tabei (1981) obtained an expression by equating the drag force on the wet particles to their buoyant weight. They evaluated the apparent drag coefficient of friction from their experimental data.

Vukovic et al. (1974) have reported the experimental data on the pressure drop and the liquid holdup in a three-phase spouted bed, a counterpart of the mobile bed. They have observed that only a part of liquid holdup is "supported" by upward flow of the gas. They have analysed the data of Chen and Douglas (1968) and showed that the ratio is in the range of 0.85 to 0.95 even for the mobile bed.

2.1.2 Bed Expansion

In literature, the bed expansion has been reported either as the ratio of the average height of the mobile bed to the height of the static bed, H/H_s , or as the gas holdup per unit volume of the mobile bed, ϵ_g .

These are related in the following way

$$H/H_s = (1 - \epsilon_{sp} + \epsilon_{sl}) / (1 - \epsilon_g) \quad (2.2)$$

In general, the expanded bed height has been found to increase with gas and liquid velocities, and diameter of the packing particles. The ratio H/H_s has been observed to be independent of H_s . The bed expansion showed a marked dependence on the free open area of the grid. For instance, with $f \geq 70\%$, the ratio H/H_s has been observed to vary linearly with U_g (Chen and Douglas, 1968; Kito et al., 1976c; Tichy and Douglas, 1972, 1973), while the trend was non-linear for $f \leq 65\%$ (Balabekov et al., 1969a, 1969b, Blyakher et al., 1967; Gel'perin et al., 1966, 1968a; Krainev et al., 1968; Levsh et al., 1968a; Strumillo et al., 1974).

Tichy and Douglas (1973) have extended their pressure drop analysis (Tichy et al., 1972) to obtain a functional form for bed expansion. To this, they have

fitted their own data and that of Chen and Douglas (1968) by regression analysis. They have found that the particle density has no effect on bed expansion.

2.1.3 Congregation Below the Upper Grid

As the gas velocity is increased at a constant U_1 , the particles start congregating below the upper grid whenever the gas velocity equals the terminal velocity of the wet particles or when the bed height reaches the upper grid at a gas velocity lower than the terminal velocity. This represents the upper limit of the normal mobile bed operation. It is referred, hereafter, as 'top grid congregation velocity' in preference to the term "flooding point" used in the literature (Uchida et al., 1977, 1980; Wen and Chang, 1978), because the term 'flooding' is generally used to describe a different physical condition prevailing in gas-liquid and liquid-liquid contactors. Uchida et al. (1977, 1980) have proposed a method of evaluating the point of congregation below the top grid.

2.1.4 Minimum Fluidization Velocity

It has been observed that the transition from static bed to mobile bed is gradual (Balabekov et al.,

1969a, 1969b; Tichy et al., 1972). The minimum fluidization velocity, U_{mf} , has been determined either by extrapolating the plots, H/H_s vs U_g , to H/H_s equal to one (Blyakher et al., 1967; Chen and Douglas, 1968; Tichy and Douglas, 1972) or from the relationship of ΔP vs U_g (Balabekov et al., 1969a, 1969b, 1971; Kito et al., 1976b) as is usually done in the case of conventional fluidized beds.

O'Neill et al. (1972) have discussed some of the apparent inconsistencies in regard to the effect of different variables on hydrodynamics of the mobile bed, especially the effect of density of the particles on U_{mf} . They have hypothesised that the mobile bed operation may be characterised as the 'fluidization with incipient flooding' or as the 'fluidization without incipient flooding'. In the former case, at the minimum fluidization the bed is under incipient flooding condition while in the latter case it is below the incipient flooding, which should obviously be the case with lighter particles. They have shown that in the former case, U_{mf} remains independent of ρ_p whereas in the latter, it is a function of ρ_p . They have predicted that the shift from one mode of fluidization to other (viz. fluidization

without incipient flooding to fluidization with incipient flooding) takes place at $\rho_p = 233 \text{ kg m}^{-3}$. The maximum value of ρ_p , beyond which the mobile bed operation is impossible, has been shown to be 1330 kg m^{-3} . In support of their contention of fluidization with incipient flooding, they have shown that the operating points reported by Douglas (1964), Chen and Douglas (1968), and Levsh et al. (1968a, 1968c) fell in between the flooding curves of the dumped packings and the drip point grids on the well-known Lobo plot.

Kuroda and Tabei (1981) have derived an expression for U_{mf} in terms of apparent coefficient of friction by equating the drag force on the wet particles to their buoyant weight. They have shown that their experimental data could be correlated by this expression with $\sim 20\%$ deviation.

2.2 AXIAL MIXING

The understanding of the axial mixing of the liquid and gas phase is essential for the determination of true values of k_l and k_g of the mobile bed contactor, and for its design and performance evaluation. Till date only three papers have appeared on the axial mixing of the liquid phase (Chen and Douglas, 1969; Koval et al., 1975a; 1975b) and none on the gas-phase axial mixing.

The details of the investigations on the liquid-phase axial mixing in mobile bed contactor are given in Table 2.3.

Chen and Douglas (1969) have determined the axial dispersion coefficient, D_L , of the liquid phase by fitting the step-function response data to the single-parameter axial dispersion model. They have reported that the values of D_L were found to increase with gas and liquid velocities. The average liquid-phase velocity \bar{U} (defined as $\bar{U} = H/\theta$), was found to be independent of gas velocity, but increased with liquid velocity. They have analyzed the data in terms of the ratio, $\frac{Pe'_1}{Pe'_0}$, where Pe'_1 and Pe'_0 are the liquid-phase Peclet numbers based on \bar{U} for the mobile bed and the packed bed at $U_g = 0$, respectively. For all the three sizes of packing particles studied, this ratio was found to be independent of the liquid velocity (and hence of \bar{U}) and to decrease with the increase in the reduced gas velocity, Δ , defined as $(U_g - U_{mf})/U_{mf}$. For Pe'_0 , they have adopted the following functional form of the correlations proposed by Otake and Kunugita (1958) and Otake et al. (1962).

$$Pe'_0 = k_1 (\bar{Re}_1)^{a_1} (Ga)^{b_1} \quad (2.3)$$

where k_1 , a_1 and b_1 are constants. They have considered that besides \overline{Re}_1 and Ga , Δ (to take care of intensity of bed motion), and $\frac{d_p}{D}$ (to account for the wall effects) should also be included in the correlation for Pe' .

Accordingly, they have proposed the following relation:

$$Pe' = k_2 (\overline{Re}_1)^{a_2} (Ga)^{b_2} f(\Delta) (d_p/D)^c \quad (2.4)$$

where k_2 , a_2 , b_2 and c are constants and $f(\Delta)$ is a function of Δ . Dividing Equation (2.4) by (2.3) and considering the fact that \bar{U} was independent of gas velocity, they simplified the relation as

$$\frac{Pe'}{Pe_o} = \frac{k_2}{k_1} (\overline{Re}_1)^{a_2-a_1} (Ga)^{b_2-b_1} f(\Delta) (d_p/D)^c \quad (2.5)$$

Since they have found, Pe' / Pe_o to be independent of \bar{U} , and the effect due to Ga can be incorporated into the term $\frac{d_p}{D}$, the Equation (2.5) was further simplified as

$$\frac{Pe'}{Pe_o} = F(\Delta) (d_p/D)^c \quad (2.6)$$

where $\frac{k_2}{k_1}$ has been coupled with $F(\Delta)$, which is a function of Δ . They have proposed the following correlation based on their experimental data:

$$\frac{Pe'}{Pe_o} = F(\Delta) (d_p/D)^{-0.304} \quad (2.7)$$

$F(\Delta)$ has been given in a graphical form.

Koval et al.(1975a) obtained the residence-time distribution curves for the liquid phase using the pulse-input of tracer into the bed through an atomizer. The height of the atomizer was varied with the bed expansion so that the tracer was uniformly distributed over the entire surface of the top layer. The second, third and fourth moments of the experimental residence-time distribution curves were calculated. Then the Peclet number Pe , defined as $\bar{U}H/D_L$, was estimated from each of these moments using the relations proposed by Kafarov et al..(1968). Since the estimated values of Pe were found to be in good agreement, they have concluded that the liquid-phase axial mixing in the mobile bed contactor can be represented by the single-parameter axial dispersion model.

Koval et al.(1975b) have determined Pe and D_L employing the step-response technique also. They have reported that the axial dispersion coefficient was found to increase with gas and liquid velocities. The effects of column diameter, and the size and density of the packing particles were found to be insignificant. The variations in D_L and Pe with the increase in gas

velocity were found to be intimately connected with the corresponding changes in the pressure drop, liquid holdup and expanded bed height. It may be pointed out that Koval et al.(1975b) used a supporting grid with a free opening of 46 % in contrast to Chen and Douglas, (1969), who used grid with $f = 70$ %. But it has been seen in the preceding section that the hydrodynamic characteristics are greatly dependent on the grid opening if it is less than 65 %. However, a good agreement has been reported by Koval et al.(1975b) between their data for $H_s = 0.30$ m and those of Chen and Douglas (1969) for $H_s = 0.305$ m, particularly at low liquid velocities.

2.3 MASS TRANSFER

Mass-transfer studies on mobile bed contactors have been reported by several investigators. Some of these studies have been reviewed by Shah (1979). A summary of the available literature, including the details of the contactor, range of variables covered, systems employed and the nature of studies conducted is given in Table 2.4. The results of these studies are briefly discussed here.

TABLE 2.4
SUMMARY OF MASS TRANSFER STUDIES ON MOBILE BED CONTACTOR

Reference	Details of contactor				Range of variables							Chemical system		Temperature	Nature of studies			
	D m	H _T m	t %	n _B	d _p (x10 ²) m	ρ _p kg m ⁻³	H ₂ m	u _L (x 10 ²) ms ⁻¹	u _g ms ⁻¹	Gas	Liquid	°C	K _g	K _l	k _g	k _l		
1	2	3	4	5	6	7	8	9	10	11	12	13	14	15	16	17	18	
Douglas et al.(1963)	0.305 (Square)	3.00	?	1	3.81	160	0.793	0.61-1.04	0 - 3.56	Air + CO ₂ % CO ₂ = 12	Alkaline process liquor pH = 11.7	65.5	✓					
				2	3.81	160	0.793	0.61-1.04	0 - 3.56	Fluegas-SO ₂ % SO ₂ = 15	Na ₂ CO ₃ solution	85.0	✓					
Douglas (1964)	0.305 (Square)	3.00	?	1	3.81	160	0.355 0.456 0.838	0.33-1.44	0.26-0.5	Air + NH ₃	Boric acid Solution Conc. = 2-4%	?	✓					
Dianov (1966)	0.096	0.50	27	1 3	1.6 1.6	250 500	0.138 0.046 0.184	0.03-0.2	2.3	Air + Br ₂	NaOH solution	?	✓					
Levash et al.(1968c)	0.176	1.2	28.8	1	rings 10.8x2 mm. 8x4x0.3 mm.	1083 1083	0.07 0.21	0.28-1.17	2-5	Desorption of Oxygen Air	Water + O ₂	?		✓				
Elenkov and Koshev (1970)	0.190		41.7 49.0 60.0 78.0	1	1.8 1.7 1.7	167 930 1090	0.08-0.2	0.56-2.4	1.2-6.4	Desorption Air	of Oxygen- Water + O ₂	Air = 16-42 Water = 14-22	✓					

TABLE 2.4(Continued)

1	2	3	4	5	6	7	8	9	10	11	12	13	14	15	16	17	18
Zhukov et al.(1978)	0.05	?	50	1	0.9	500	0.05 - 0.25	0.36-1.39	2.2-5.3	Desorption of CO ₂ Air	Water, CO ₂	?		✓			
	0.10				1.6	245											
	0.16				2.9	110											
	0.20																
McMicheal et al. (1976) Wer and Chang (1978)	0.23	0.8	?	3			0.136 - 0.254 (each stage)	?	?	Flue gas + SO ₂ SO ₂ = 4500 ppm	Lime and Limestone Slurry	Inlet - slurry Temp = 15-50	✓				
	1.52 (Square)	3.8	?	3			0.127 (each stage)	?	?								
Strumillo et al.(1978)	0.20		?		2.0		0.3	1.39	5	Air + SO ₂ % SO ₂ = 0-5	Mg(OH) ₂ Solution		✓				
	0.50		?	3	2.5	170		?	?	Flue gas + Fluorine	Water		✓				
Kudra et al.(1978)	0.30		50	4	2.5	170	0.15 on each stage	1.67-5.85	0.2-0.7	Desorption of H ₂ S Air	Water, H ₂ S		✓				
Gal'perin et al.(1968)	0.08	1.5	40	3	1.0	600	Upper stage = 0.05 Lower stage = 0.05 Middle stage = 0.05 - 0.10		0 - 60	Rectification with total Reflux ethyl alcohol (3-5%) + Water							

1	2	3	4	5	6	7	8	9	10	11	12	13	14	15	16	17	18
Groeneveld (1967)	0.45	1.5	70	1	3.73	73.6	0.12 0.25 0.35 0.44	0 - 0.2	2 - 7	Air, O ₂ % O ₂ = ?	Na ₂ SO ₃ M = 0.66 CaSO ₄ Catalyst, 4) (M = 0.10)	30					✓
Gel'perin et al. (1970)	0.20	1.8	33 47 61	3			≤ 0.18	0.55 - 2.75	1.5 - 4.0	Flue gas, Co ₂ % Co ₂ = 10	Monoethanol amine solution	40					✓
Gel'perin et al. (1972)	0.145	?	19 30 40 45	2	1.55	470	0.045	0.55 - 1.67	1.5 - 4.0	Air, Co ₂ % Co ₂ = ?	NaOH KOH LiOH, MEA	?					✓
Wozniak and Østergaard (1972, 1973)	0.10	1.0	?	1	0.97	388	0.22	0.02 - 0.07	0.7	Air, Co ₂ % Co ₂ = 5	NaOH M = 0.15 - 1.5	25		✓			✓
Kito et al. (1976a)	0.05 0.10	1.5	31.5 1.27	1	1.1 2.65 2.87	1000 590 590	0.05 0.20	"Stagnant"	0.05 - 4.0	Air, Co ₂ % Co ₂ = 5	NaOH M = 0.05	15 - 25		✓			✓
Wozniak (1977)	0.20	?	60	2	1.96	266	0.29 On each stage	0.5 - 3.0	1.7 - 3.0	Air, Co ₂ % Co = 1.5 - 2.3	NaOH M = 0.15 - 1.5	25		✓			✓
Strumillo and Kudra (1977)	0.085	0.5	65	1	1.0 0.75 0.50	1050	0.02 0.16	0.9 - 3.0	0.5 - 3.5	Air, Co ₂ % Co ₂ = 3 - 4	NaOH M = 2 - 3	30				✓	✓

2.3.1 Overall Mass-transfer Coefficients

Douglas et al.(1963) and Tomony (1964) have reported about the several studies conducted on a relatively large mobile bed contactor (0.305 m x 0.305 m square cross section and 3.05 m long). The absorption of carbon dioxide into an alkaline process liquor, sulfur dioxide into aqueous solution of sodium hydroxide, and into the magnesium hydroxide slurry were studied. The mass-transfer data have been reported in terms of volumetric overall gas-phase mass-transfer coefficient, $K_g a_{st}$, based on the static volume of the packing. Douglas et al.(1963) have presented a comparative study of the performance of a mobile bed contactor and that of a coke-packed tower (1.2 m ID and 11.3 m long) for the absorption of carbon dioxide into an alkaline process liquor. It has been shown that the values of $K_g a_{st}$ obtained in the mobile bed contactor were 70 times higher than the corresponding values in the coke-packed tower. Similar other striking observations led to the installation of several large scale plants for the preparation of process liquors in a number of Canadian and US pulp mills (Douglas et al., 1963; Tomony, 1964; Douglas, 1964; Anon., 1964).

Douglas (1964) determined the height of transfer unit, H_{og} , and $K_g a_{st}$, using the absorption of ammonia from air into boric acid solution. He observed that the values of H_{og} were much lower than the corresponding reported values for the packed bed absorbers.

Dianov (1966) has determined $K_g a_p$ (based on the surface area of the packing) for the absorption of bromine from air into aqueous solution of sodium hydroxide. $K_g a_p$ was found to be independent of U_1 . He has also examined the effect of sectionalizing the column and has reported that the three-stage mobile bed contactor was found to remove 99 % of bromine as compared to 80-81 % in the single-stage contactor.

Using plastic rings as packings, Levsh et al. (1968b) have determined $K_g a_B$ (based on the volume of the expanded bed) for the desorption of oxygen from water. They have stated that the values of $K_g a_B$ were found to be 2-20 times greater than the corresponding values reported for "ordinary" absorbers. $K_g a_B$ was found to decrease with the increase in gas velocity and the static bed height, whereas it decreased with the increase in liquid velocity. The large sized rings gave higher values of $K_g a_B$. They have examined and found that the recovery of oxygen was considerably improved by sectionalizing the column.

The desorption of oxygen from water was also employed by Elenkov and Kosev (1970) but they have reported their data in terms of overall liquid-phase mass-transfer coefficient, K_1A' , based on the cross-section of the bed. They have stated that the value of K_1A' was found to be 1.5 - 2 times greater than the corresponding value obtained in some "plate" columns. K_1A' was found to increase linearly with the increase in liquid velocity at lower values of static bed height and free open area of the supporting grid. But for higher values of static bed height and free open area of the supporting grid, K_1A' was found to increase first and then to decrease with the increase in liquid velocity. This decrease was attributed to the 'inhomogeneity' observed in the bed at higher values of liquid velocity and static bed height.

Zhukov et al. (1976) determined the overall liquid-phase mass-transfer coefficient, K_1A' (based on the cross section of the column), using the desorption of carbon dioxide from water into air. They have computed K_1A' assuming complete mixing of the liquid phase and plug flow of the gas phase as well as by taking into account of the axial mixing of the liquid phase. Employing the relations proposed by Hartman and Standart (1967) and the values of Pe reported by Chen and Douglas (1969) and

Koval et al.(1975b), they have estimated the Murphree tray efficiency, the number of transfer units and the 'true' values of K_1A' . They have reported that the values of K_1A' estimated, neglecting the axial mixing, were too high compared to the corresponding true values. The ratio between these two was found to vary between 1.5 and 2.0 in the case of low range of gas velocity ($U_g = 2.5 - 3.0 \text{ m s}^{-1}$) and between 3 and 5 for $U_g > 3 \text{ m s}^{-1}$. The true values of K_1A' were found to increase with the increase in gas velocity, liquid velocity and static bed height and the increase was sharp for $U_g > 3 \text{ m s}^{-1}$. This increase was attributed to the increase in expanded bed height and the liquid holdup which also increase the interfacial area. K_1A' was found to be almost independent of the diameter and size of the packing and diameter of the column. They have shown that the volumetric overall mass transfer coefficient, $\frac{K_1A'}{H}$, was independent of gas velocity and hence, they have concluded that the increase in 'true' values of K_1A' was mainly due to the increase in liquid holdup. They have proposed a correlation for the true values of K_1A' .

A number of studies using different sizes of mobile bed contactor have been reported by Strumillo and co-workers for the absorption of SO_2 into $\text{Mg}(\text{OH})_2$ solution,

CO_2 into NaOH solution, fluorine gas into water (Strumillo et al., 1976) and desorption of H_2S by air from 'deposit' water of sulphur mines (Kudra et al., 1978). It has been stated in general that high values of overall mass-transfer coefficients were obtained and these experiments confirmed the possibility of continuous operation of the mobile bed contactors with the liquid containing considerable amount of suspended solid particles. It has been reported that based on the above investigations two large sized mobile bed columns (each of 4.7 m ID and 17 m long) were installed for the desorption of H_2S from 'deposit' water. The absorption efficiency of these columns was found to be twice as large as that of the packed columns (with Raschig rings) of the same diameter but 45 m long.

Gel'perin et al. (1968b) have reported results of a study on the rectification of ethyl alcohol - water mixture (3-5 wt % alcohol) using a three-stage mobile bed contactor under total reflux condition. The static bed height was kept constant at 50 mm in the lower and the upper stages and it was varied from 50 to 150 mm in the middle stage. They have determined the Murphree tray efficiency of the middle stage. It has been reported that for $H_s = 50$ mm, the Murphree tray efficiency

increased linearly from 90 to 180 % with the increase in vapor phase velocity from 1 to 6 m s⁻¹. The efficiency was also found to increase with the increase in static bed height. They have reported that the Murphree tray efficiency was 5 - 6 times that of the tray columns.

McMichael et al.(1976) and Wen and Chang (1978) have reported that under the sponsorship of the Environmental Protection Agency (EPA) of USA, several small-scale and large-scale mobile bed contactors and spray columns were tested for the efficient removal of sulfur dioxide from flue gases, using lime and lime stone - magnesium oxide slurry. It has been already mentioned that Uchida et al. (1977) have proposed correlations for pressure drop and liquid holdup by analyzing the data obtained by Epstein et al.(1975) on these contactors. McMichael et al.(1976) have analyzed the mass-transfer data. They have considered the mobile bed to be composed of two sections viz., the packed (fluidized) section and the spray section and proposed correlations for mass-transfer coefficients for both the sections. It has been reported that these correlations were found to predict, within 5 % deviation, the SO₂ removal performance of a number of mobile bed contactors of widely differing sizes and over a wide range of static bed heights.

Wen and Chang (1978) have reported that when lime or lime stone slurry was used, some data indicated that the total pressure drop was higher than the value estimated from the correlations proposed by Uchida et al. (1977). In addition, they have noted that whenever the higher pressure drops were observed, the mass-transfer efficiencies were also higher. This increase in pressure drop has been attributed to the increase in liquid holdup which in turn influenced the mass-transfer rates. Accordingly, Wen and Chang (1978) have modified the correlations proposed by McMichael et al. (1976) to take into account the effect of liquid holdup.

The above investigations indicate that the performance of the mobile bed contactor is better compared to the packed bed and plate columns. In general, it has been observed that the overall mass transfer coefficient increased with gas velocity and decreased with static bed height, but was almost independent of liquid velocity. Whenever the bed was sectionalized, an improvement in the performance was observed, indicating that the axial mixing has a significant effect. However, these investigations can be used in designing a mobile bed contactor only for the specific systems studied and that too

within the limited range of variables covered. To gain further insight and to obtain general correlations for the design, the individual mass-transfer coefficients and interfacial area are needed. The investigations aimed at evaluating these parameters have been reviewed in the following section.

2.3.2 Individual Mass-transfer Coefficients and Interfacial Area

Groeneveld (1967), Kosey et al.(1971), Gel'perin et al. (1972), Rangwala (1973), Wozniak and Østergaard (1972, 1973), Kito et al.(1976a), Wozniak (1977) and Strumillo and Kudra (1977) have made attempts to determine the individual mass-transfer coefficients and the interfacial area using the chemical-absorption method (Danckwerts and Sharma, 1966; Danckwerts, 1970; Charpentier, 1982).

Groeneveld (1967) has used the absorption of oxygen from air into aqueous solution of sodium sulfite with cobaltous sulfate as catalyst. The total interfacial area, a_T , was determined using the relation:

$$\frac{1}{2} V_1 \frac{\Delta C_{SO_3}}{\Delta t} = a_T \left(\frac{2}{3} k_2 D_{O_2} C_{O_2}^* \right)^{0.5} C_{O_2}^* \quad (2.8)$$

subjected to the condition

$$\frac{\left(\frac{2}{3} k_2 D_{O_2} C_{O_2}^*\right)^{0.5}}{k_1} \gg 2 \quad (2.9)$$

where V_1 = volume of sulfite solution, m^3

ΔC_{SO_3} = change in sulfite concentration, $kmol\ m^{-3}$

Δt = change in time, s

a_T = total interfacial area, m^2

k_2 = second-order rate-constant for reaction of oxygen, $m^3\ kmol^{-1}\ s^{-1}$

D_{O_2} = diffusivity of dissolved oxygen in the solution, $m^2\ s^{-1}$

$C_{O_2}^*$ = concentration of dissolved oxygen in equilibrium with gas at the interface, $kmol\ m^{-3}$

k_1 = liquid-film mass-transfer coefficient, $m\ s^{-1}$

Groeneveld has reported that the value of a_T was found to increase with the increase in gas and liquid velocities, but to decrease marginally with the increase in static bed height. A sharp increase in the interfacial area has been reported in the higher range of gas and liquid velocities when the particles congregated below the upper grid. This increase in a_T has been attributed to the change in the liquid holdup which was also found to exhibit a similar trend.

All the other earlier mentioned investigators have used the absorption of carbon dioxide from air into aqueous solution of sodium hydroxide. They have employed 2 to 5 volume percent of carbon dioxide and upto 3N solution of sodium hydroxide.

Gel'perin et al.(1972) have assumed that the liquid and gas-phase mass-transfer coefficients k_l and k_g , respectively could be neglected. In view of this, they determined the interfacial area per unit cross-section of the mobile bed column, A' , using the relation:

$$A' = \frac{(RA')}{n_B C_{CO_2}^* (k_2 D_{CO_2} C_{OH})^{0.5}} \quad (2.10)$$

They have considered the contactor to be composed of two sections viz., the fluidized section and the spray section, and represented A' as

$$A' = A'_f + A'_s \quad (2.11)$$

where A'_f and A'_s are the interfacial areas for the fluidized and spray section, respectively. The interfacial area for the spray section was determined by varying its height under the same operating conditions. They have proposed the following correlations:

$$A'_s = 1.3 \times 10^5 \times U_1^{0.35} U_g^{0.31} (H_T - H) \quad (2.12)$$

$$\text{and} \quad A'_f = A'_b \left[\frac{1.635 \times 10^5 \times f}{A'_b{}^{1.55} U_g^{0.29}} \right] 10^3 \times H_s \quad (2.13)$$

where A'_b is the interfacial area per unit cross-section of the column when operated without the packing particles and is given by

$$A'_b = 58.73 U_1^{0.44} (U_g/f)^{0.92} \quad (2.14)$$

The values of A' estimated using the above correlations were found to be in agreement with the observed values within the error limit of $\pm 15\%$. They have also determined the interfacial area for the absorption of carbon dioxide into aqueous solutions of KOH, LiOH and monoethanolamine, and found that the value of A' was in agreement with the above correlations. In another investigation Gel'perin et al. (1970) determined the interfacial area in a three stage mobile bed contactor of 0.2 m ID, using the absorption of carbon dioxide from synthesis gas (CO_2 10 % by volume) into the aqueous solutions of monoethanolamine. The values of A' for the large size contactor were found to be about 30 % lower than those computed from the above correlations. The deviation has been attributed to the end-and wall-effects,

the higher concentration of carbon dioxide in the gas phase, the monoethanolamine in the liquid phase and the errors due to the extrapolation of physico-chemical data for the elevated temperatures ($\sim 40^\circ\text{C}$).

Wozniak and Østergaard (1972, 1973), Kito et al. (1976a) and Wozniak (1977) have also assumed the liquid-phase mass-transfer coefficient, k_1 , to be negligible, but they have considered the gas-phase resistance. For the determination of the interfacial area and the gas-phase mass-transfer coefficient, they have employed the relation:

$$\frac{P_{\text{CO}_2}}{(R a_{\text{st}})} = \frac{1}{K_g a_{\text{st}}} = \frac{1}{k_g a_{\text{st}}} + \frac{1}{a_{\text{st}} H_{\text{CO}_2} (k_2 D_{\text{CO}_2} C_{\text{OH}})^{0.5}} \quad (2.15)$$

Wozniak and Østergaard (1972, 1973) employed a static bed height of 0.22 m and a gas velocity of 0.7 m s^{-1} and varied the liquid velocity in the range from 0.02 to 0.07 m s^{-1} . They have reported that the interfacial area per unit volume of the static bed, a_{st} , was found to increase with the liquid velocity. It has been stated that the values of interfacial area expressed as per unit volume of the total column were in the same order of magnitude ($1.2 - 3.0 \text{ cm}^2 \text{ cm}^{-3}$) as observed in bubble columns and were little lower than the values obtained

for turbine, paddle and propeller agitators. k_g was found to decrease with the increase in liquid velocity. Its value was in the range of 1×10^{-3} to 4×10^{-3} $\text{kmol KN}^{-1} \text{ks}^{-1}$. In view of the low values of k_g , the authors have concluded that the mobile bed contactor may not be suitable for gas-phase resistance controlled absorption.

Wozniak (1977) has reported that the value of a_{st} (measured on a two-stage mobile bed contactor) was found to increase with the increase in both gas and liquid velocities. They have proposed the following correlation for the interfacial area in terms of dimensionless groups consisting of ΔP , ϵ_g and H :

$$a_p = 6.189 \times 10^{-7} \left[\frac{\epsilon_g}{1-\epsilon_g} \right]^{0.8022} \left[\frac{H \Delta P}{U_g \epsilon_g} \right]^{0.9337} \quad (2.16)$$

The data for $k_g a$ has not been reported, but it has been pointed out that if the mass-transfer resistance in the gas phase is ignored it would lead to an error of 15 to 20 % in the value of interfacial area.

Kito et al. (1976a) kept the liquid flow as 'stagnant' (i.e., no liquid flow) in the mobile bed and the gas was

passed through the bed of particles and the liquid held in the bed. They have reported that at higher gas velocities, the magnitude of $(k_g a_L)$ (where a_L = interfacial area per unit liquid volume) were of the same order as those obtained by Kosev et al.(1977), but smaller than those obtained by Wozniak and Østergaard (1972, 1973). $k_g a_L$ was found to decrease with the increase in gas velocity for $U_g > 2 \text{ m s}^{-1}$. This is in agreement with the observation of Levsh et al.(1968b). The value of a_B was found to increase with the increase in gas velocity upto $U_g = 2 \text{ m s}^{-1}$ and then to decrease. a_B was found to be independent of the free open area of the grid, the static bed height, the column diameter and the size and density of the packing particles. However, it is not clear from this study whether the liquid holdup would be the same both under the liquid-stagnant condition and the liquid flow condition.

Strumillo and Kudra (1977) have emphasized that k_L should not be neglected in the mobile bed contactors. Using the absorption of pure carbon dioxide into sodium hydroxide solution, they have shown that the gas-film resistance was less than 3 % of the total mass-transfer resistance. They have determined the interfacial area,

A' , and the surface renewal rate, s , using the Danckwerts' plot, which is based on the relation:

$$(RA' / C_{CO_2}^*)^2 = (A')^2 D_{CO_2} (k_2 C_{OH} + s) \quad (2.17)$$

They have reported that the value of A' was found to increase with the increase in liquid velocity but to decrease with the increase in size of the packing particles. A' exhibited a maxima with the gas velocity and the static bed height. The decrease in A' with the gas velocity ($U_g > 3 \text{ m s}^{-1}$) and the static bed height ($H_s > 0.12 \text{ m}$) has been attributed to the inhomogeneity in the bed occurred at higher gas velocities and static bed heights. The following correlation for A' has been proposed:

$$A' = 16.25 U_g^{0.92} U_l^{0.34} H_s^{0.83} d_p^{-0.94} \quad (2.18)$$

for $U_g \leq 3 \text{ m s}^{-1}$ and $H_s \leq 0.12 \text{ m}$

The data for surface renewal rate has not been reported but it has been indicated that the surface renewal rate was comparable with the pseudo-first order chemical reaction rate-constant $k_1 (= k_2 C_{OH})$.

CHAPTER 3

EXPERIMENTAL SET-UP AND MEASUREMENT TECHNIQUES

In this chapter, the details of the experimental set-up and measurement techniques employed for the studies on hydrodynamics, axial mixing and mass transfer in mobile bed contactor have been presented.

3.1 EXPERIMENTAL SET-UP

It consisted of a mobile bed contactor, a blower and a liquid feed pump, tracer injection and monitoring systems, sampling and recording devices. A schematic diagram of the experimental set-up is shown in Figure 3.1.

3.1.1 Mobile Bed Contactor

The mobile bed contactor was designed to carry out studies on hydrodynamics, axial mixing and mass-transfer. The main test section (E) was a, 0.15 m ID and 1.1 m long, cylindrical glass column. The bottom section (F) was a, 0.3 m ID and 1.0 m long, mild steel cylindrical section. It was provided with a gas inlet, a liquid outlet, a liquid level indicator, a gas-liquid disengager (G), a conductivity cell (H) and a pressure tap. A corrugated conical baffle was used to facilitate smooth disengaging

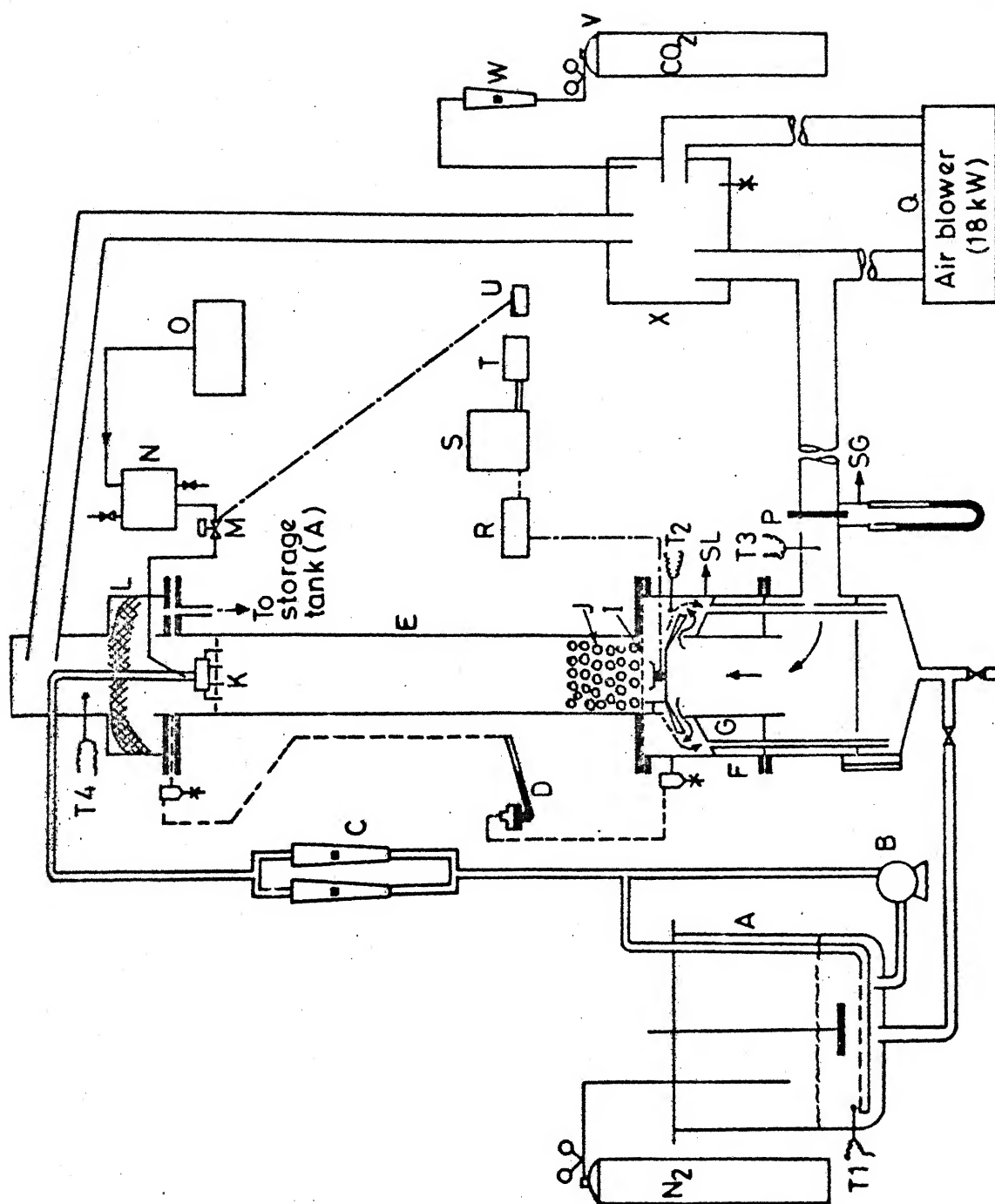


**Fig. 3.1 Schematic diagram of the experimental set-up.
(Legend on page 45)**

Legend for Figure 3.1

A - liquid storage tank
B - centrifugal pump
C - rotameters
D - inclined manometer
E - mobile bed column
F - bottom section
G - gas-liquid disengager
H - conductivity cell
I - bottom supporting grid
J - packing particles
K - liquid distributor
L - top section
M - solenoid valve
N - tracer-reservoir
O - air-compressor
P - orifice meter

Q - air-blower
R - conductivity meter
S - automatic data acquisition system
T - desktop computer
U - microswitch
V - CO₂ gas cylinder
W - rotameter
X - mixing tank

Sampling points

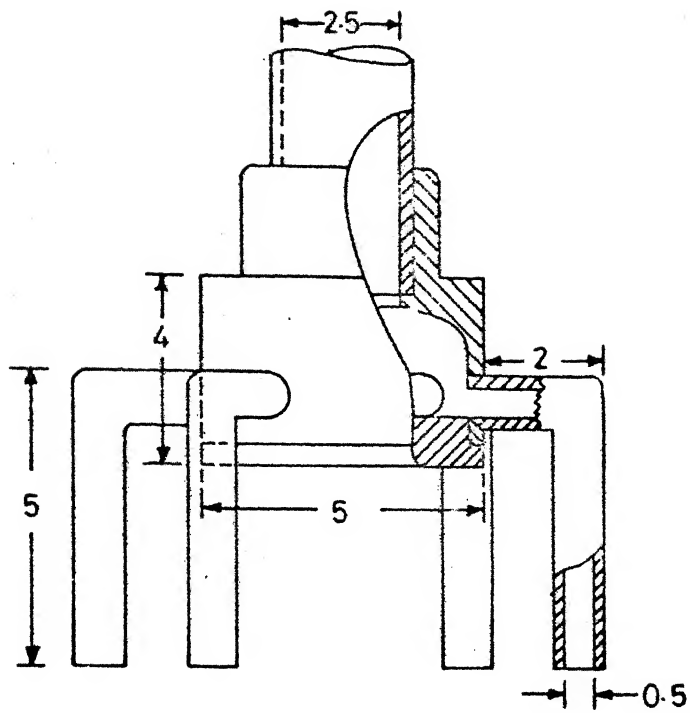
SL - for liquid sample
SG - for gas sample

Temperature monitoring points

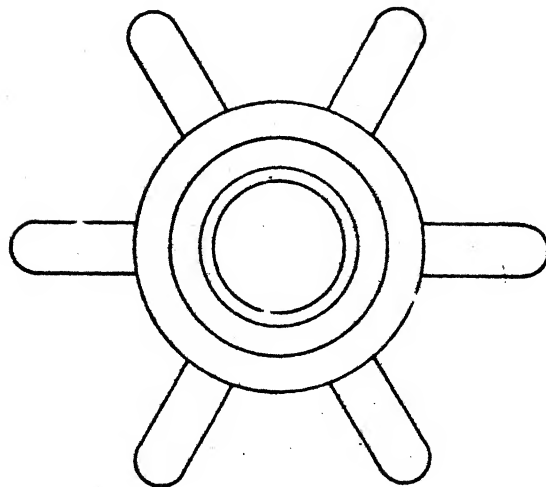
T1 - inlet liquid stream
T2 - outlet liquid stream
T3 - inlet gas stream
T4 - outlet gas stream

of gas and liquid without splashing. A stainless steel wire mesh with square openings (each of dimension 0.0055×0.0055 m) was used as the bottom supporting grid (I). The free open area of the grid was found to be 70 % and its characteristic factor, $(f \frac{d}{D})$ to be 0.028. The top section (L) was a 0.3 m ID and 0.25 m long perspex column. The upper portion of this was packed with 0.05 m thick layers of fine stainless steel wire meshes to serve as entrainment separator. An upper grid and a liquid distributor (K) with provision for tracer injection were fitted in the top section.

A sketch of the liquid distributor is shown in Figure 3.2. It was a 0.05 m ID and 0.04 m long teflon cylindrical section having six "L" - shaped plastic nozzles, each of 0.005 m ID. In order to avoid the dispersion of the liquid before it reaches the upper surface of the expanded bed, a rod-like flow of liquid through the nozzles was ensured by attaching 0.005 m ID and 0.03 m long plastic tubes to these nozzles. Prior to fixing the distributor in the set-up, uniform liquid flow distribution through each of these nozzles was ensured by proper adjustment of the projection of the nozzles into the cylindrical section. The flow distribution pattern for different liquid flow rates is given in Table 3.1.



Front view



Top view

(all dimensions in cm)

Fig. 3.2-Sketch of the liquid distributor.

TABLE 3.1

LIQUID FLOW DISTRIBUTION PATTERN THROUGH NOZZLES OF DISTRIBUTOR

Liquid flow cc s ⁻¹	Flow through nozzles, cc s ⁻¹						Net flow through six nozzles, cc s ⁻¹
	1	2	3	4	5	6	
80	13.2	13.2	13.2	14.2	12.4	13.2	79.4
300	47.6	47.6	47.6	51.7	47.6	47.6	289.7
600	101.0	97.0	96.5	104.5	97.0	98.5	594.5
800	133.4	131.6	133.4	131.6	133.0	131.6	794.6

Air was supplied to the mobile bed contactor by a twin lobe water cooled blower (Q) (18 kW; SLM-MANEKIAL Industries Ltd., Type RP-40). The flow rate of air was measured using an orifice meter (P). It was a 0.025 m diameter, sharp-edged orifice made of stainless steel and located in a 0.8 m ID pipe. This orifice meter was designed as per the specifications recommended in Chemical Engineers' Handbook (Perry and Chilton, 1973). The pressure drop across the orifice was measured using a manometer with carbon tetrachloride as the manometric fluid, and at very high gas flow rates with mercury as the fluid.

A centrifugal pump (B) was used to circulate the liquid and its flow rate was measured by means of two calibrated rotameters (C).

The pressure drop across the mobile bed was measured by means of an inclined manometer (D) with water as the manometric fluid.

3.1.2 Tracer Injection System

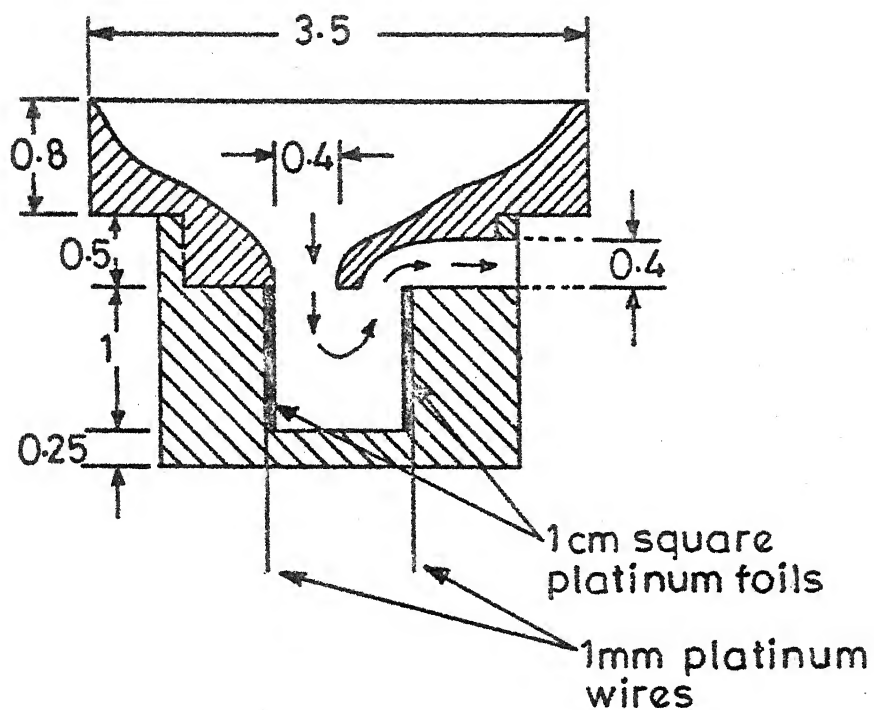
For the injection of tracer, a 1.5 mm ID teflon capillary tube was connected to the liquid inlet just above the distributor as shown in Figure 3.1. The tracer

injection system consisted of an air-compressor (O), a stainless steel reservoir (N) for tracer and a solenoid valve (M) coupled with a microswitch (U).

3.1.3 Tracer Monitoring System

The tracer monitoring system consisted of an electrical conductivity cell (H), a conductivity meter (R) (SYSTRONICS, DRCM; type-303), an automatic data acquisition system (S) (HEWLETT PACKARD, Model 3052A) and a desktop computer (T) (HEWLETT PACKARD, Model 9825A).

The electrical conductivity cell (H) was located in the mobile bed contactor about 0.03 m below the center of the bottom grid and was mounted on the corrugated conical baffle. A drawing of the conductivity cell is given in Figure 3.3. Its construction was similar to the one used by Dunn et al. (1977) for the axial dispersion studies on a packed bed column. The funnel-shaped top portion of the cell collected the liquid sample and drained it to the lower portion of 1 cm ID and 1 cm long cylindrical bore in which two platinum foils (each of 0.01 x 0.01 m square cross-section) were embedded on the wall opposite to each other. After passing through the space in between the platinum foils, the liquid left the



(all dimensions in cm)
Material -Teflon

Fig.3.3 - Cross-sectional drawing of the conductivity cell.

cell through the side port located just above the bore. The two platinum foils (working as electrodes) were connected to the input terminals of the conductivity meter. The output from the conductivity meter was fed to the data acquisition system.

3.1.4 Modification for Mass Transfer Studies

For mass transfer studies, both the gas (CO_2 + air mixture) and the liquid (NaOH solution) streams were recycled in order to minimise the consumption of the reagents. The recycling of the gas also ensured that the air entering the mobile bed was saturated with water vapor, which otherwise would have interfered with the absorption of CO_2 into the solution. Similar recycling of the gas and the liquid streams has been employed by Porter et al.(1966) and Pohorecki (1975,1976). Carbon dioxide was fed from a CO_2 gas cylinder (V) to the mixing tank (X) located in the gas loop where it was mixed with the recirculating gas. The feed rate of carbon dioxide was measured using a ~~calibrated~~ rotameter (W).

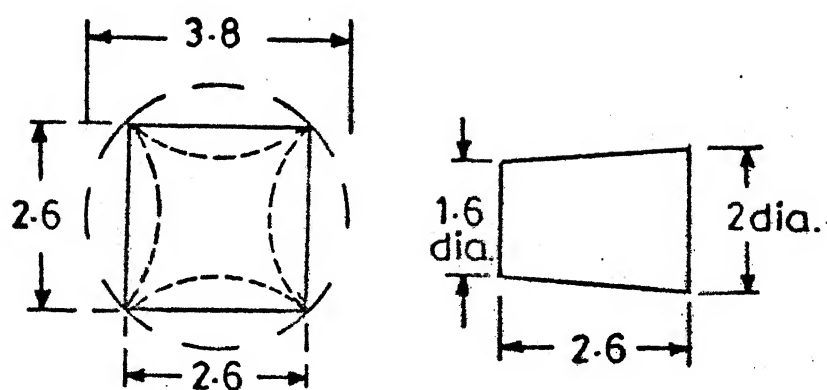
The CO_2 -gas regulator and the cylinder valve were heated using a heating tape to ensure free flow of carbon dioxide which otherwise was found to stop due to the solidification of carbon dioxide in the regulator.

During a mass-transfer run the complete mixing of NaOH solution in the storage tank (A) was ensured by having a stirrer. In addition to this the bypass from the pump was fed uniformly into the tank using a 2 m long perforated polyethylene tube immersed into NaOH solution. In order to prevent the absorption of CO_2 from the atmospheric air by NaOH solution, a blanket of nitrogen was provided by introducing the gas just above the solution throughout the run.

The liquid samples were drawn from the bottom section just below the grid. The gas samples were drawn from the high pressure point of the orifice meter. These sampling points SL and SG, are shown in Figure 3.1. Temperatures of liquid and gas streams at inlet and outlet points (T1, T2, T3 and T4 as shown in Figure 3.1) were measured with a multi-point temperature indicator (ALNOR, Type 1200-8) with an accuracy of $\pm 0.5^\circ\text{C}$.

3.2 PACKING PARTICLES

Hollow spherical and irregular shaped polyethylene particles and tapered cork particles were used for the hydrodynamic and axial mixing studies. Sketches of irregular and cork particles are shown in Figure 3.4. The



Irregular particle

Cork particle

(all dimensions in cm)

Fig.3.4 - Sketches of a irregular and a cork particle.

irregular shaped particles were made from spherical particles (0.038 m diameter; $\rho_p = 53 \text{ kg m}^{-3}$) in the following manner. A pinhole was made in the particle and then it was squeezed from the four sides as shown in Figure 3.4. After getting the desired shape, the pinhole was closed with "araldite", an epoxy resin.

To check whether the cork particles were getting soaked with water during a run, the difference in weights, before and after soaking the cork particles in water for 48 hours, was measured. It was found that the difference was negligible. A preliminary test was also performed to detect any adsorption of the dilute NaCl-solution on to the surface of the cork particles. For this purpose, some dry cork particles were placed in a beaker and were covered with 0.2 N solution of sodium chloride. The particles were allowed to soak with the solution for 48 hours, and then any change in the concentration of the NaCl solution was measured and was found to be negligible.

For the mass transfer studies, two types of spherical particles of same size but of densities 53 and 148 kg m^{-3} , respectively were used. The irregular particles could not be used as it was observed in the preliminary runs that the particles got filled with the liquid because the araldite used to fill the pinhole came off due to the

action of hot sodium hydroxide solution. The cork particles also could not be used because they reacted with sodium hydroxide solution. The characteristics of the particles used in different studies are given in Table 3.2.

3.3 EXPERIMENTAL PROCEDURE

3.3.1 Tracer Monitoring Technique

The emf vs concentration of NaCl in tap water was determined at 25°C, 30°C and 35°C. It was found that the plots of emf vs concentration were linear. A typical plot is shown in Figure 3.5. The linear relationship was used in computing the normalised concentration $\frac{C}{C_0}$ directly from the emf measured with the data acquisition system.

The suitability of pulse-and step-input of tracer injection was examined in a number of preliminary runs. In the case of pulse-input, the errors were found to be large since the residence time of the liquid phase in the bed was only 2 to 7 s. Hence the step-response technique was selected. Nearly saturated NaCl solution was used as tracer. Its flow rate was less than 2 % of the liquid flow rate through the bed. Depending upon

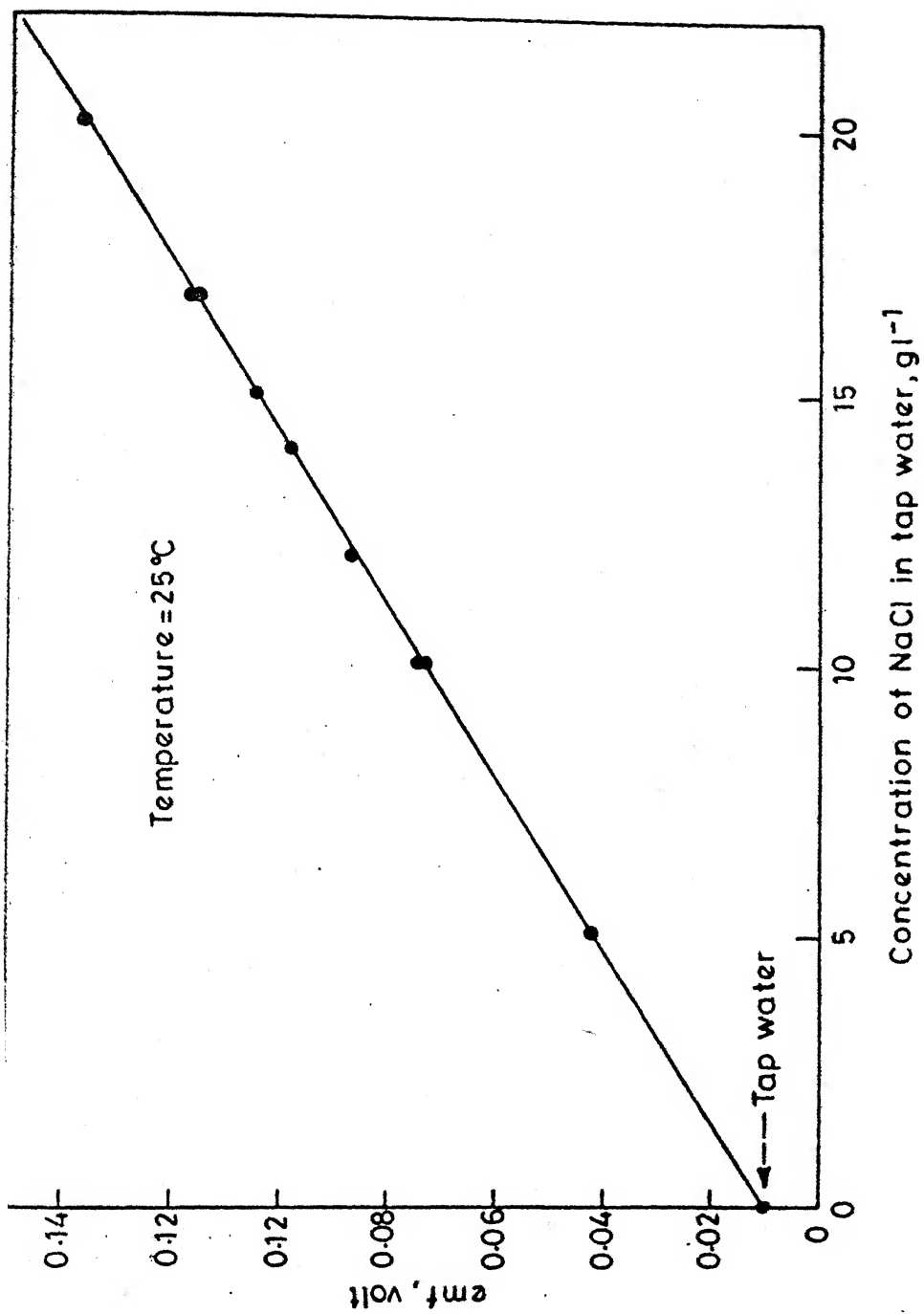


Fig.3.5 - A typical plot of concentration of NaCl in tap water versus emf recorded by data acquisition system.

TABLE 3.2

CHARACTERISTICS OF PARTICLES

characteristics	For hydrodynamic and axial mixing studies			For mass transfer studies	
Particle	Spherical	Irregular	Cork	Spherical	Spherical
d_p	0.038	0.0312	0.0237	0.038	0.038
ϕ_s	1	0.675	0.822	1	1
β_p	53	112	183	53	148
ϵ_{sp}	0.475	0.470	0.480	0.475	0.475
η_p	40	66	175	40	40

the average residence time, the sampling rate of the concentration was adjusted between 14 to 20 readings per second. It may be recalled that the step-response technique has been used also by Chen and Douglas (1969) and Koval et al.(1975b).

3.3.2 Determination of Delay Time of Tracer Injection

Ideally the tracer should be injected just above the top layer of the mobile bed and its detection just at the supporting grid. It was not possible physically to follow such a procedure due to the fluctuations in the bed height. Hence, the delay time, caused by the end effects resulting due to the fixed positions of the tracer injection, was accounted in the following manner. The average residence time of the liquid phase was determined for the empty column with supporting grid for three different spacings between the distributor and the grid viz. 0.3, 0.7 and 1.1 m and for liquid flow rates ranging from 0.011 to 0.044 m s⁻¹. Five to eight breakthrough curves were obtained for each set of spacing and liquid flow rate. A plot of average residence time versus spacing with liquid flow rate as a parameter is shown in Figure 3.6. The delay time of the liquid phase for a given bed expansion was determined using this figure. In

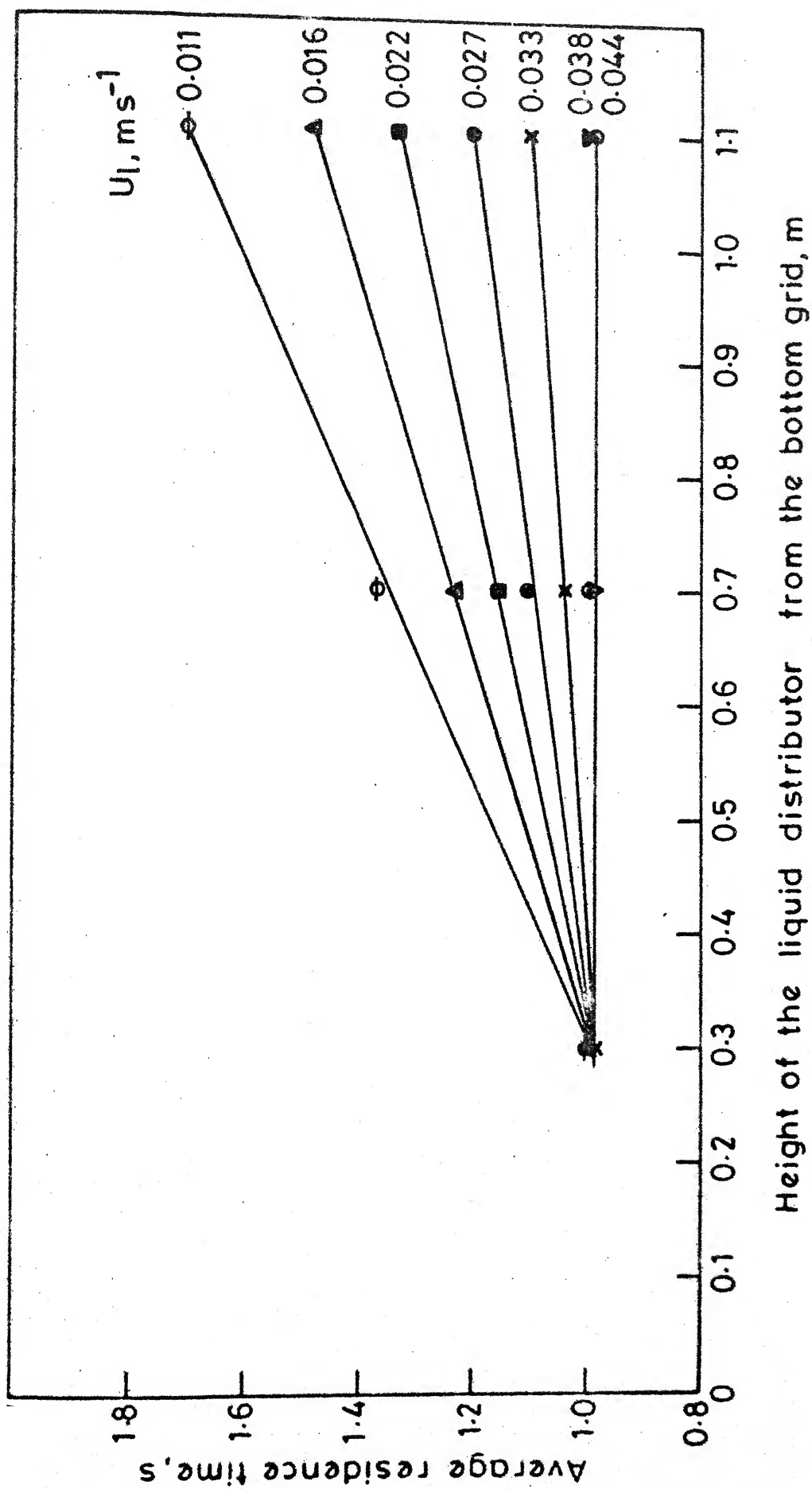


Fig.3.6 - Average residence time of the liquid flow with respect to height through empty column (without gas flow).

all the runs the breakthrough curves ($\frac{C}{C_0}$ vs t) were observed to be nearly vertical lines indicating the plug flow behaviour of the liquid phase through the empty column. A similar method for determination of delay time has been used by Schiesser and Lapidus (1961) for the packed beds.

3.3.3 Bed Expansion, Pressure Drop and Minimum Fluidization Velocity

The measurements were made after operating the bed for a minimum period of 15 min to allow the transients to die down. The height of the mobile bed fluctuated widely and as a consequence the level in the inclined manometer also fluctuated. The movement of the top surface of the bed was observed for a period of 5 min and the most frequently occurring maximum and minimum values were recorded. The average of these were taken as the expanded bed height. The manometer readings were also recorded in a similar manner. The minimum fluidization velocity was determined by extrapolating the plot, H/H_s vs U_g , to $H/H_s = 1$.

3.3.4 Breakthrough Curves

Once the above measurements were made for a given static bed height and for different values of gas and

liquid velocities, then based on the visual observations, gas velocities were chosen so as to cover evenly the range of velocities from minimum fluidization to congregation of particles below the upper grid for the determination of the breakthrough curves.

Before injecting the tracer, the emf for the tap water was monitored for 30 s. The injection and detection of tracer were started simultaneously by switching on, at a stroke, both the microswitch to activate the solenoid valve and the 'RUN-Key' of the computer. The measurement was continued till the data-acquisition system displayed fairly constant values over a period of 10 s. A typical experimental breakthrough curve obtained for the cork particles is shown in Figure 3.7. The processing of the data was immediately performed after eliminating the number of initial readings corresponding to the delay time for the observed expanded bed height.

The experimental breakthrough curves could be analysed on the basis of the single parameter axial dispersion model considering the mobile bed as a closed-closed system. This has been discussed in detail in section 4.1.1 of Chapter 4. The average residence time, liquid holdup, variance, Peclet number and axial

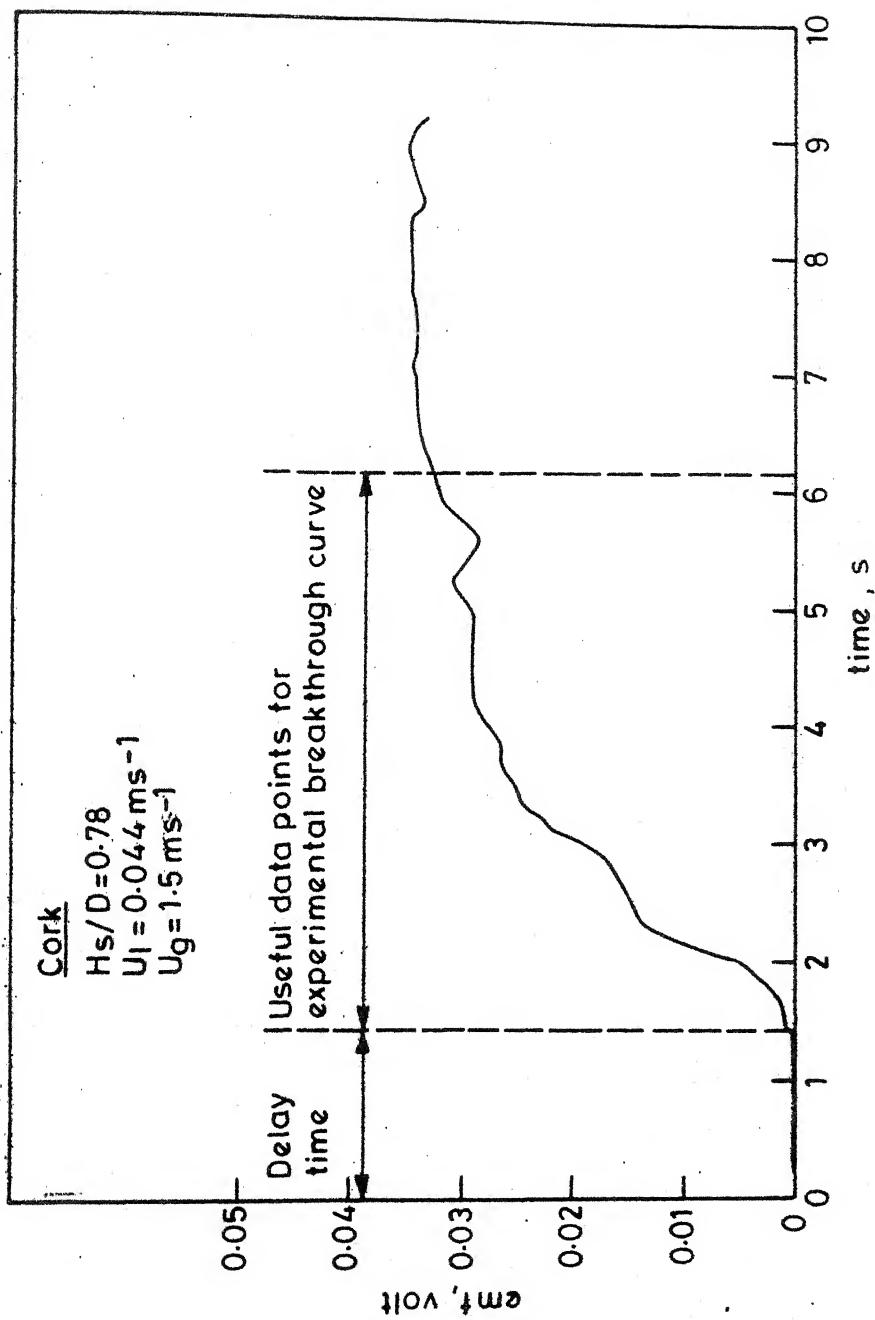


Fig. 3.7 A typical plot of emf versus time for the cork particles.

dispersion coefficient were evaluated using the relations given in Table 3.3. Five to ten breakthrough curves were obtained for each run depending on the fluctuations in the values of average residence time and Peclet number.

3.3.5 Range of Variables Covered in Hydrodynamic and Axial Mixing Studies

System	: Air-water
Static bed height	: 0.12, 0.24, 0.36, 0.48 m
Liquid velocity	: 0.011 - 0.044 m s ⁻¹
Gas velocity	: 0 - 5 m s ⁻¹

3.3.6 Mass Transfer Measurements

A known volume of 2N NaOH solution, prepared using distilled water, was charged into the storage tank. First air was circulated through the closed loop. In the beginning, the temperature of air rose rapidly above the ambient by about 15°C. Then the solution was circulated through the bed at the desired rate. After a while both solution and air attained steady state temperatures. At this stage, carbon dioxide was fed into the loop till its composition reached to 2 - 4 %. Then the feed rate of carbon dioxide was readjusted to a lower

TABLE 3.3

RELATIONS EMPLOYED FOR THE EVALUATION OF AVERAGE RESIDENCE
TIME, LIQUID HOLDUP, PECLET NUMBER AND AXIAL DISPERSION
COEFFICIENT FROM EXPERIMENTAL BREAKTHROUGH CURVES

Function	Relation
Normalised step-input response curve, F	$F = \frac{C}{C_0}$ versus t
Normalised pulse-input response curve, E	$E = \frac{dF}{dt}$ for closed-closed system (Levenspiel, 1972)
First moment, μ_t	$\mu_t = \int_0^{\infty} t E dt$
Average residence time, θ	$\theta = \frac{\mu_t}{t}$
Liquid holdup, h_1	$h_1 = \theta U_1$
Second moment, δ_t^2	$\delta_t^2 = \int_0^{\infty} t^2 E dt - \frac{\mu_t^2}{t}$
Variance, σ^2	$\sigma^2 = \delta_t^2 / \theta^2$
Peclet number, Pe	$\sigma^2 = \frac{2}{Pe} - \frac{2}{Pe^2} (1 - \exp(-Pe))$ for closed-closed system (Levenspiel, 1972)
Axial dispersion coefficient, D_L	$Pe = \frac{\bar{U} H}{D_L}$ where $\bar{U} = H/\theta$

value (based on the preliminary runs) and it was kept constant throughout the run. The measurements of gas and liquid compositions and temperatures were made at 10 min intervals. Thus an experimental run was completed in about 2 hours depending upon the final concentration of sodium hydroxide in the solution.

3.3.7 Methods of Analysis

The liquid samples were analyzed by the double titration technique using hydrochloric acid as the reagent and phenolphthalein and methyl orange as indicators (Vogel, 1961; Shapiro, 1972). All titrations were carried out in carbon dioxide free atmosphere. During sampling, storage and titration care was taken to prevent absorption of carbon dioxide from atmosphere.

The gas samples were analyzed using NaOH solution with the aid of an Orsat-type analyzer. The details of the analyzer and the method of analysis have been given in Appendix A.

3.3.8 Range of Variables Covered in Mass Transfer Studies

Chemical system	: Air + CO ₂ - NaOH solution
Static bed height	: 0.24 m
Liquid velocity	: 0.022, 0.033, 0.0411 m s ⁻¹
Gas velocity	: 0.5 - 2.75 m s ⁻¹
% CO ₂ in gas-phase	: 2 - 6 %
NaOH concentration	: 2N
Temperature	: 30 - 45 °C

CHAPTER 4

RESULTS AND DISCUSSION

In this chapter, the results of the studies on hydrodynamics, axial mixing and mass transfer have been presented.

4.1 HYDRODYNAMICS4.1.1 Bed Behaviour-Visual Observations

The transition from static bed to mobile bed was observed to be gradual as reported by Balabekov et al. (1969a, 1969b) and Tichy et al. (1972). The top surface of the mobile bed, though it was not flat, could be distinguished clearly. Only in the cases of $H_s/D = 2.4$ and 3.2 and that too at low gas velocities slugging of the bed was observed. In other cases smooth fluidization characterised by random motion of individual particles was observed. However, the magnitude of fluctuations increased gradually as the gas velocity increased.

During an otherwise normal fluidization it was observed that the particles started lining up at the wall. Once a single particle layer was set on the grid around the wall, subsequent stacking of the remaining particles as one layer over the other took place within a minute.

This sort of monolayer stacking of the particles will be, hereafter, referred as "congregation at the wall". The only other investigators to report the occurrence of such phenomenon are Tichy et al.(1972).

This phenomenon was observed with the spherical and irregular particles for H_s/D equal to 1.6, 2.4 and 3.2. But, in the case of cork particles it was observed even for $H_s/D = 0.78$. The maps of the regions, in which congregation at the wall was observed, are depicted in Figure 4.1. In the case of spherical particles the congregation was seen to form and break off on its own, but in the case of irregular and cork particles once formed it remained intact. This could be attributed to the greater force of adhesion of the particles to the wall. This force of adhesion, which arises as a result of the interfacial tension, is proportional to the circumference of the liquid bridge formed between the particles and the wall and it was more in the case of irregular particles. Interestingly enough, the formation of congregation was observed even for dry irregular and cork particles. It can be seen from Figure 4.1 that the congregation of dry particles is more pronounced in the case of irregular particles.

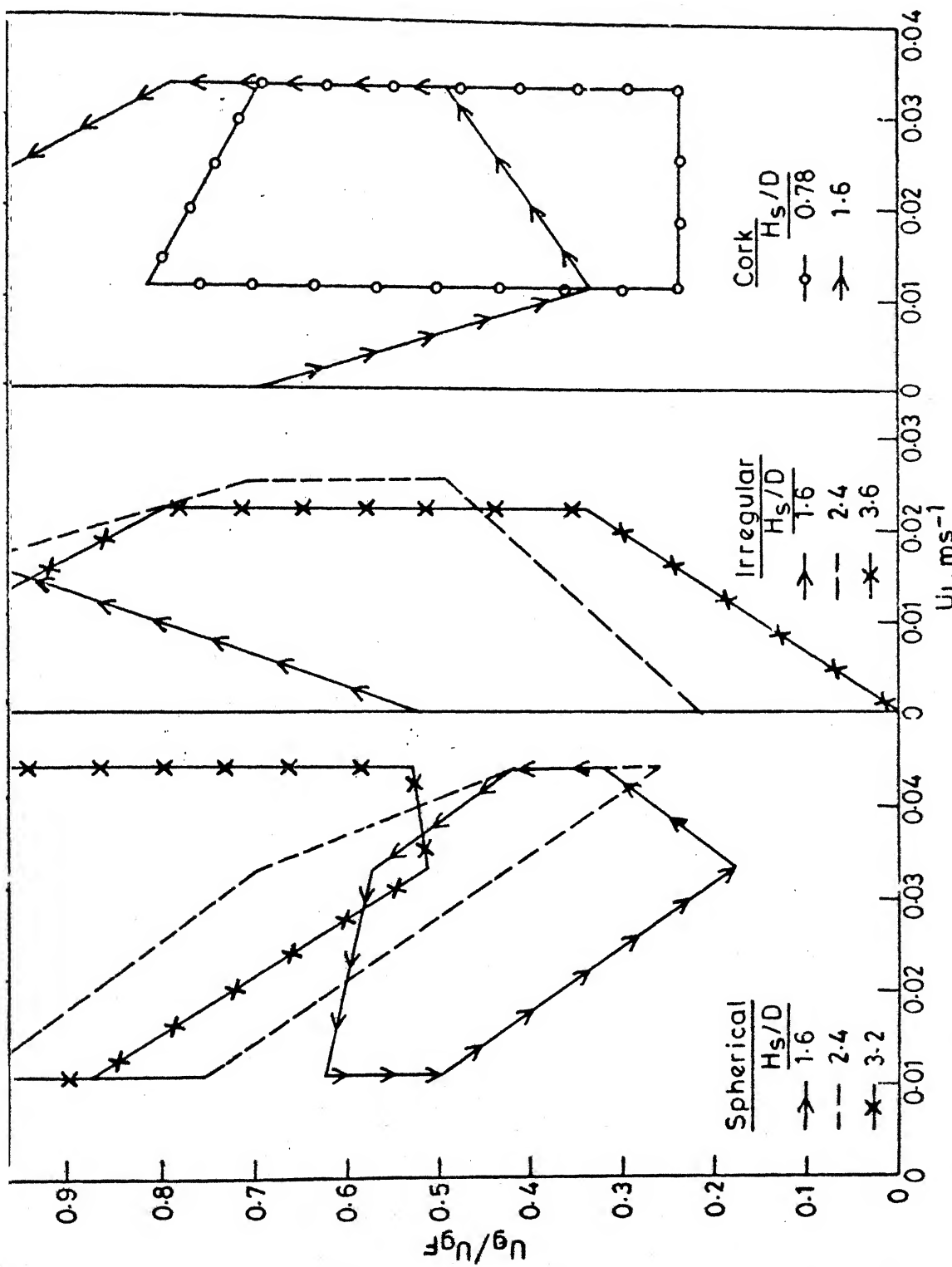


Fig. 4.1 - Maps depicting the regions of congregation at the wall.

Since the contact area is more for these particles, greater stability of support is provided by one layer of particles to the next layer.

As expected, the pressure drop and the liquid holdup decreased drastically once the congregation was formed as the gas and the liquid passed through the particle-free core. Whenever the congregation took place during a run, it was broken by sudden increase in liquid flow rate and then the flow rate was reset to the previous value. This resulted in apparent smooth fluidization though in some cases persistent tendency to form congregation in the lower half of the bed was seen. In the regions depicted in Figure 4.1, several breakthrough curves could be taken before the congregation took place again. In the case of cork particles for $H_g/D = 2.4$ and 3.2, frequent congregation did not permit the measurements.

4.1.2 Liquid Holdup and Pressure Drop

As a consequence of the bed height fluctuations the measured liquid holdup was found to be fluctuating. It may be expected because the average residence time of the tracer was about the same magnitude as that of the average 'cycle' time of the bed height fluctuations.

Hence, for each run 5 to 10 measurements of liquid holdup were taken depending on the nature of fluctuations and the average values are reported. The percent standard deviation of the liquid holdup ranged from 5 to 20 %.

The plots of measured liquid holdup versus gas velocity with liquid velocity as a parameter are given in Figures 4.2 through 4.5. It was observed that h_l increased with the increase in U_l and H_s . It has been found to be independent of U_g for $H_s/D = 0.78$ except in the case of spherical particles where it increased linearly with U_g . Similar trends have been reported also by Groeneveld (1967) whose experimental conditions were close to those under discussion. For the other H_s/D values, h_l was found to be nearly independent of U_g for $U_l = 0.011 \text{ m s}^{-1}$, but for $U_l > 0.011 \text{ m s}^{-1}$ its dependence on U_g did not exhibit a definite trend as can be seen from Figures 4.3 through 4.5. It may be due to the inherent tendency of the particles to congregate at the wall.

The total pressure drop was found to be independent of U_g in all the cases. Typical plots are shown in Figure 4.6.

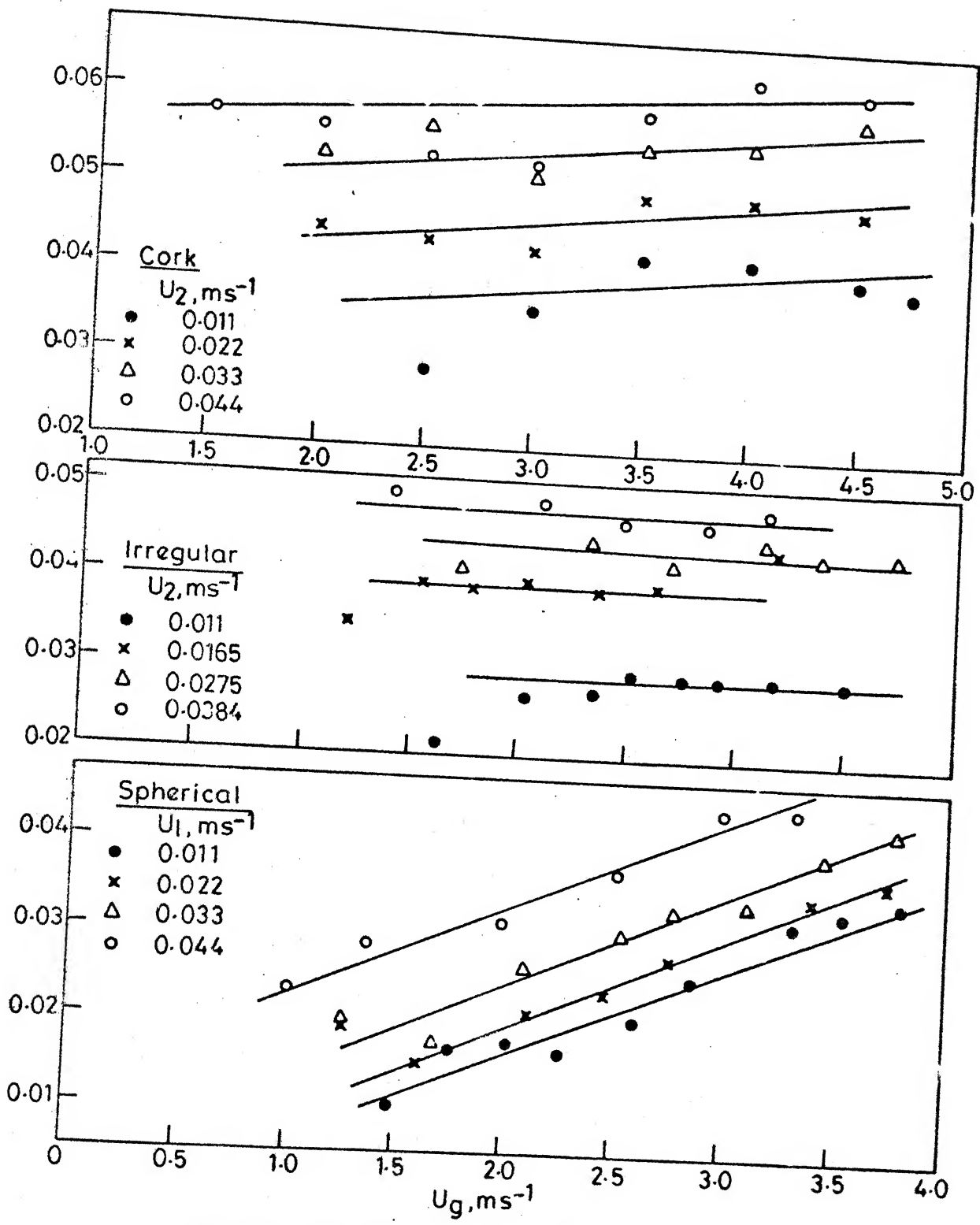


Fig.4.2 - h_l versus U_g for $H_s/D = 0.78$.

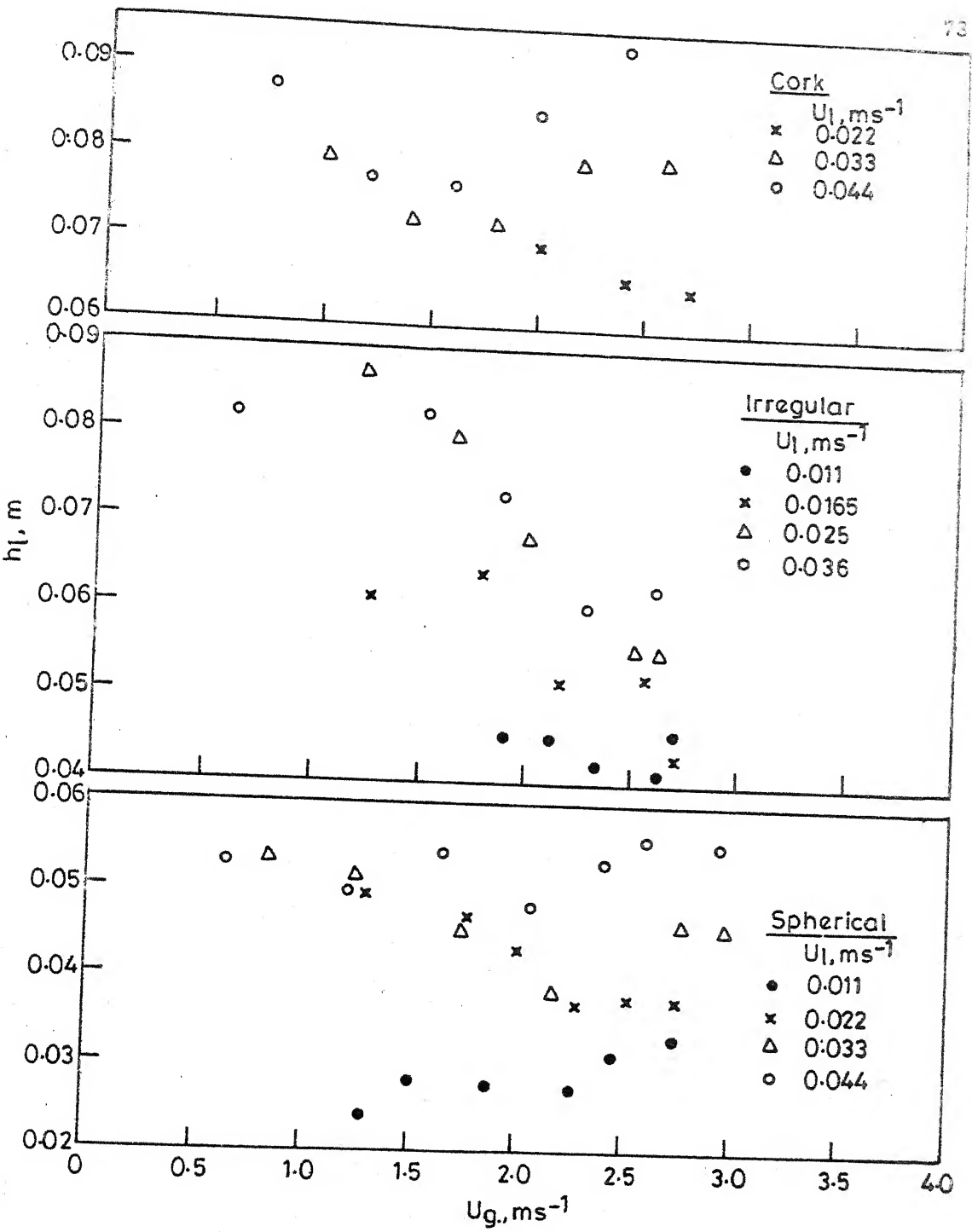


Fig.4.3 - h_l versus U_g for $H_s/D=1.6$.

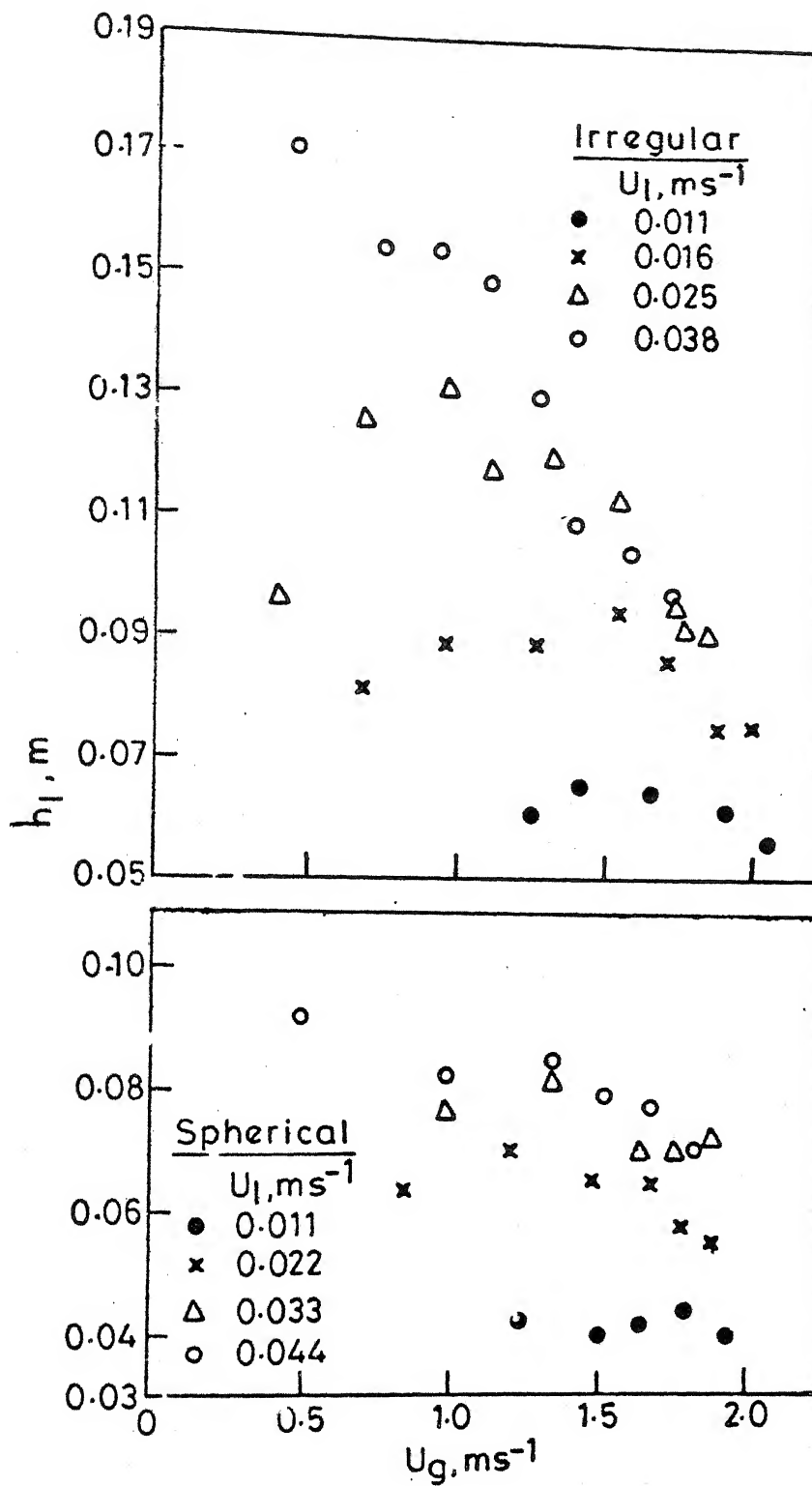


Fig.4.4 - h_1 versus U_g for $H_s/D = 2.4$.

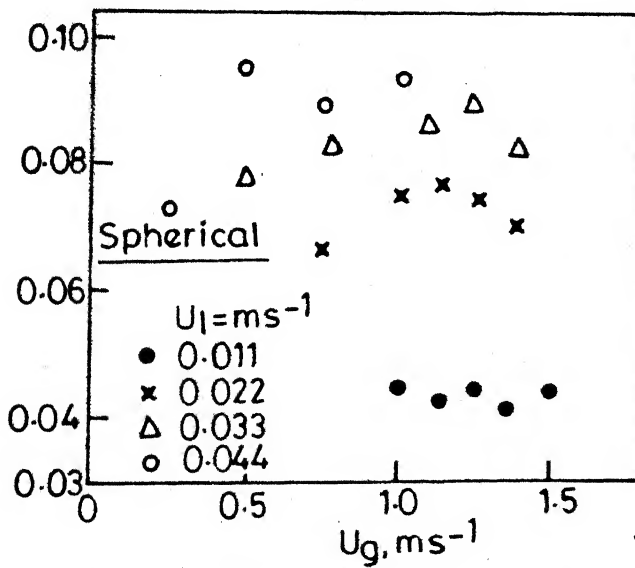
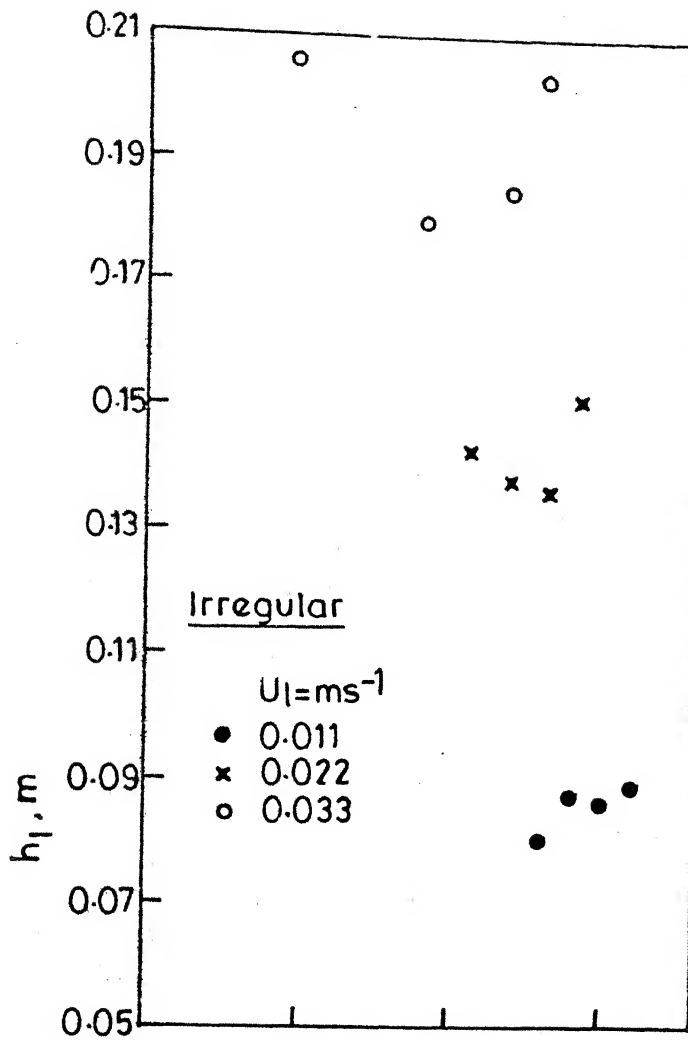


Fig. 4.5 - h_1 versus U_g for $H_s/D=3.2$.

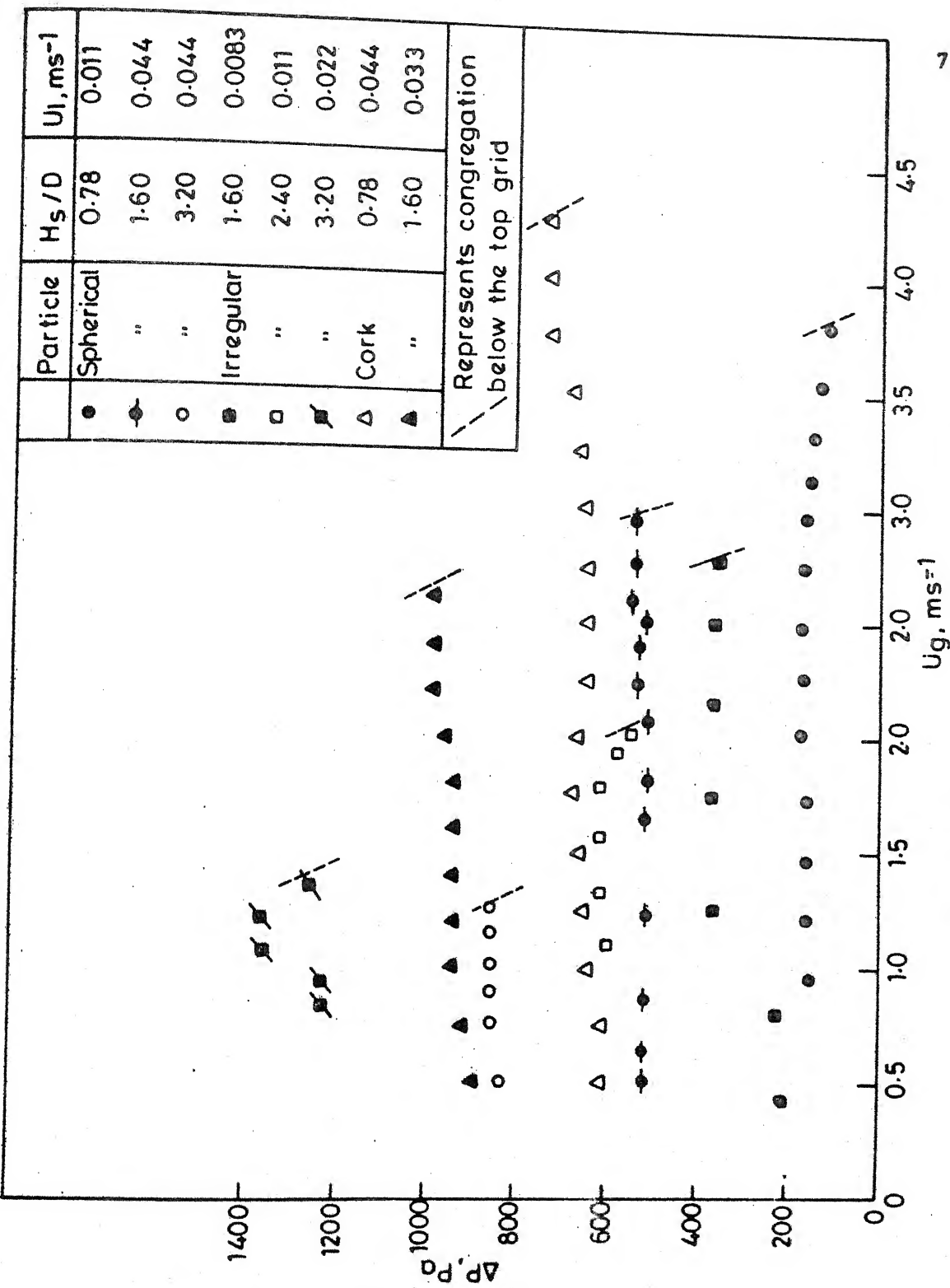


Fig.4.6 - Typical plots of ΔP versus U_g .

It has been generally assumed (for instance Kito et al., 1976b) that the liquid holdup in the bed is fully supported by the upward flow of gas like in conventional fluidized beds, and that it can be evaluated from the pressure drop measurement by the relation:

$$\Delta P_{1B} = \Delta P - \Delta P_p \quad (4.1)$$

For the sake of comparison of ΔP_{1B} with $h_1 \Delta P_{1B}$ was evaluated in terms of height of water and has been denoted by $\Delta P'_{1B}$. In the case of spherical particles for $H_s/D = 0.78$ and $U_1 = 0.011 \text{ m s}^{-1}$, the ratio $\Delta P'_{1B}/h_1$ was found to decrease from 0.9 to 0.22 with an increase in gas velocity. An analysis of the data of Groeneveld (1967) (under similar conditions) revealed that h_1 is about 4 to 5 times $\Delta P'_{1B}$. For other bed conditions, the ratio $\Delta P'_{1B}/h_1$ was observed to vary between 1.0 and 0.6. The ratio tended to 1.0 at high liquid flow rates and for low static bed heights.

Kito and co-workers (1976c, 1978) have measured and proposed correlations for $\Delta P'_{1B}$ and h_1 . The ratio $\Delta P'_{1B}/h_1$ computed from these correlations is found to vary between 0.97 and 0.7 for different sizes and densities of particles and for $H_s/D = 1$. It may be recalled that Vuković et al. (1974), who have reported

the experimental data on the pressure drop and the liquid holdup in a three-phase spouted bed, have observed that only a part of the liquid holdup is "supported" by upward flow of the gas. They analysed also the data of Chen and Douglas (1968) and showed that the ratio is between 0.85 and 0.95 even for the mobile bed.

From the above discussion it is clear that only a part of the liquid held in the bed is supported by upward flow of the gas while the rest is under free fall.

4.1.3 Correlations for h_L and $\Delta P'_{LB}$

The liquid holdup correlation proposed by Kito et al. (1978) appears to be general as it covers a wide range of variables and could fit the data of several other investigators. The functional form of this correlation was adapted to correlate the data of h_L and $\Delta P'_{LB}$. To make an account for the shape of the particles, d_p was replaced by $d_p \phi_s$ in the Kito-Tabei-Murata correlation. The correlations for the data of h_L and $\Delta P'_{LB}$ are shown in Figures 4.7 and 4.8. It may be pointed out that each point in Figure 4.7 is an average of the values measured at different gas velocities at a constant value of U_L . It can be seen from this figure that the data of h_L fell above the line representing Kito et al. correlation. Interestingly enough,

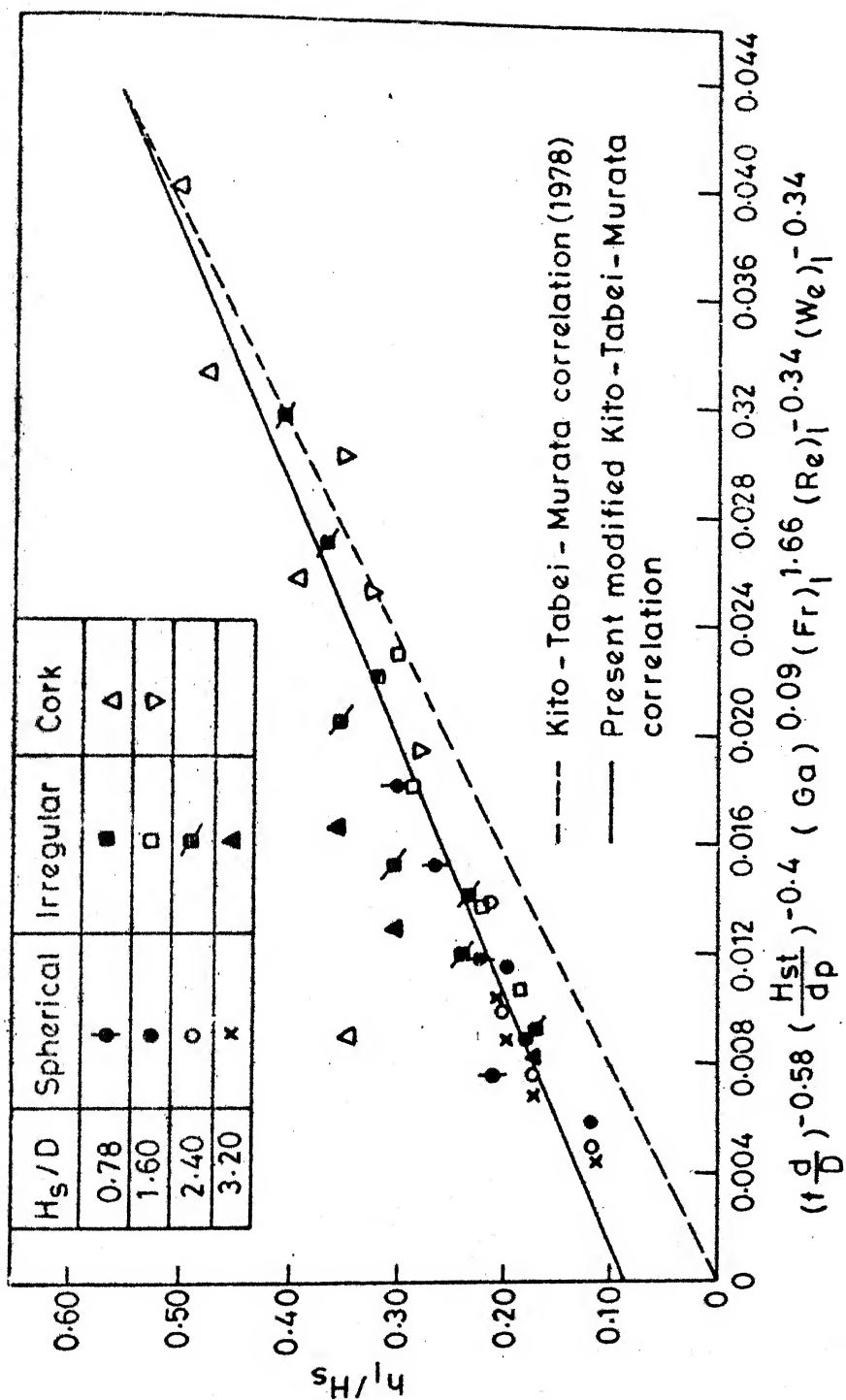


Fig. 4.7 - Comparison of data of h_1 with Kito-Tabei-Murata correlation.

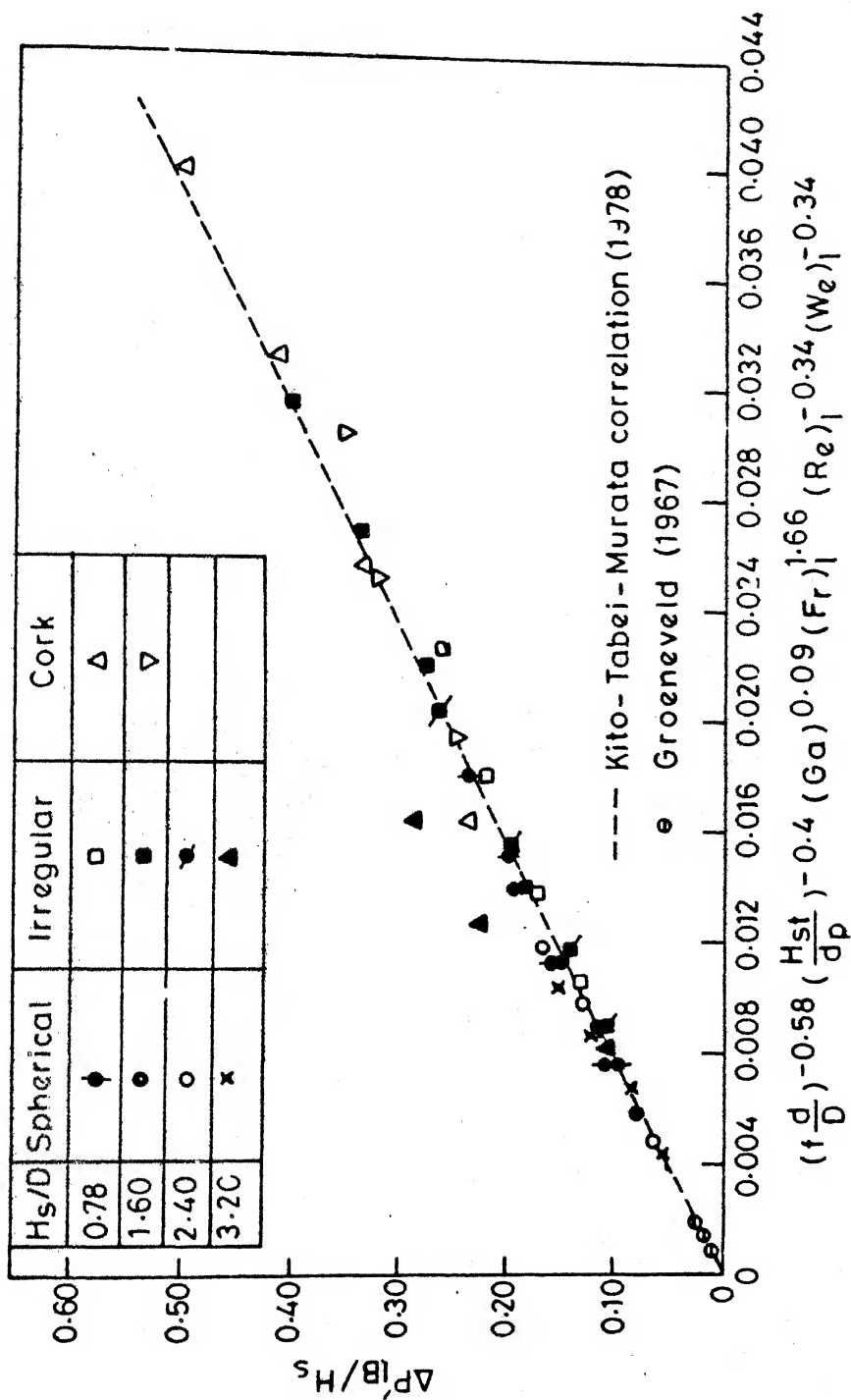


Fig. 4-8-Comparison of data of $\Delta P'_{IB}$ with Kito-Tabei-Murata correlation.

the correlation gave a good fit to the data of $\Delta P'_{LB}$ (see Figure 4.8). The modified Kito-Tabei-Murata correlations for h_l and $\Delta P'_{LB}$ are given below:

$$h_l/H_s = 0.086 + 11 (H_s/d_p)^{-0.4} (fd/D)^{-0.58} (Ga)^{0.09} \times \\ (Fr)_l^{1.66} (Re)_l^{-0.34} (We)_l^{-0.34} \quad (4.2)$$

$$\Delta P'_{LB}/H_s = 12.8 (H_s/d_p)^{-0.4} (fd/D)^{-0.58} (Ga)^{0.09} \times \\ (Fr)_l^{1.66} (Re)_l^{-0.34} (We)_l^{-0.34} \quad (4.3)$$

4.1.4 Bed Expansion

The ratio H/H_s was found to be independent of H_s . It varied linearly with gas velocity. Typical plots of H/H_s versus U_g are shown in Figure 4.9. Also included in this figure are the estimates of H/H_s computed from the correlations proposed by Tichy and Douglas (1972) and Kito et al. (1978). It can be seen that the difference between the estimated and the observed values increased considerably with the increase in gas velocity. A similar trend was observed for all other bed conditions. Except for the shape, the cork particles had characteristics similar to the particles used by Tichy and Douglas (1972). Hence, the difference in the bed expansion may be attributed to the shape of the particles. The expansion of the

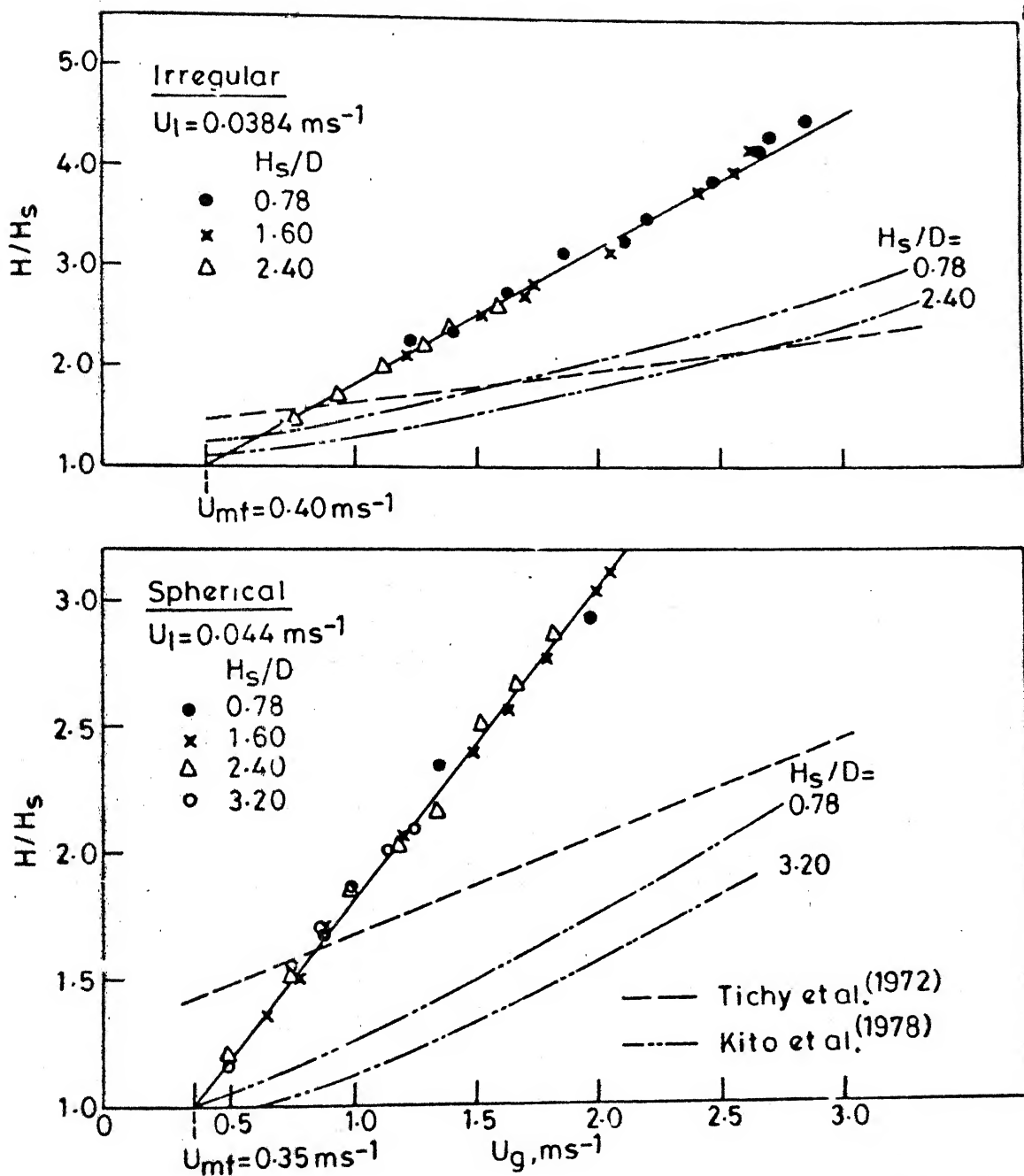


Fig.4.9 - Typical plots showing the comparison of the data of H/H_s with other correlations.

bed of cork particles showed a nature different from the other two, hence two separate empirical correlations are proposed. They are:

$$H/H_s = 2.132 d_p^{0.12} U_l^{0.31} + 1.02 d_p^{-1.7} \rho_p^{-1.2} U_l^{0.2} U_g \quad (4.4)$$

for the spherical and irregular particles and,

$$H/H_s = -1.07 + 43 U_l + 1.545 U_g \quad (4.5)$$

for the cork particles.

4.1.5 Minimum Fluidization Velocity

The transition from the static bed to the mobile bed was gradual and the transition zone had a spread over a considerable range of gas velocity. This range increased with an increase in H_s and decreased with an increase in liquid velocity. The minimum fluidization velocity was determined by H/H_s vs U_g plots as stated earlier. Hence, the correlations given in Equations (4.4) and (4.5) can be used to estimate U_{mf} by substituting H/H_s equal to 1. The observed values of U_{mf} were compared with the values calculated from Equations (4.4) and (4.5) as well as from the correlation proposed by Kito et al. (1976b) in Figure 4.10.

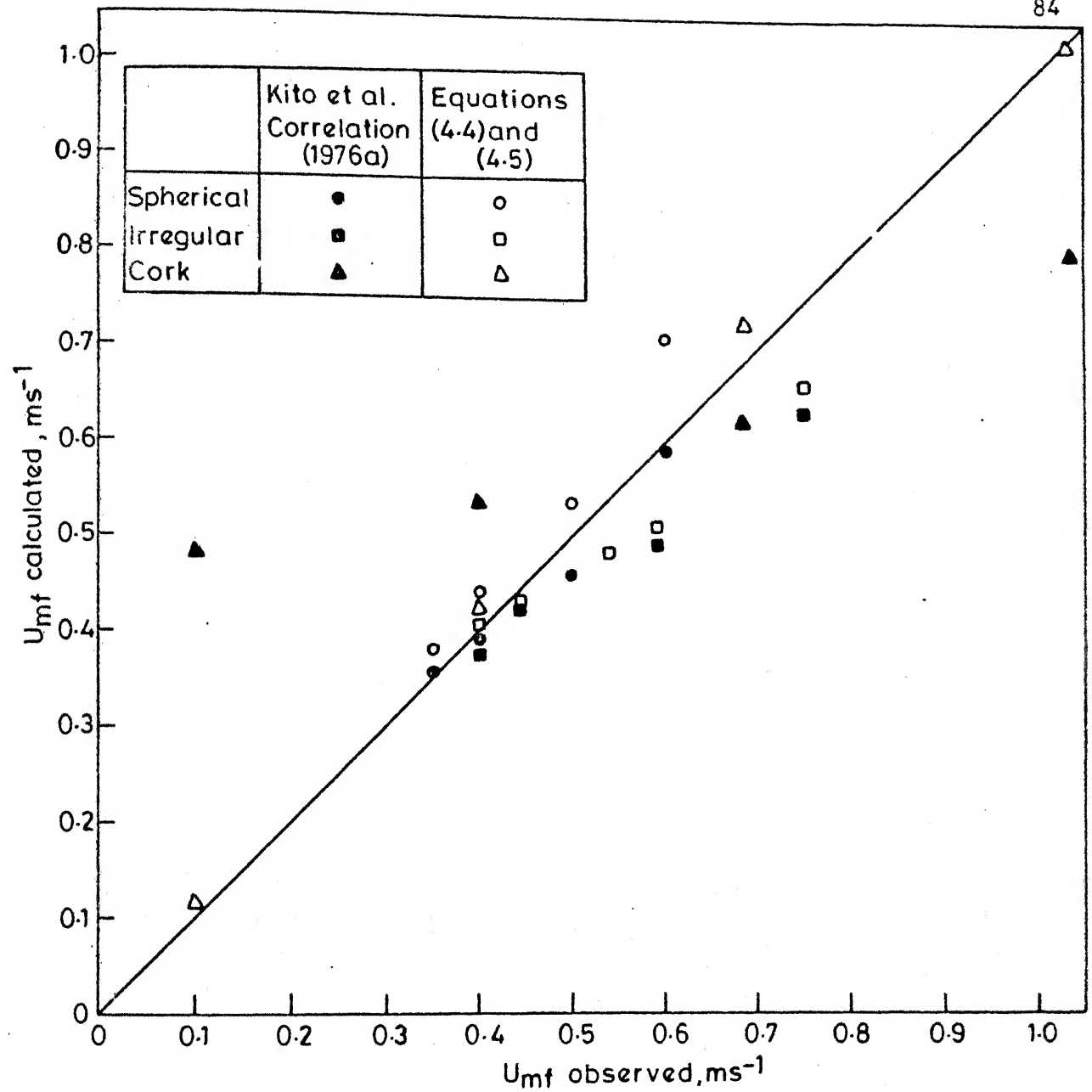


Fig. 4.10- Comparison of the observed values of U_{mf} with those calculated from Equations (4.4) and (4.5) and other correlation.

4.2 AXIAL MIXING

4.2.1 Interpretation of Breakthrough Curves

The studies, in which the motion of the fluid particles of the flowing phase could be considered sufficiently random, indicate that the axial mixing characteristics of the phase may be adequately described by the single-parameter axial dispersion model (Shah et al. 1978; Shah, 1979). This model assumes uniform radial concentration in the phase and characterises the axial mixing by a single parameter namely axial dispersion coefficient, D_L . It may be recalled that Chen and Douglas (1969) and Koval et al. (1975a, 1975b) have also adopted this model in order to describe the axial mixing of the liquid phase in the mobile bed contactor. To check the applicability of this model, the breakthrough curves obtained in the present study were analyzed as described below.

Since the breakthrough curves obtained for the liquid flow through the empty column indicated a plug flow behaviour of liquid phase, it was assumed that the liquid phase is in plug flow before and after the mobile bed section. Thus the mobile bed was considered as a closed-closed system (van deer Laan, 1958; Levenspiel, 1972).

When step input of a tracer is imposed on the liquid stream entering the tracer-free mobile bed, the concentration of tracer in the bed can be described by the one-dimensional axial dispersion equation and initial and boundary conditions:

$$\frac{\partial C}{\partial t} = D_L \frac{\partial^2 C}{\partial x^2} - \bar{U} \frac{\partial C}{\partial x} \quad (4.6)$$

$$\text{I.C. : } C = 0 \text{ at } t = 0 \text{ and } 0 < x < H \quad (4.7)$$

$$\text{B.C. at inlet: } \bar{U}C - D_L \frac{\partial C}{\partial x} = \bar{U}C_0 \text{ for all } t > 0 \text{ and } x = 0 \quad (4.8)$$

$$\text{B.C. at outlet: } -D_L \frac{\partial C}{\partial x} = 0 \text{ for all } t > 0 \text{ and } x = H \quad (4.9)$$

where

$C = C(x, t)$ = tracer concentration.

C_0 = tracer concentration in the inlet liquid stream.

t = time from the commencement of the displacement.

x = distance from the point of the introduction of the displacing fluid.

\bar{U} = average interstitial velocity of the fluid.

D_L = axial dispersion coefficient.

H = expanded height of the mobile bed.

The set of Equations (4.6) through (4.9) can be cast in dimensionless forms as

$$\frac{\partial C^*}{\partial T} = \frac{1}{Pe} \frac{\partial^2 C^*}{\partial X^2} - \frac{\partial C^*}{\partial X} \quad (4.10)$$

$$\text{I.C. : } C^* = 1 \text{ at } T = 0 \text{ and } 0 < X < 1 \quad (4.11)$$

$$\text{B.C. at inlet: } Pe C^* - \frac{\partial C^*}{\partial X} = 0 \text{ for all } T > 0 \text{ and } X = 0 \quad (4.12)$$

$$\text{B.C. at outlet: } \frac{\partial C^*}{\partial X} = 0 \text{ for all } T > 0 \text{ and } X = 1 \quad (4.13)$$

where

$$C^* = \bar{C}(X, T) = 1 - \frac{C}{C_0}$$

$$Pe = \text{Peclet number} = \frac{\bar{U}H}{D_L}$$

$$X = \frac{x}{H}$$

$$T = \frac{t}{\theta}$$

and θ = average residence time of the liquid phase.

The solution of Equation (4.10) for initial and boundary conditions, given by Equations (4.11) through (4.13), has been given by Yagi and Miyauchi (1953) and Brenner (1962). The theoretical breakthrough curve

($\frac{C}{C_0}$ versus t/θ) can be expressed as

$$\left(\frac{C}{C_0}\right)_{x=H} = 1 - C^*(1, T) = 1 - \exp(2P - PT) \times \sum_{k=1}^{\infty} \frac{\lambda_k \sin(2\lambda_k)}{\lambda_k^2 + P^2 + P} \left(\exp - \frac{\lambda_k^2 T}{P}\right) \quad (4.14)$$

where $P = Pe/4$ and λ_k ($k = 1, 2, \dots$) are the positive roots (in increasing order) of the transcendental equation

$$\tan 2\lambda_k = \frac{2\lambda_k P}{\lambda_k^2 - P^2} \quad (4.15)$$

from which the trivial root λ_0 is to be excluded (Carslaw and Jaeger, 1959). The numerical values of these roots at various values of P can be obtained by the relations

$$\begin{aligned} \lambda_{2n-1} &= \beta_n \\ \text{and } \lambda_{2n} &= \gamma_n \end{aligned} \quad (4.16)$$

for $n = 1, 2, 3, \dots$

where β_n and γ_n are the positive roots (in increasing order) of the transcendental equations.

$$\beta_n \tan \beta_n - P = 0 \quad (4.17)$$

$$\text{and } \gamma_n \cot \gamma_n + P = 0 \quad (4.18)$$

Using Equations (4.17), (4.18) and (4.14) the theoretical breakthrough curves were computed for the Peclet numbers evaluated from the second moments of the experimental breakthrough curves (as described in section 3.3.4). First 12 terms of the series solution given by Equation (4.14) were found sufficient for convergence.

For a number of randomly selected runs at various gas and liquid velocities and static bed heights, the agreement between the theoretical and experimental breakthrough curves was found to be good. Four typical plots are shown in Figures 4.11 through 4.14. The good agreement between theoretical and experimental breakthrough curves justifies the validity of the single-parameter axial dispersion model to describe the axial mixing of the liquid phase in the mobile bed contactor.

4.2.2 Peclet Number of the Liquid Phase

As described in section 3.3.4, 5-10 breakthrough curves were obtained for each run depending upon the nature of fluctuations in Peclet numbers. The Peclet numbers were found to be deviating considerably at low gas velocities particularly when the mobile bed exhibited a slugging nature. But the deviations were very small at higher gas velocities because of the smooth fluidization

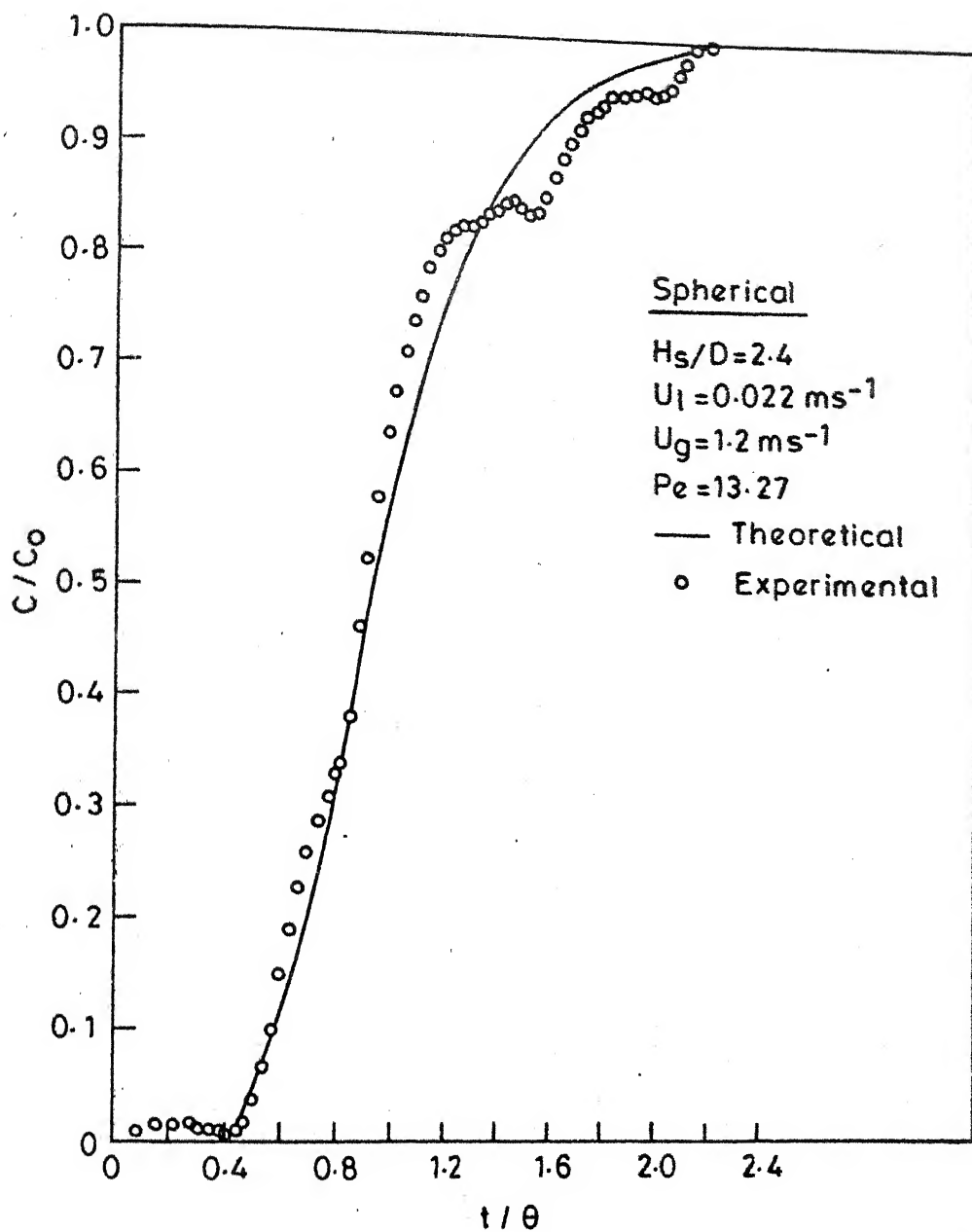


Fig.4.11 Comparison of an experimental breakthrough curve with the theoretical curve for spherical particles.

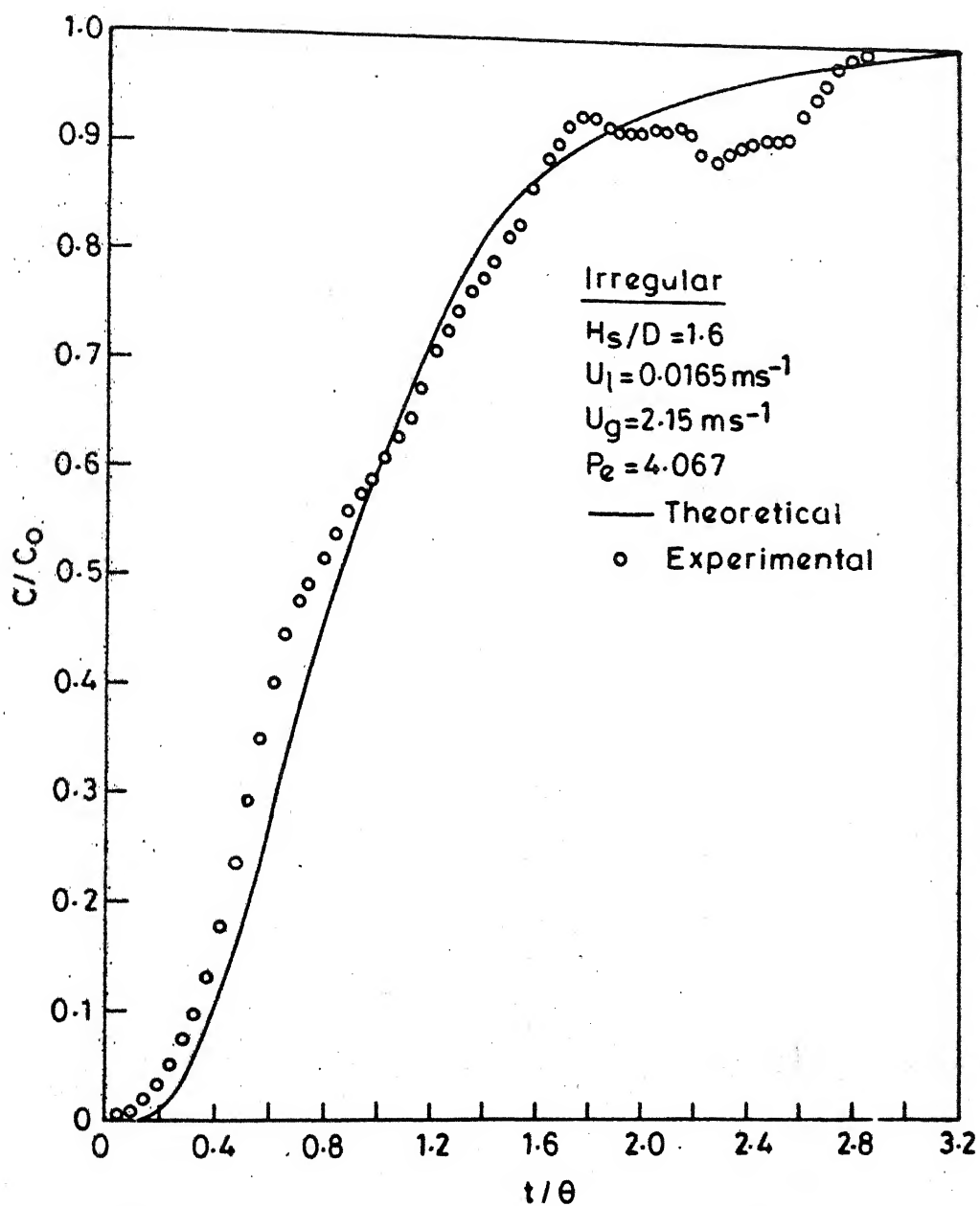


Fig. 4.12 Comparison of an experimental breakthrough curve with the theoretical curve for irregular particles.

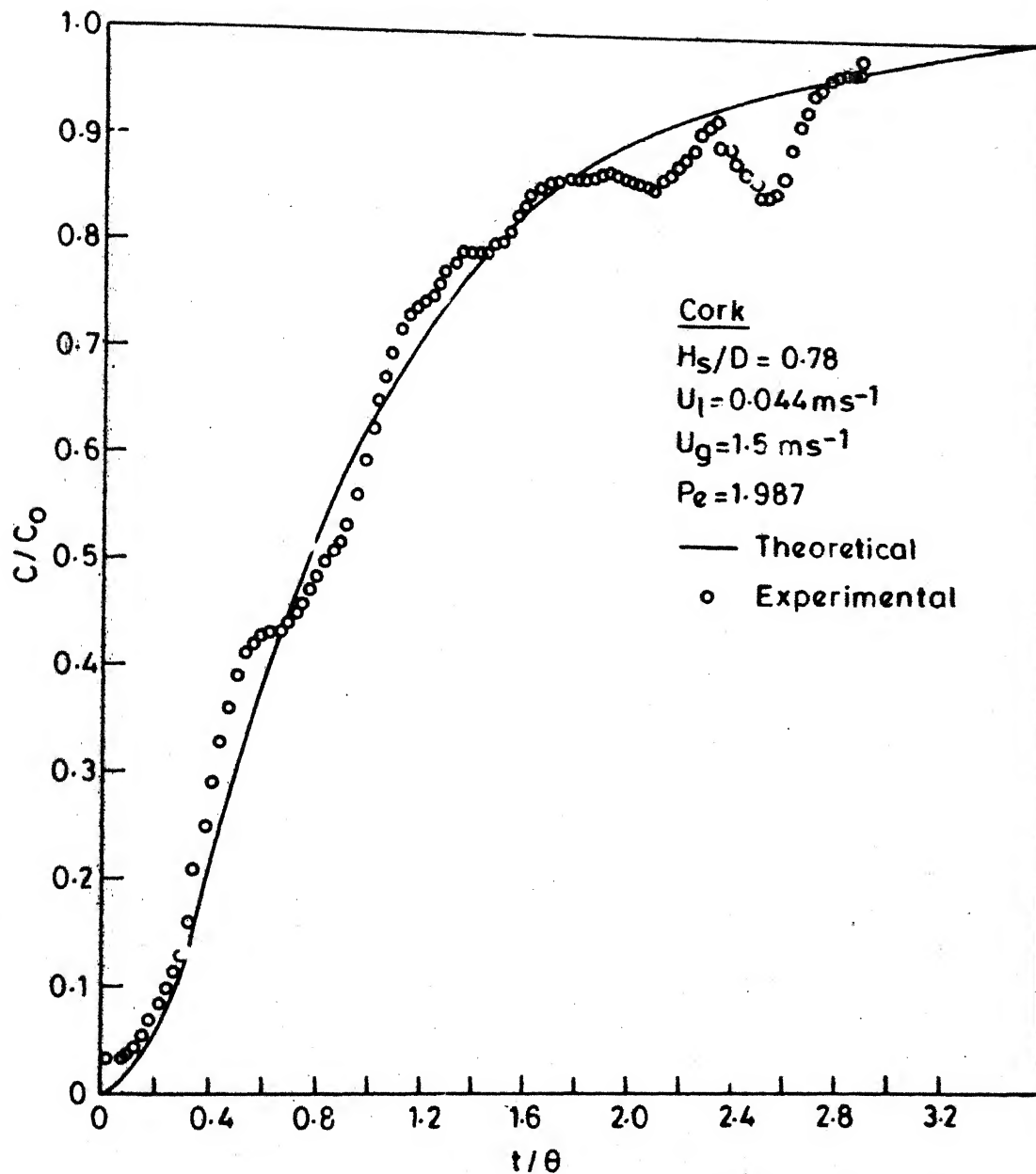


Fig.4.13 Comparison of an experimental breakthrough curve with the theoretical curve for cork particles.

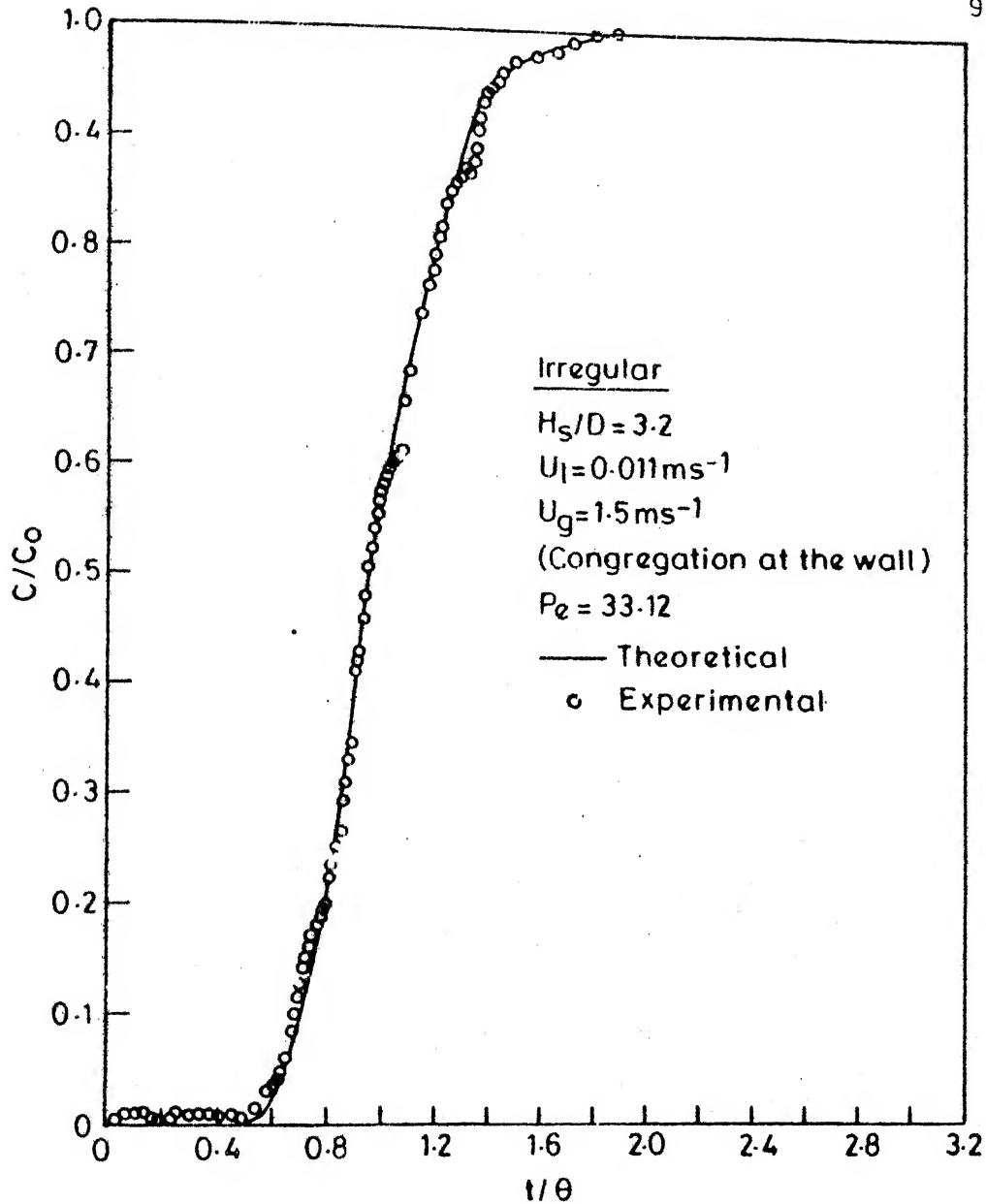


Fig. 4.14. Comparison of an experimental breakthrough curve with the theoretical curve in the case of congregation of irregular particles at the wall.

at these velocities. Two typical sets of Peclet numbers for low and high gas velocities are given in Table 4.1. The kinks observed in the breakthrough curves (see Figures 4.11 through 4.14) can be attributed to the slugging nature of the bed. It may be pointed out that even for packed bed the Peclet numbers, reported by Dunn et al.(1977) for the liquid phase, show a 20 to 50 % deviation. The average Peclet number evaluated from the breakthrough curves obtained for a given run have been reported here and it has been referred simply as Peclet number.

The plots of Peclet number versus gas velocity with liquid velocity as a parameter are given in Figures 4.15 through 4.19 for all the three sizes of packing and different static bed heights. It can be seen from Figures 4.15 and 4.16 that for low static bed heights ($H_s/D = 0.78$ and 1.6) the Peclet number was found to decrease with the increase in liquid velocity whereas it remained independent of gas velocity. This trend is consistent with the observations of Chen and Douglas (1969) and Koval et al.(1975b). Also Peclet numbers for lower static bed heights were of the same magnitude as those reported by these investigators.

TABLE 4.1

TWO TYPICAL SETS OF PECLET NUMBERS AT LOW AND HIGH GAS
VELOCITIES IN THE CASE OF SPHERICAL PARTICLES

$$U_1 = 0.011 \text{ m s}^{-1}; H_g/D = 3.2$$

U_g m s^{-1}	Average residence time, s	Peclet number
1.00	3.95	16.01
	4.48	13.56
	3.57	11.20
	3.60	13.62
	3.66	10.50
	4.05	18.93
	3.22	14.94
	3.70	11.70
	4.17	13.52
1.79	4.00	13.00
	3.96	10.81
	3.97	10.99
	3.86	10.81
	3.92	10.32
	4.34	11.63
	3.96	10.72

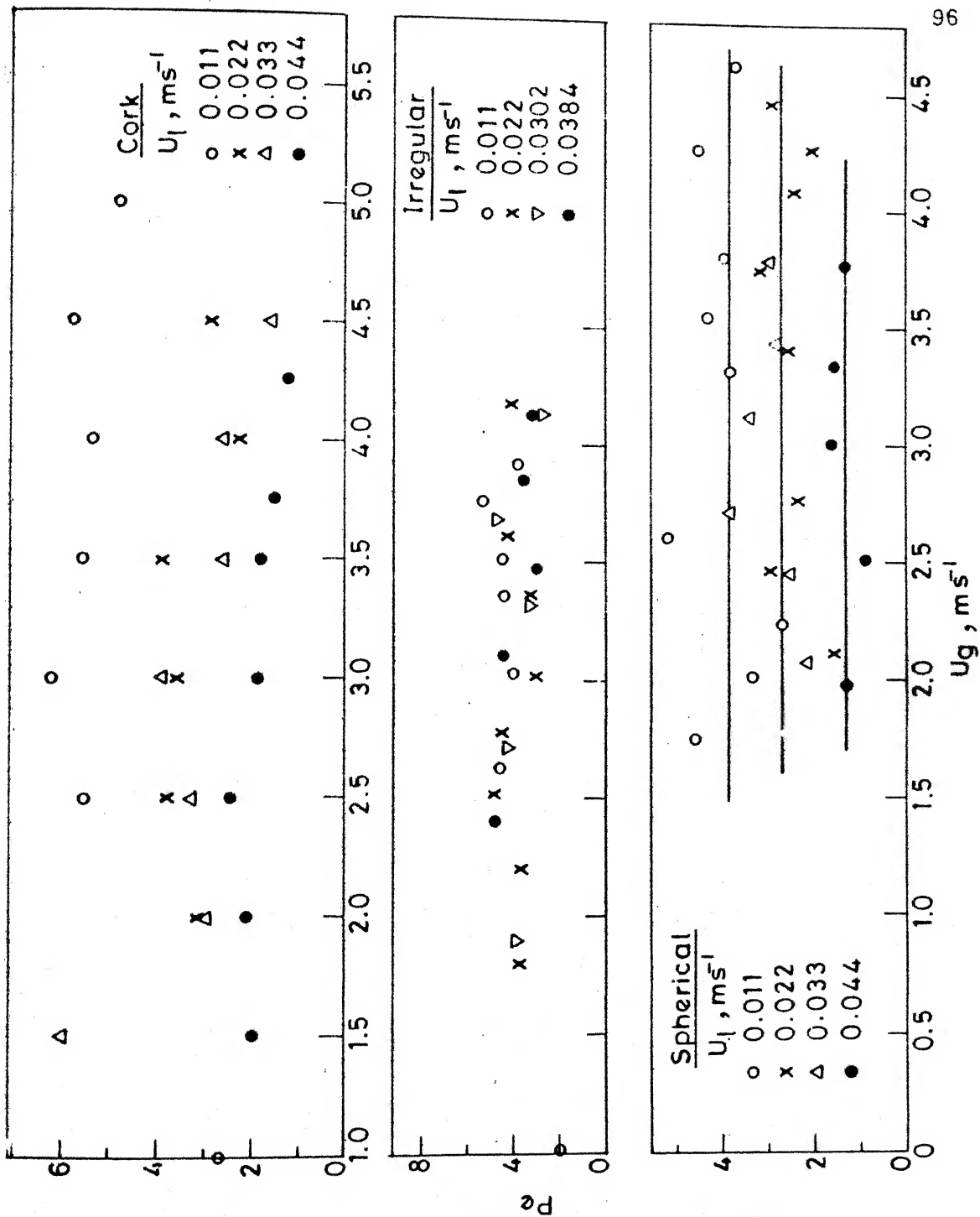


Fig . 4:15 Pe versus U_g for $H_s/D = 0.78$.

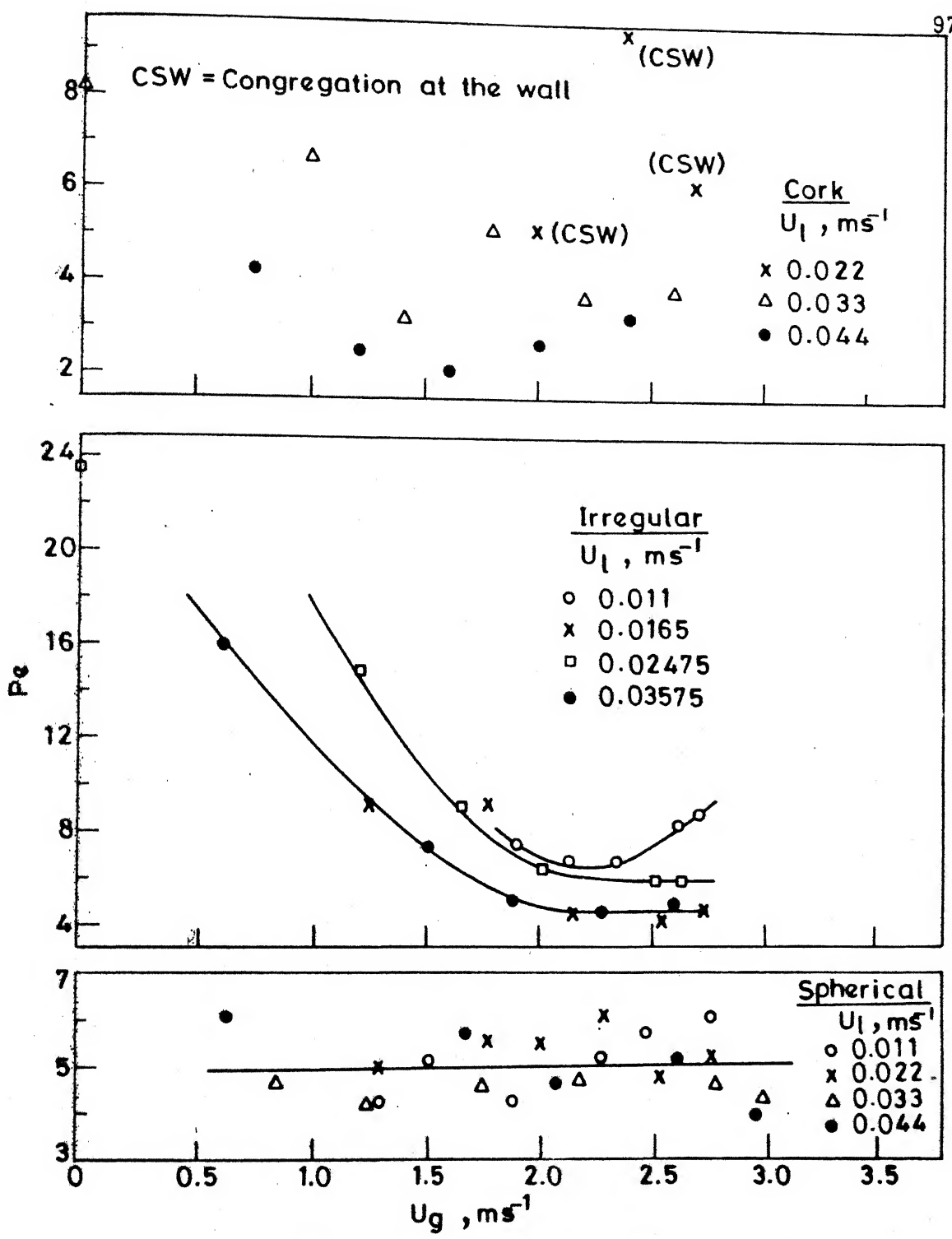


Fig . 4.16 Pe versus U_g for $H_s/D = 1.6$.

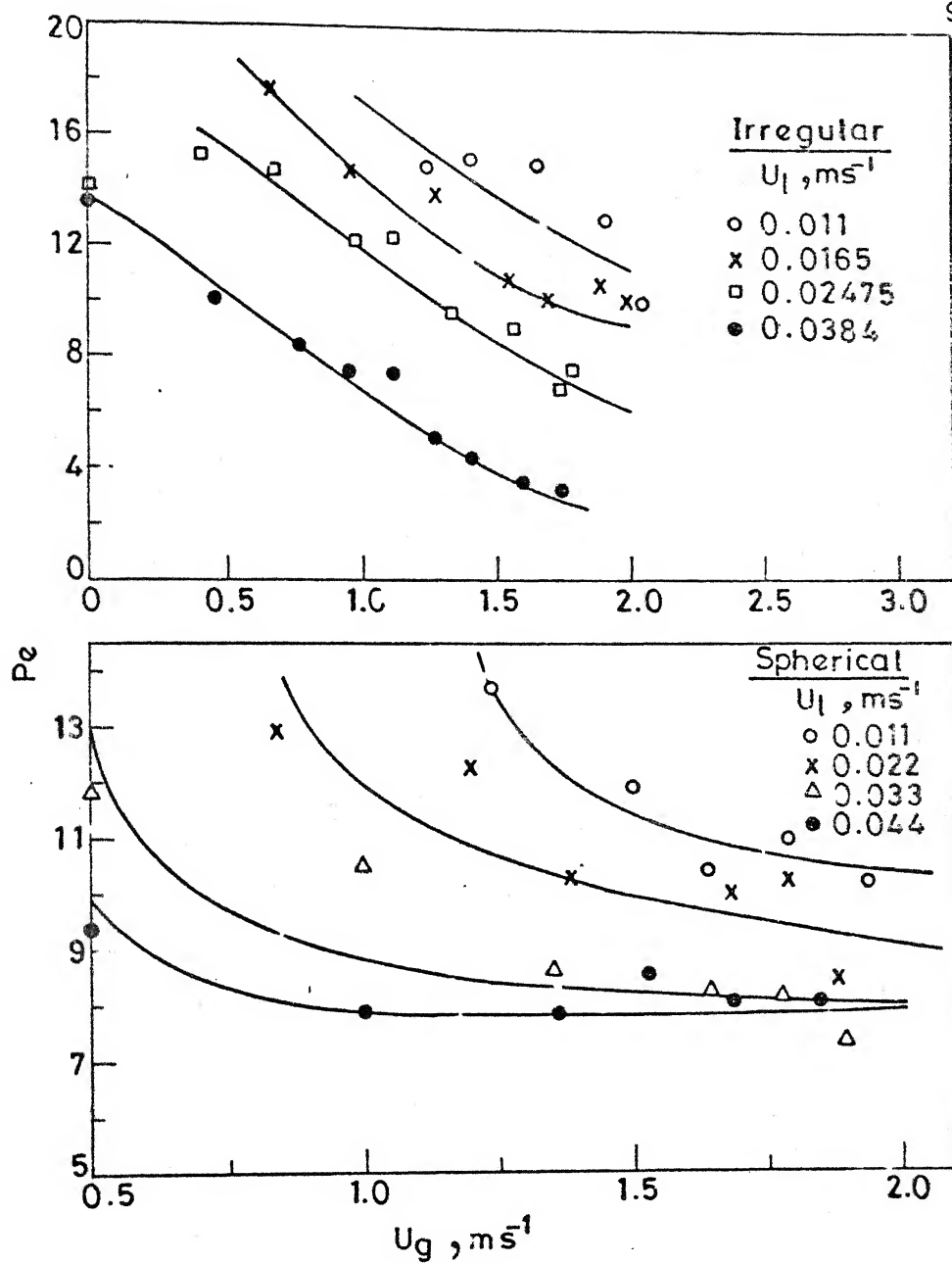


Fig .4.17 Pe versus U_g for $H_s/D = 2.4$.

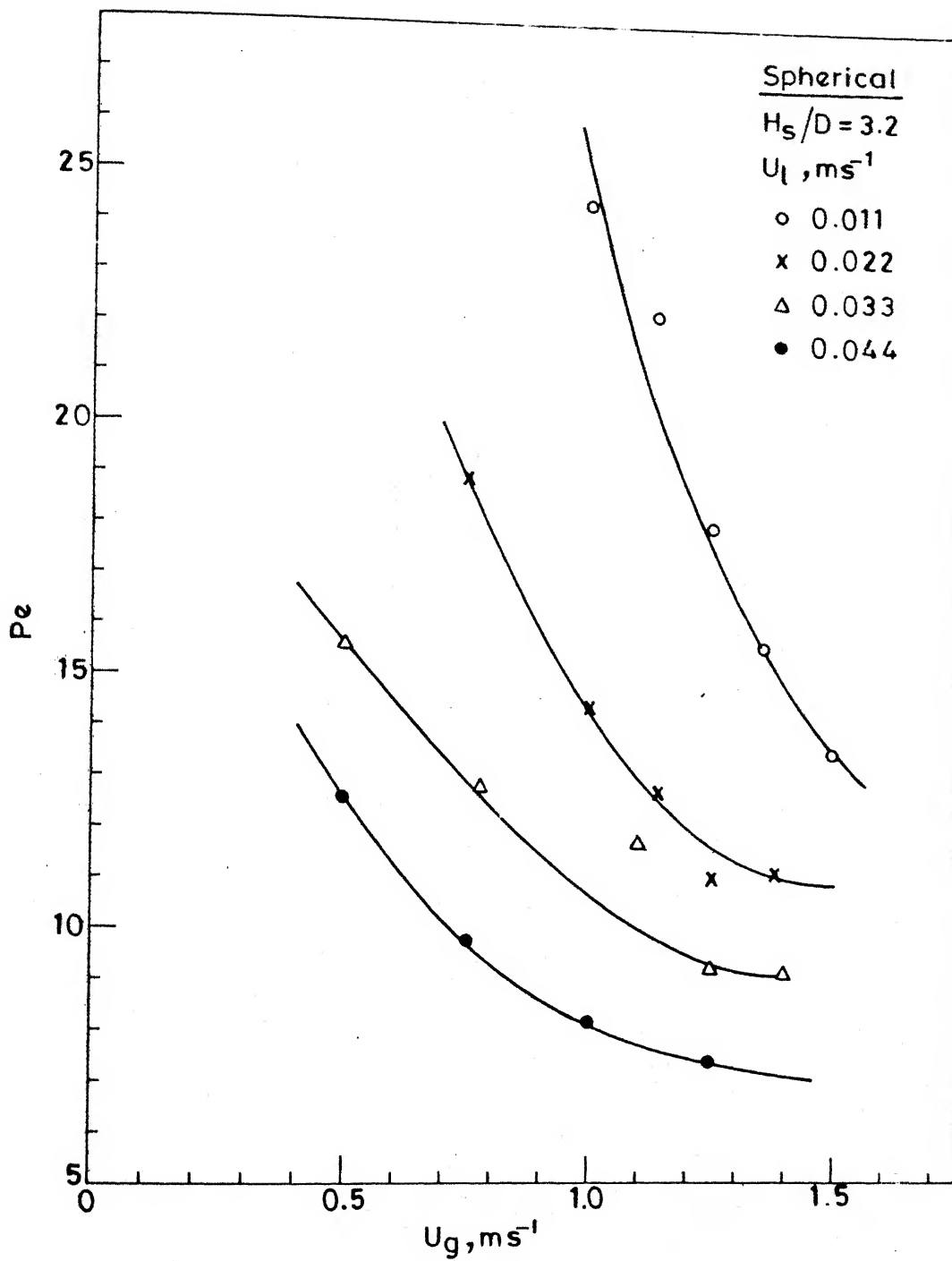


Fig. 4.18 Pe versus U_g for $H_s/D = 3.2$ in the case of spherical particles.

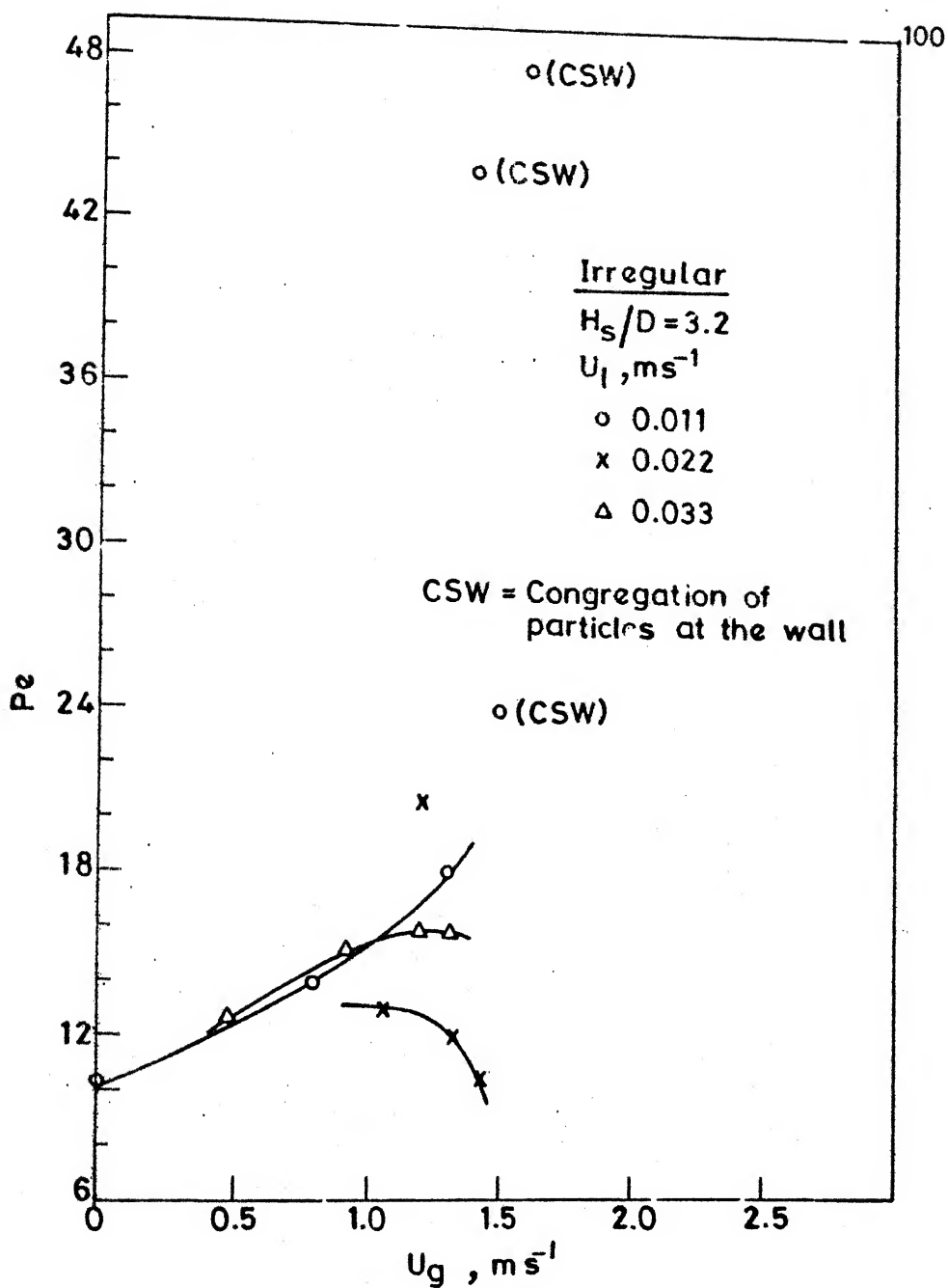


Fig. 4.19 Pe versus U_g for $H_s/D = 3.2$ in the case of irregular particles.

It can be seen from Figures 4.17 and 4.19 that for higher static bed heights ($H_s/D = 2.4$ and 3.2) the Peclet number decreased with the increase in gas and liquid velocities. It may be pointed out that with the increase in gas velocity the increase in D_L is such that it has more than offset the increase in H^2 and as a result the Peclet number decreased. But the values of Pe at higher static beds were much higher than those obtained at lower static bed heights. Therefore, a near plug flow of liquid phase could be achieved with higher static bed heights.

Due to frequent congregation of irregular particles at the wall, reliable measurements over the entire range of gas velocities could not be obtained for $H_s/D = 3.2$. However, the data points obtained for some gas velocities were found to be in conformity with the above mentioned trend (see Figure 4.19). The data points, which are far above the rest are the Peclet numbers when congregation occurred. In such a situation most of the liquid passed through the particle-free core resulting in a nearly plug flow of the liquid phase.

Due to frequent congregation of cork particles, the breakthrough curves could not be obtained for $H_s/D = 2.4$ and 3.2 .

4.2.3 Axial Dispersion Coefficient

The axial dispersion coefficient was evaluated from the data of the average Peclet number and using the relation $D_L = \frac{\bar{U}H^2}{Pe}$. The plots of axial dispersion coefficient versus gas velocity with liquid velocity as a parameter are shown in Figure 4.20 through 4.22 for all the three sizes of packing particles and different static bed heights. It can be seen from these figures that D_L increased with the increase in both the gas and liquid velocity, but the effect of static bed height on D_L was marginal. The effect of shape of the particles on D_L was examined. From the plots of D_L versus U_g (see Figure 4.20) it is found that $D_L \propto U_g^{2.26}$ for the spherical particles. Chen and Douglas (1969) and Koval et al. (1976b) have used spherical particles of different densities and sizes, and their data also yielded the same relation (see Figure 4.23). But it is found that $D_L \propto U_g^{2.41}$ for the irregular particles (see Figure 4.21) and $D_L \propto U_g^{2.56}$ for the cork particles (see Figure 4.22). The marginal higher value of the exponent may be attributed to the shape of the particles. However, the plots of D_L versus \bar{U} indicated that $D_L \propto \bar{U}^{2.92}$ for all the three particles. Therefore, it appears that D_L depends on liquid holdup which is ofcourse inturn affected by the shape of the particles. In the

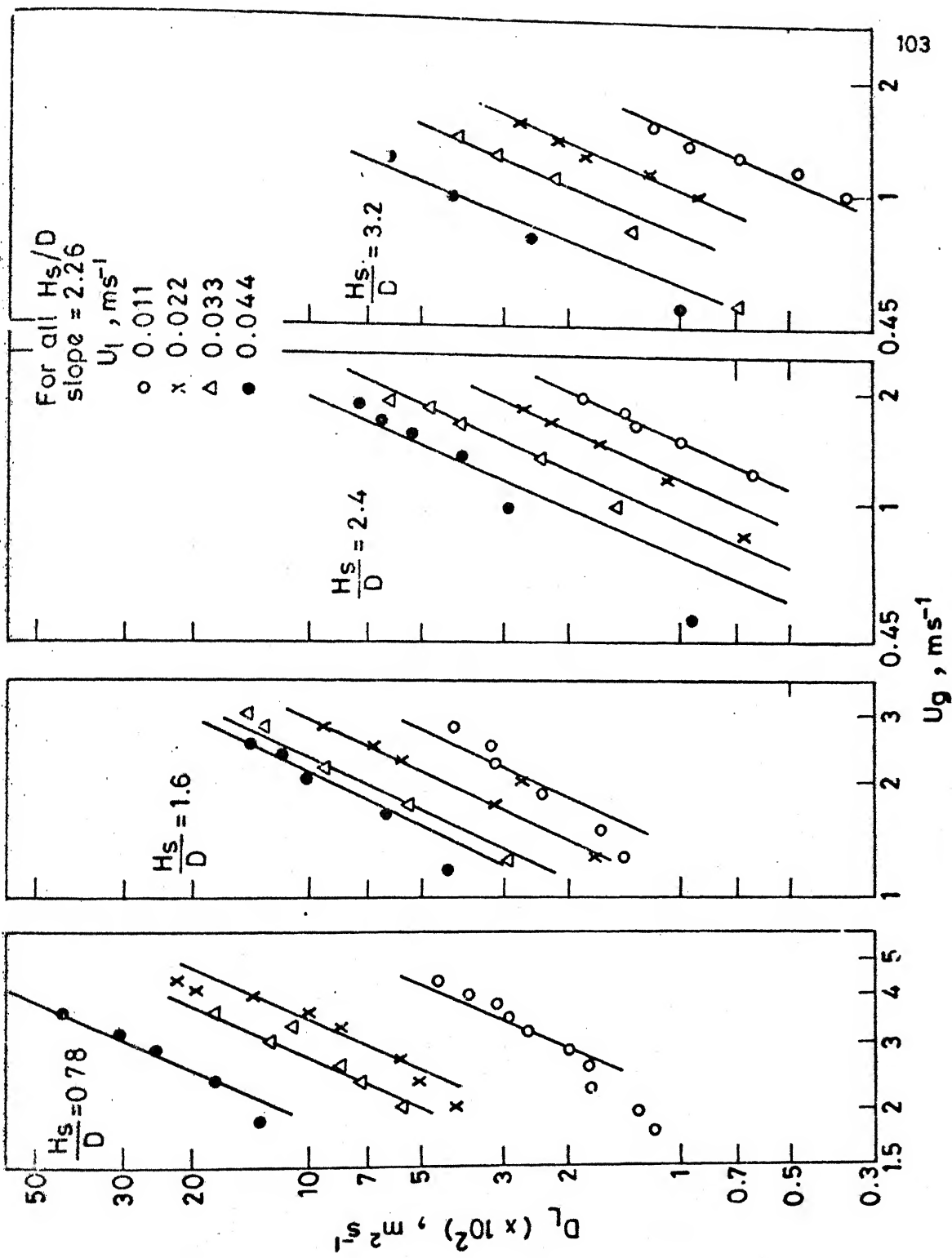


Fig. 4.20 D_L versus U_g for the spherical particles.

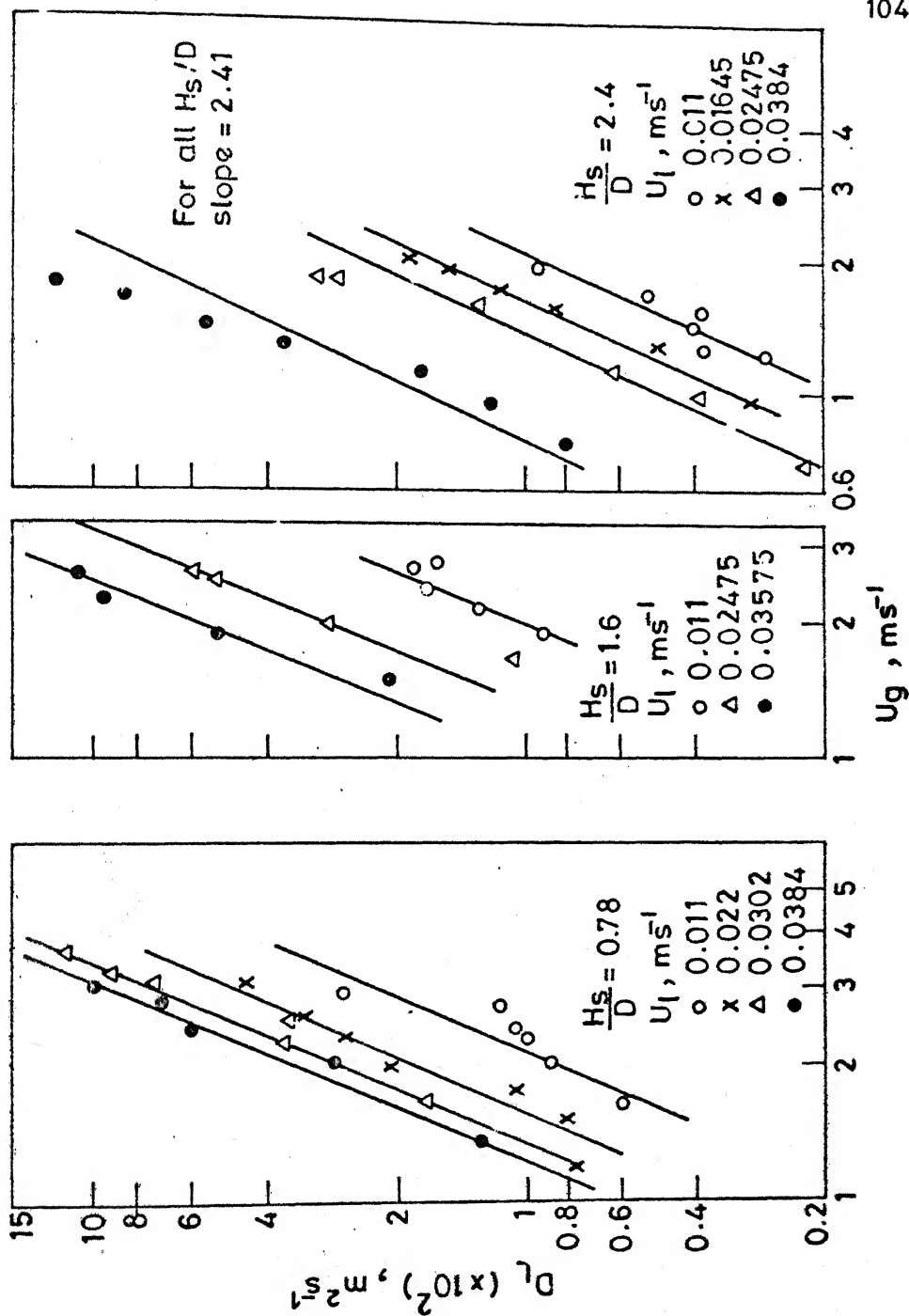


Fig. 4.21 D_L versus U_g for the irregular particles.

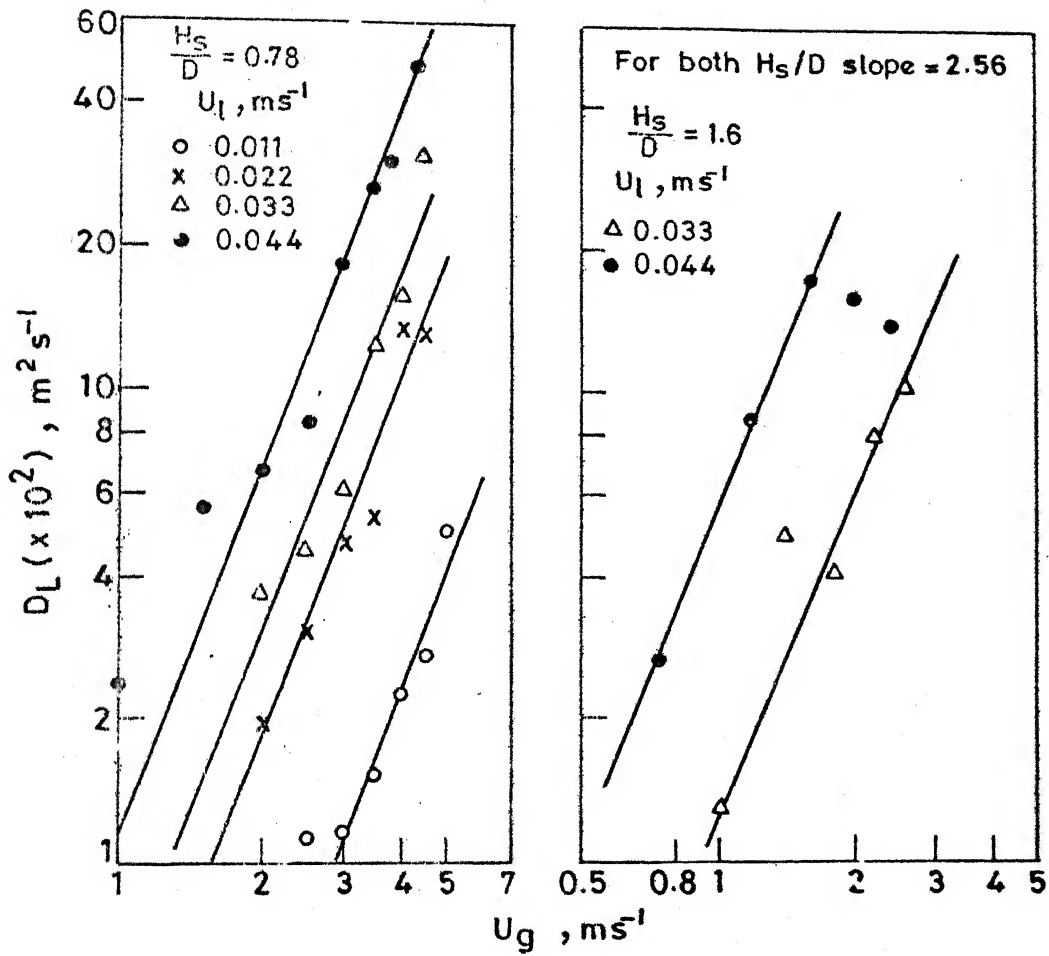


Fig. 4.22 D_L versus U_g for the cork particles.

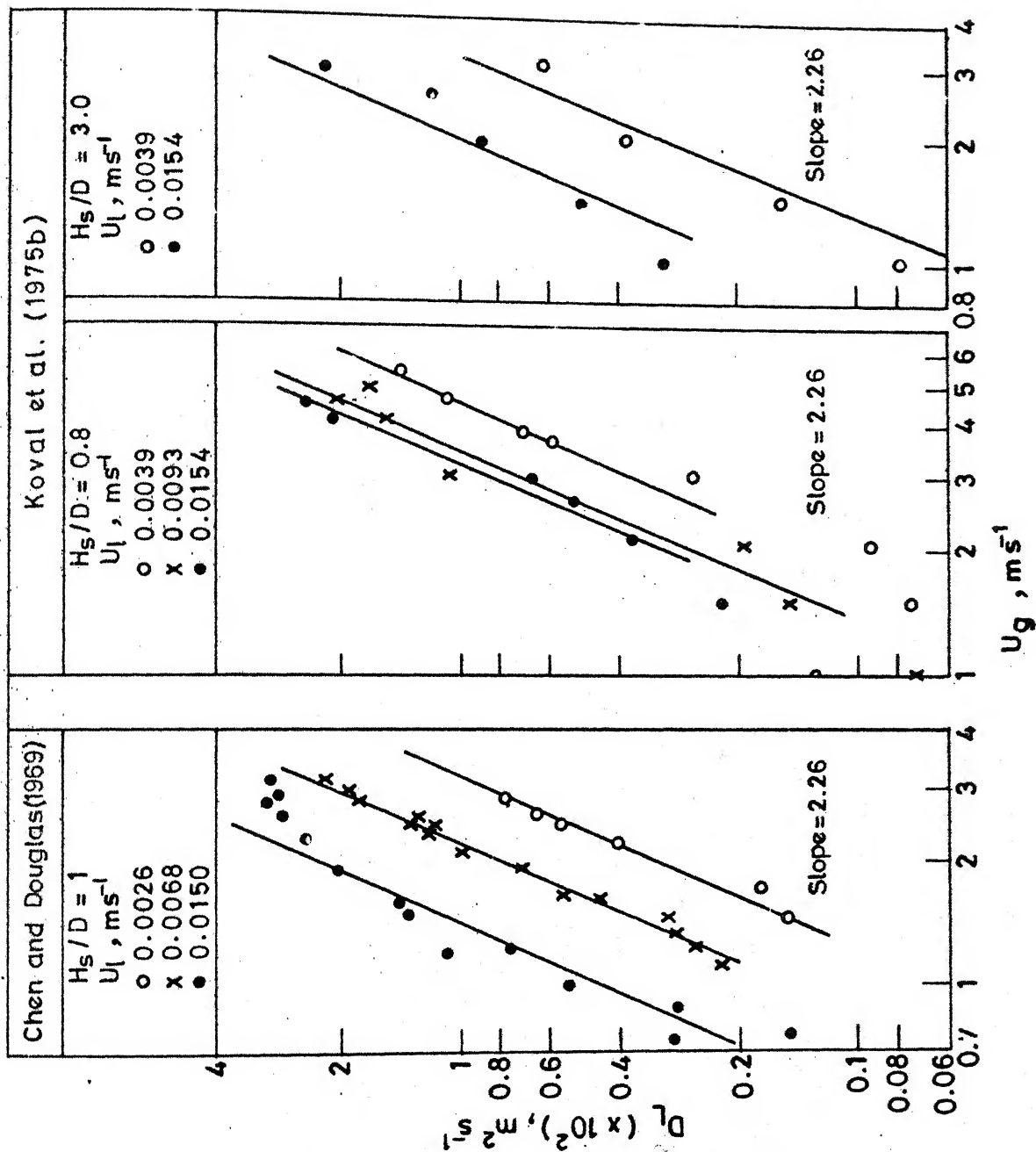


Fig. 4.23 D_L versus U_g for the data of Chen and Douglas (1969) and Koval et al. (1975b)

correlations presented below the equivalent diameter ($d_p \phi_s$) has been employed to account the shape of the particles.

4.2.4 Correlations for Pe and D_L

The Peclet number and the axial dispersion coefficient can be expected to be functions of operating parameters U_1 (or \bar{U}), U_g , H_s , $d_p \phi_s$, D and properties of gas and liquid. Using the exponent multiple regression analysis technique several functional forms of correlations consisting of appropriate dimensionless groups formed by taking different combinations of the above variables were tested, and the following correlations were found to fit the 90 % of the data within a deviation of ± 35 % :

$$Pe = 10^{4.49} (Re)_1^{-0.47} (Re)_g^{-0.308} (Ga)^{-0.165} \times (H_s/d_p)^{0.824} (d_p/D)^{1.464} \quad (4.19)$$

$$Pe = 10^{3.25} (\bar{Re})_1^{-0.59} (Re)_g^{0.2} (Ga)^{-0.097} \times (H_s/d_p)^{0.95} (d_p/D)^{1.562} \quad (4.20)$$

and

$$D_L = 10^{-13.85} (\bar{Re})_1^{1.82} (Re)_g^{0.47} (Ga)^{0.27} \times (H_s/d_p)^{-0.068} (d_p/D)^{-2.8} \quad (4.21)$$

The observed and calculated values of Pe and D_L were compared and are shown in Figures 4.24 through 4.26. The data of Chen and Douglas (1969) and Koval et al. (1975b) were compared with the calculated values using Equation (4.19) (see Figure 4.27). It can be seen from this figure that the data of Chen and Douglas (1969) are in good agreement with the Equation (4.19) especially at gas velocities far above the minimum fluidization velocity. It may be pointed out that Chen and Douglas have covered relatively a narrow range of the expanded bed height ($H/H_g = 1 - 1.5$) whereas in the present study, a much wider range of bed expansion was covered and the lowest H/H_g was above 1.5. The data of Koval et al. (1975b) fell below the line representing Equation (4.19). It may be noted that Koval et al. employed a grid only of 46% free opening (in contrast to $f = 70\%$ used in the present study and by Chen and Douglas). As has been discussed in section 2.1.1 that the free opening of the bottom grid has a strong influence on the liquid holdup which increases with the decrease in f . Hence lower values of Pe observed by Koval et al. are perhaps due to lower grid opening.

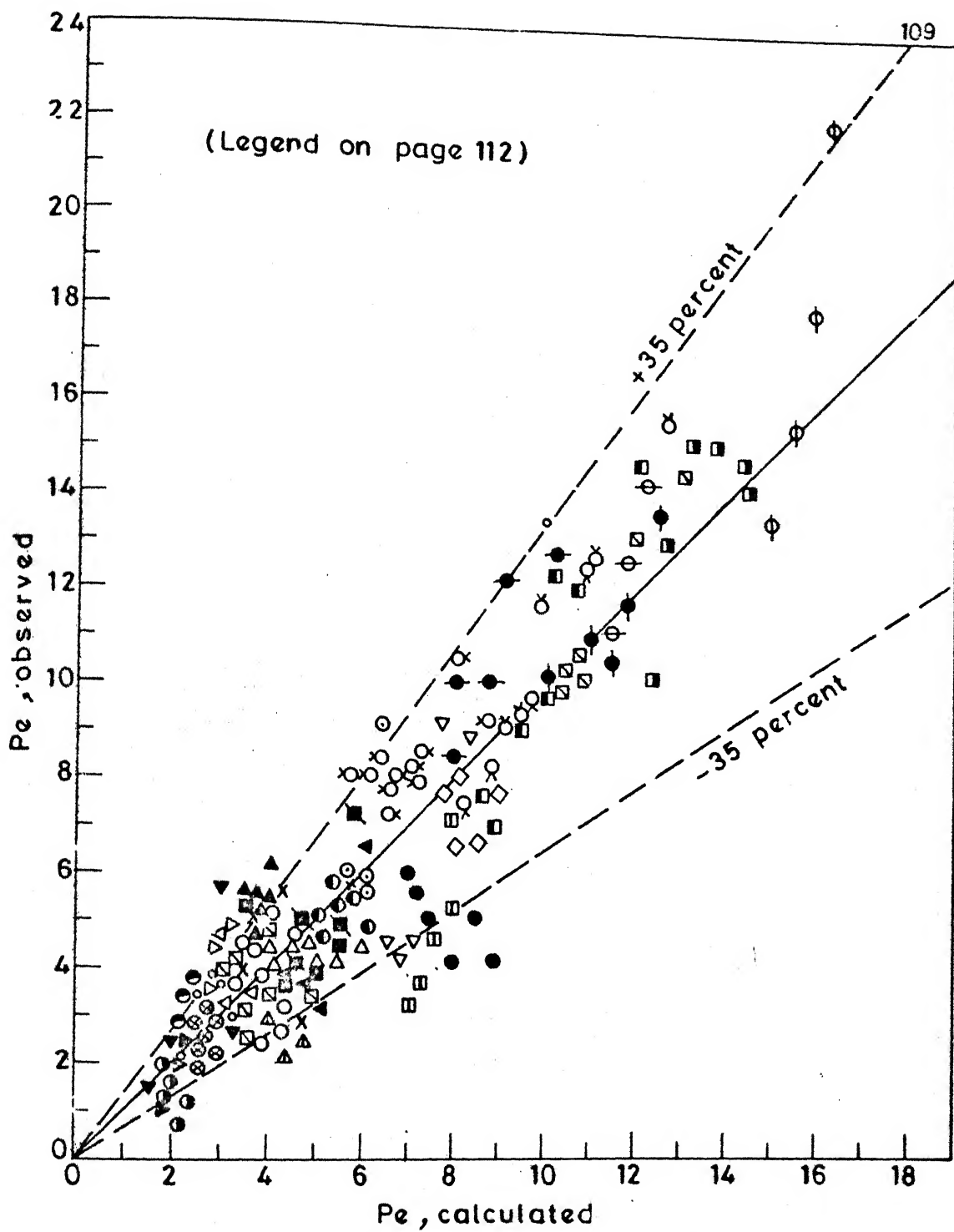


Fig. 4.24 Comparison of observed values of Pe with the values estimated using Equation (4.19)

(Legend on page 112)

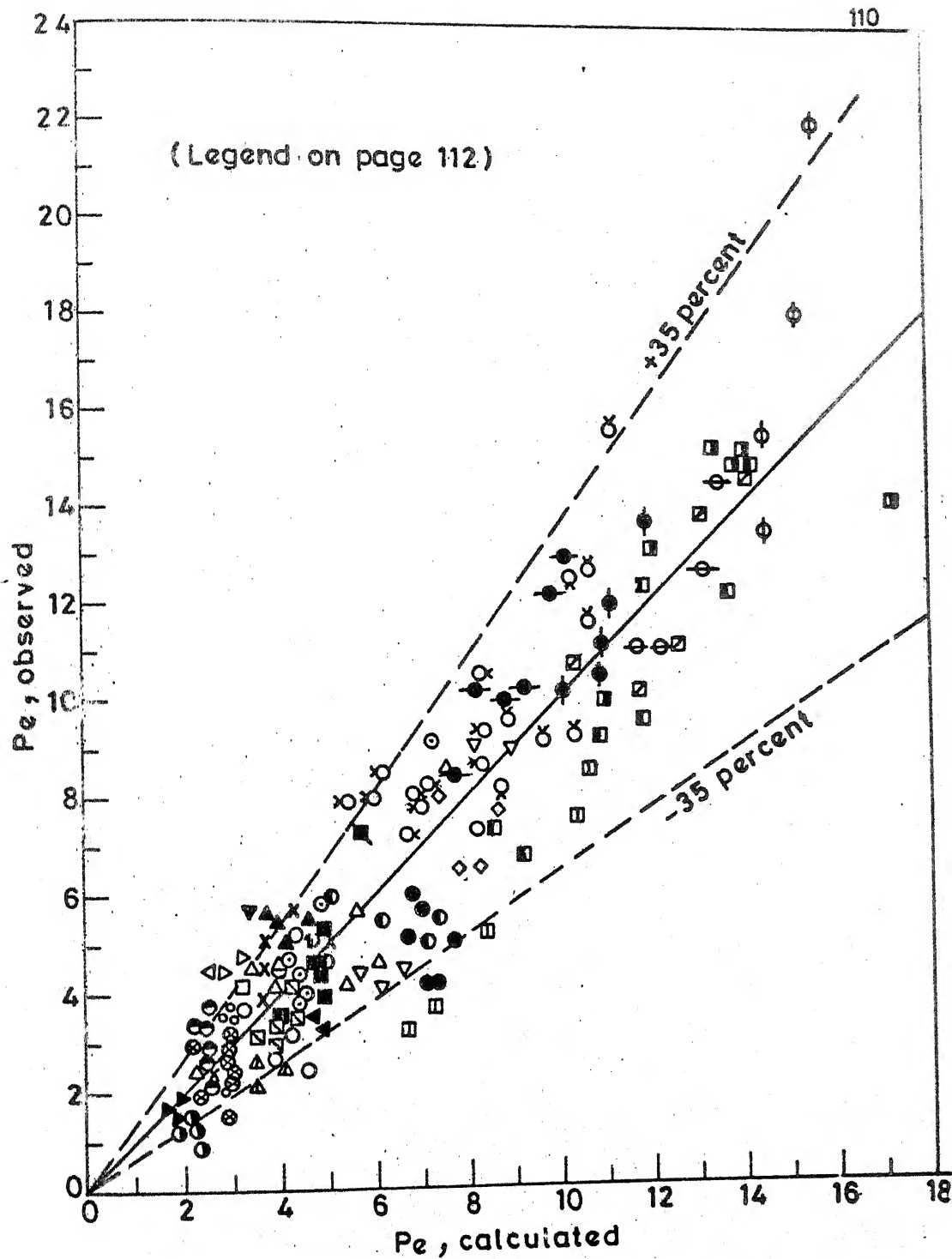


Fig. 4.25 Comparison of observed values of Pe with the values estimated using Equation (4.20)

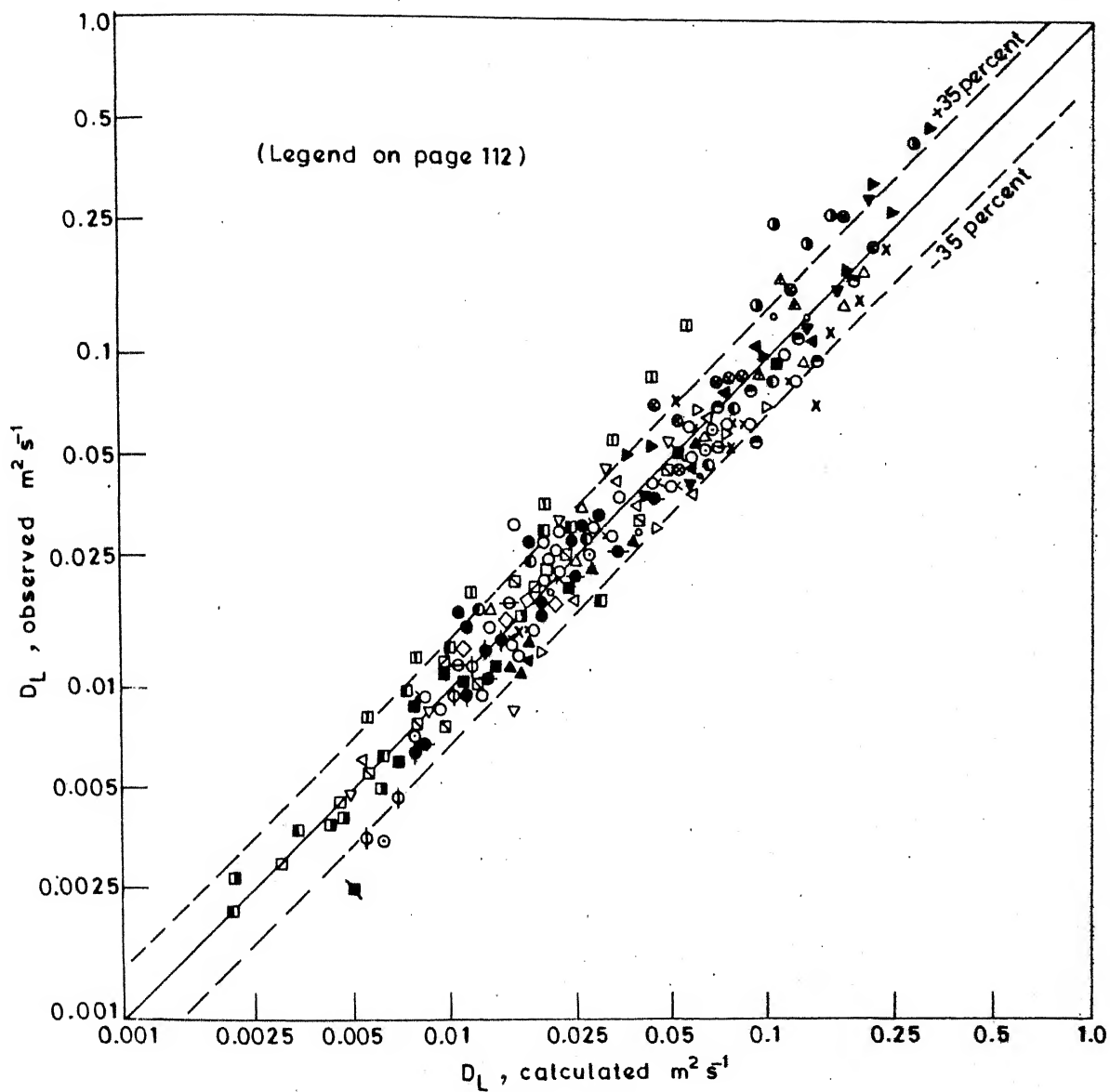


Fig. 4.26 Comparison of observed values of D_L with the values estimated using Equation (4.21).

Legend for Figures 4.24, 4.25 and 4.26

Spherical			Irregular		
H_s/D	$U_{1,m}$	s^{-1}	H_s/D	$U_{1,m}$	s^{-1}
○	0.78	0.011	■	0.78	0.011
⊗	0.78	0.022	▣	0.78	0.022
⊙	0.78	0.033	◁	0.78	0.0302
⊖	0.78	0.044	▷	0.78	0.0384
●	1.6	0.011	◊	1.6	0.011
⦿	1.6	0.022	▽	1.6	0.0165
△	1.6	0.033	⊙	1.6	0.02475
×	1.6	0.044	⦿	1.6	0.03575
⊕	2.4	0.011	▣	2.4	0.011
⊗	2.4	0.022	▣	2.4	0.0165
⊙	2.4	0.033	▣	2.4	0.02475
⊖	2.4	0.044	▣	2.4	0.0384
⊕	3.2	0.011	Cork		
⊗	3.2	0.022	H_s/D	$U_{1,m}$	s^{-1}
⊙	3.2	0.033	▲	0.78	0.011
⊖	3.2	0.044	○	0.78	0.022
			▼	0.78	0.033
			▷	0.78	0.044
			◁	1.6	0.033
			△	1.6	0.044

	$U_l, \text{m s}^{-1}$	d_p, cm	$\rho_p, \text{kg m}^{-3}$	H_s/D	Reference
a	0.0026	2.54	174	1.0	Chen and Douglas (1969)
b	0.0068				
c	0.015				
x	0.00386	1.6	283	0.8	Koval et al. (1975 b)
y	0.00925				
z	0.01536				

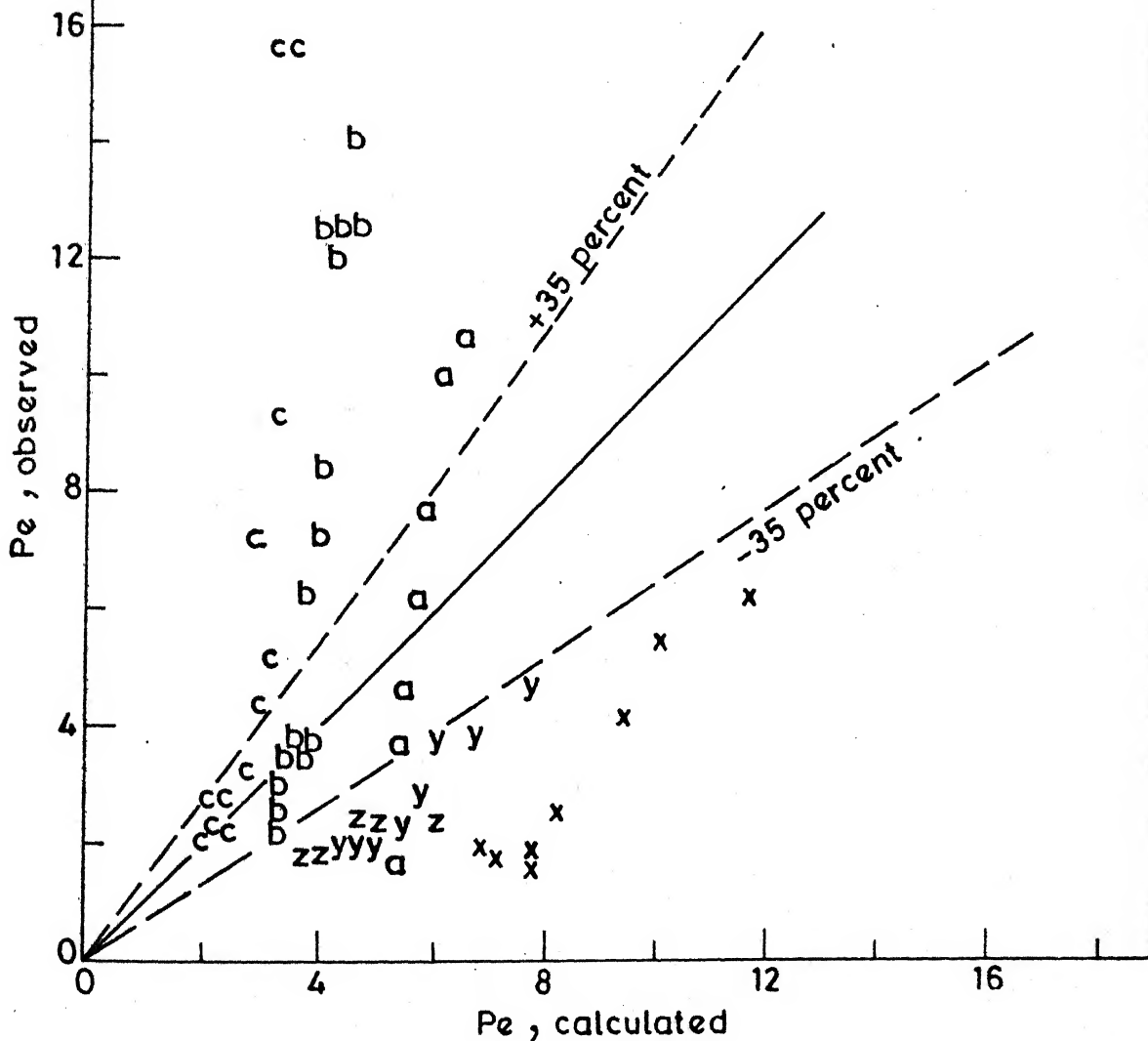


Fig.4.27 Comparison of observed values of Pe with the values estimated using Equation (4.19) for the data of Chen and Douglas (1969) and Koval et al. (1975 b).

4.3 MASS TRANSFER

4.3.1 Variations of Compositions and Temperatures of Gas and Liquid Streams During a Run

As mentioned in section 3.3.6, when temperatures of both the circulating gas and liquid streams became steady CO_2 was fed to the closed-loop. After allowing 10 min. for the initial transients to die down, the measurements of temperatures and compositions were started. It was observed that the concentration of NaOH solution decreased linearly whereas the composition of CO_2 in the gas stream increased in all the runs. It was observed that the temperatures of the inlet and outlet liquid streams were equal. The temperature of the inlet gas stream was higher than that of the outlet because as the gas passed through the blower it got heated up. The temperature difference between the inlet and outlet gas streams was observed to be in between 1°C and 5°C . Depending upon the ratio of bypass stream and the stream that was fed to the bed, the temperature difference between the solution and that of the inlet gas stream during a run was observed to be in between -2°C and 5°C . The solution was found to be at higher temperature particularly when low gas velocity was used. Two typical

plots showing the liquid and gas compositions and the solution temperature with time are shown in Figures 4.28 and 4.30 for the lighter ($\rho_p = .53 \text{ kg m}^{-3}$) and heavier ($\rho_p = 148 \text{ kg m}^{-3}$) particles, respectively. Similar variations of composition and temperature have been reported by Porter et al. (1966), who employed the recycling arrangements for the gas and liquid streams for the evaluation of interfacial area, using CO_2 -NaOH system, in a large bubble-cap tray (0.915 m ID). Strumillo and Kudra (1977) have also observed a linear decrease in NaOH concentration in the solution.

Since the liquid-side heat-transfer coefficient is several times higher than that of the gas-side and that the involved temperature difference was small, it was assumed that the temperature of the solution right upto the interface was uniform and hence the physico-chemical properties (required for the evaluation of interfacial area) were estimated using the solution temperature.

4.3.2 Evaluation of Interfacial Area and Surface-renewal Rate

Based on the study of the absorption of pure CO_2 into NaOH solution in mobile bed contactor, Strumillo and Kudra (1977) have shown that the error in neglecting the gas-side mass-transfer resistance is less

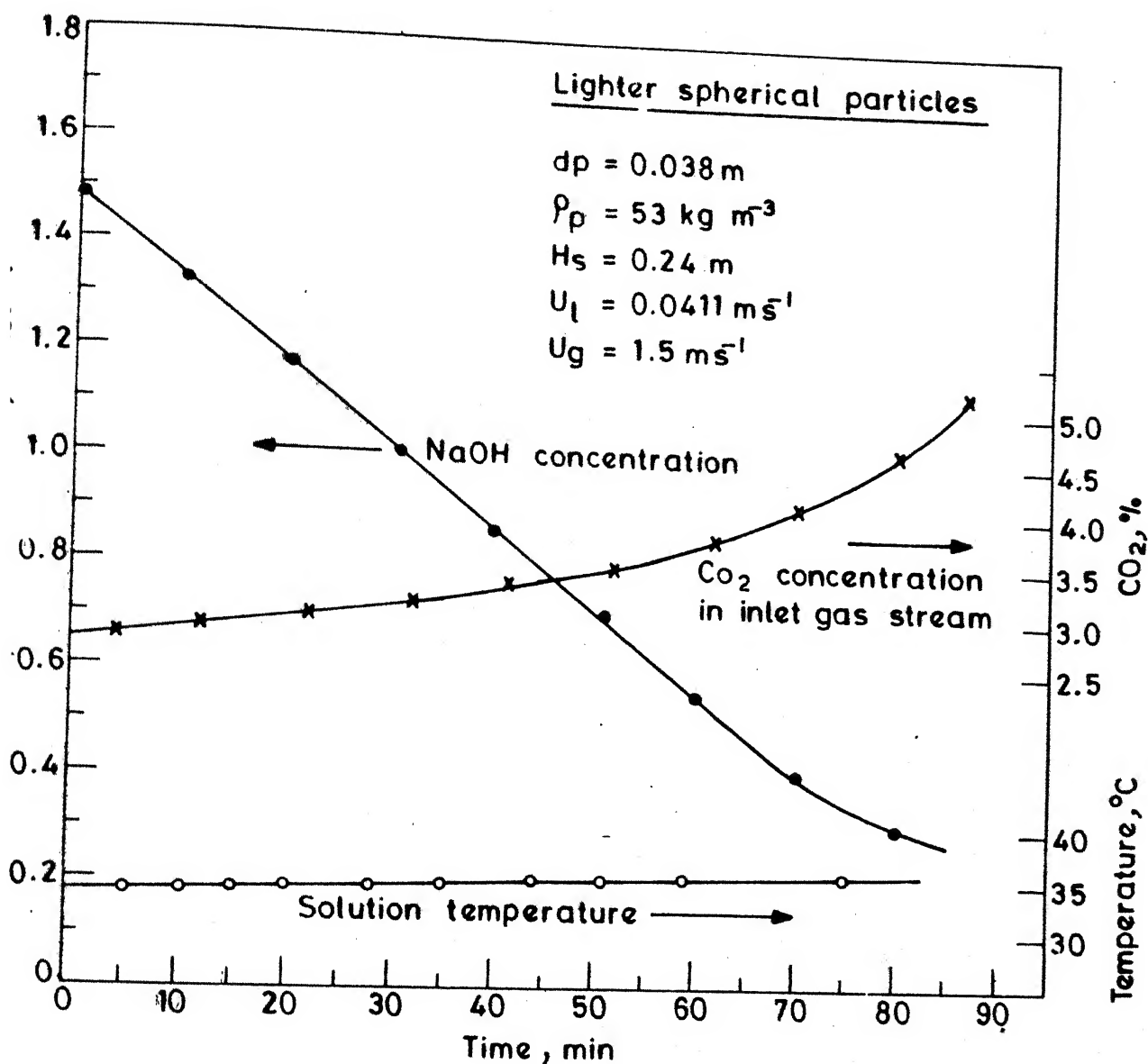


Fig. 4.28 Variations of liquid and gas compositions and temperature with time during a mass-transfer run with lighter spherical particles.

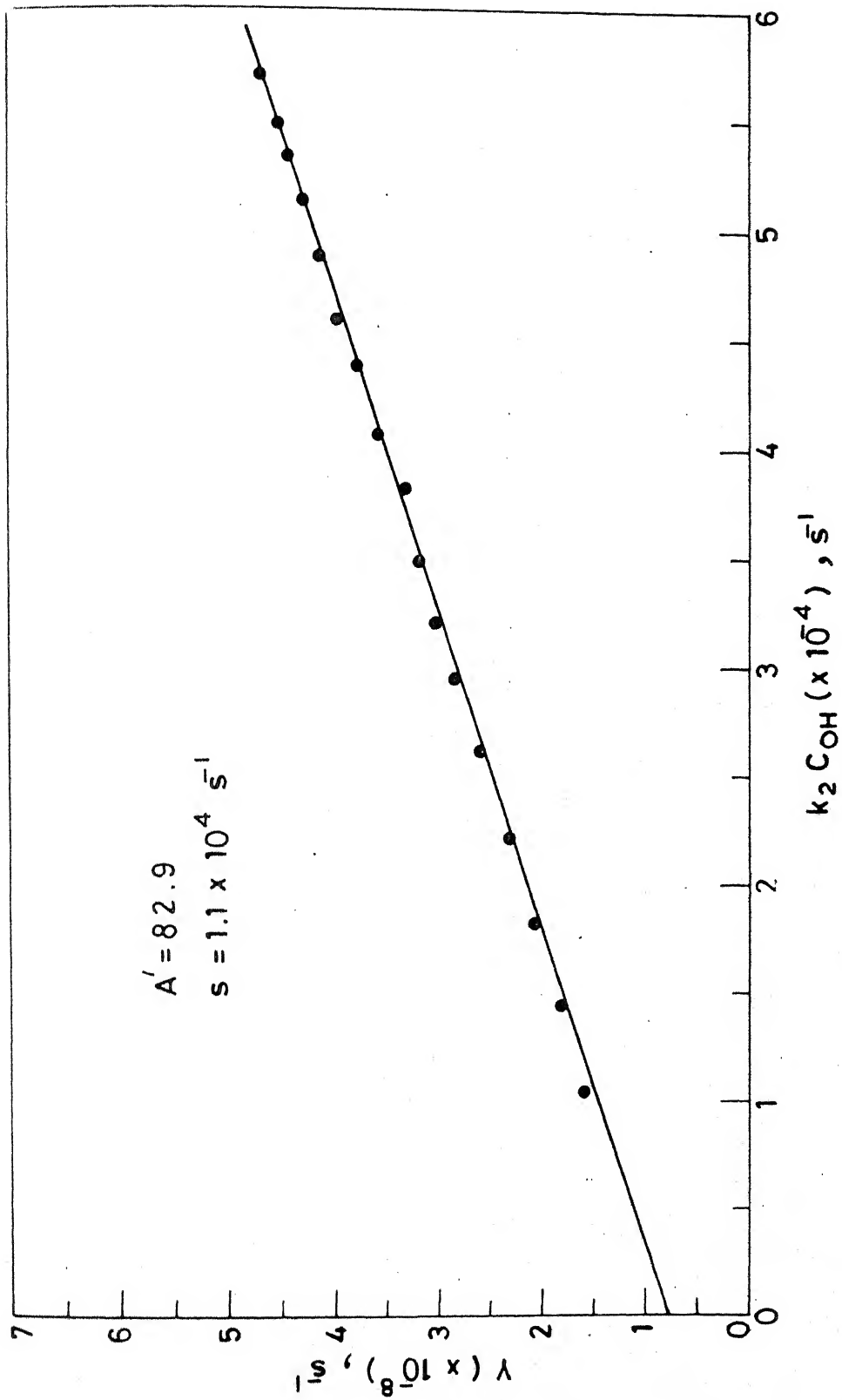


Fig. 4.29 Danckwert's plot for the run depicted in Figure 4.28

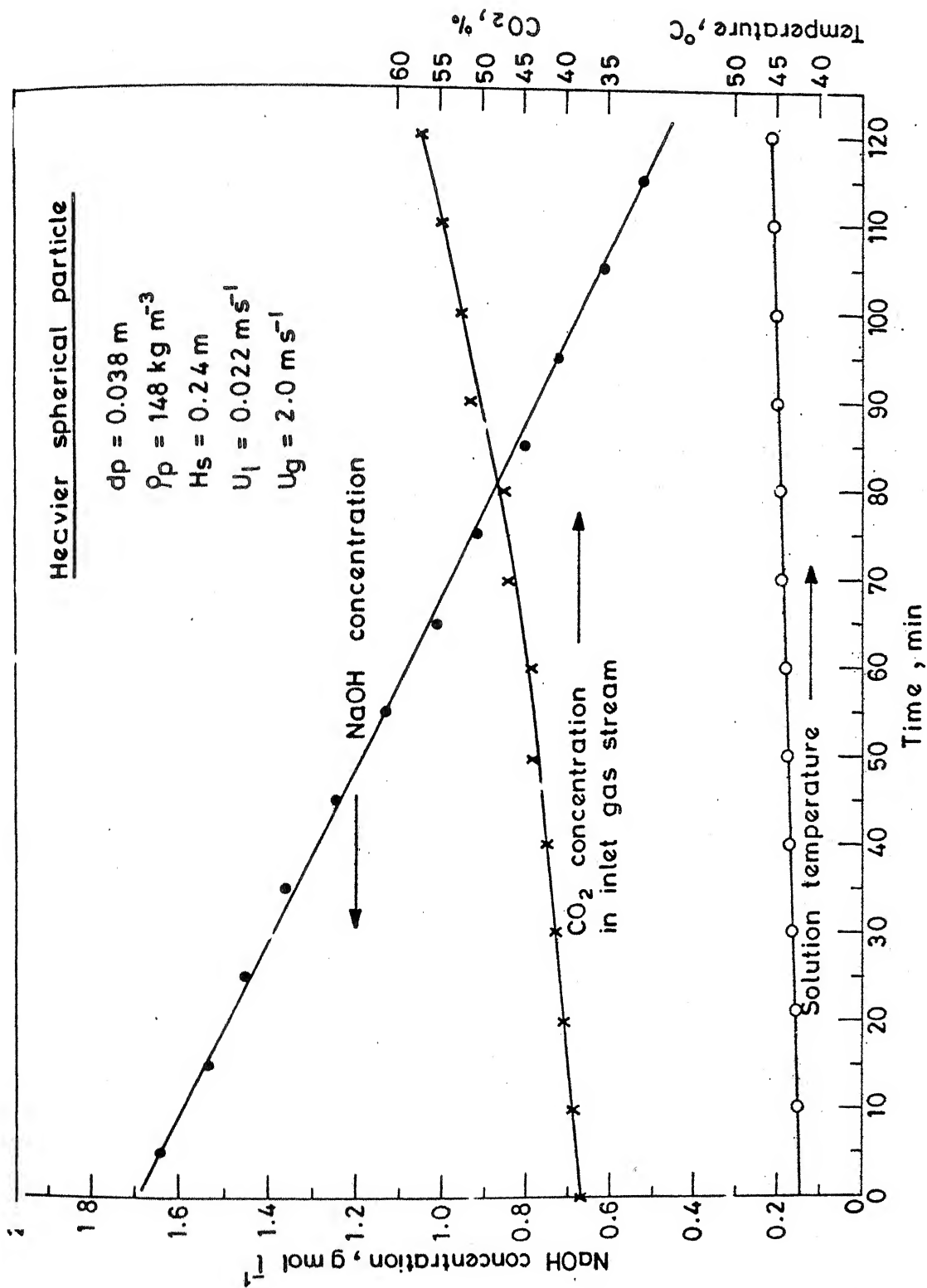


Fig. 4.30 Variations of liquid and gas compositions and temperature with time during a mass-transfer run with heavier spherical particles.

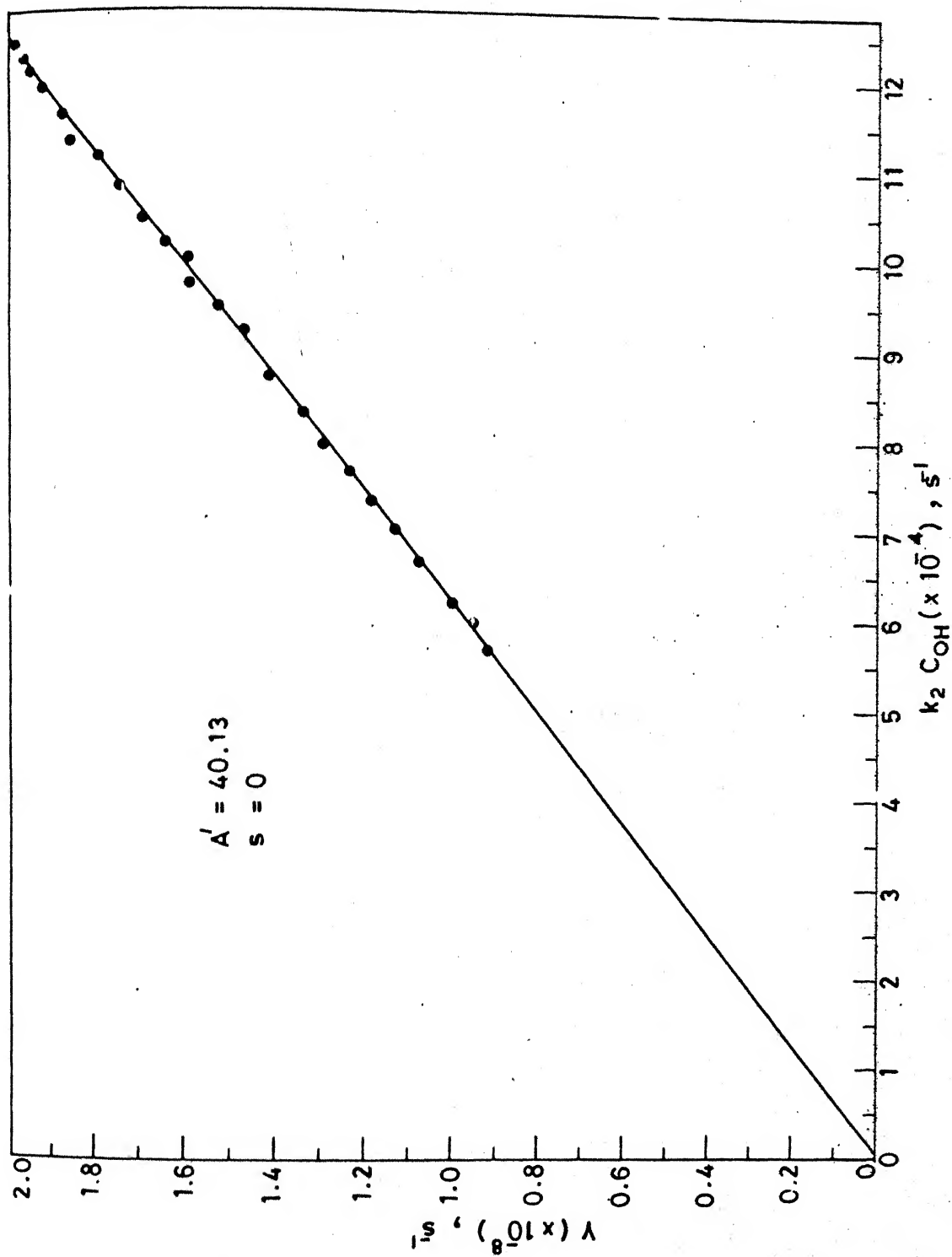


Fig. 4.31 Danckwerts' plot for the run depicted in Figure 4.30

than 5 % when composition of CO_2 used is 3 to 4 volume%. As pointed out earlier that the other investigators too have considered the gas-side mass-transfer resistance to be negligible. Under this condition, the rate of absorption for the pseudo-first-order reaction is given by the relation

$$(RA') = A' C_{\text{CO}_2}^* \sqrt{D_{\text{CO}_2} (k_2 C_{\text{OH}} + s)} \quad (4.22)$$

provided the following condition is satisfied (Danckwerts and Sharma, 1966; Danckwerts, 1970):-

$$\sqrt{D_{\text{CO}_2} k_2 C_{\text{OH}}} = \frac{1}{2} k_1 \left(1 + \frac{C_{\text{OH}}}{z C_{\text{CO}_2}^*} \right) \quad (4.23)$$

Equation (4.22) can be rewritten as

$$Y = \frac{(RA')^2}{C_{\text{CO}_2}^* D_{\text{CO}_2}} = A'^2 (k_2 C_{\text{OH}} + s) \quad (4.24)$$

and the well-known Danckwerts' plot (Y versus $k_2 C_{\text{OH}}$) can be constructed to evaluate interfacial area and surface-renewal rate. It may be recalled that all the other investigators neglected the surface-renewal rate (and hence the liquid-phase mass transfer coefficient, k_1) in comparison to $k_2 C_{\text{OH}}$, but Strumillo and Kudra (1977) have pointed out that it has to be considered in the case of mobile bed contactor. For the evaluation of Y and

4.3.3 Interfacial Area and Surface-renewal Rate

It was found for the bed with lighter particles that the intercept ($A'^2 s$) of Danckwerts' plot was greater than zero except for one run, whereas for bed with heavier particles $A'^2 s = 0$ for most of the runs.

The estimated interfacial area and surface-renewal rates are listed in Tables 4.2 and 4.3 along with the average expanded bed height, H , and interfacial area per unit volume of the expanded bed, a_B . It can be seen in one of the runs that s is very high. The tedious nature and the magnitude of error in measurements with a large set-up like this have been discussed by Wozniak (1977). Since the surface-renewal rate is about an order of magnitude smaller than $k_2 C_{OH}$, the values of s reported can be considered to give only order of magnitude. The variation of A' with gas velocity for both the particles is shown in Figure 4.32.

It can be seen from this figure that for the bed with lighter particles, A' was found to increase with liquid velocity but to decrease with increase in gas velocity. Whereas for the bed with heavier particles, A' decreased with increase in gas velocity but the trend indicates that it decreased with increase in liquid velocity.

TABLE 4.2

SUMMARY OF MASS TRANSFER RESULTS WITH LIGHTER SPHERICAL PARTICLES

$$d_p = 0.038 \text{ m}; \quad \rho_p = 53 \text{ kg m}^{-3}; \quad H_s = 0.24 \text{ m}$$

U_1 m s^{-1}	U_g m s^{-1}	H m	A' $\text{m}^2 \text{ m}^{-2}$	a_B $\text{m}^2 \text{ m}^{-3}$	$S (x 10^{-4})$ s^{-1}
0.022	0.5	0.28	66.14	236.21	1.03
	1.25	0.45	62.25	138.33	12.0
	1.50	0.50	61.64	123.28	0.00
	2.0	0.625	62.58	100.53	1.92
	2.0	0.625	58.74	93.98	2.67
	2.0	0.625	64.35	102.96	0.48
	2.5	0.75	60.83	81.11	1.757
0.033	0.5	0.33	77.46	234.73	0.95
	1.25	0.525	72.11	137.35	0.96
	1.25	0.525	74.16	141.26	0.91
	2.00	0.725	72.28	99.70	1.24
	2.00	0.725	70.36	97.05	0.61
0.041.1	0.8	0.38	80.00	211.00	0.78
	1.25	0.50	79.42	158.84	0.71
	1.25	0.50	81.39	162.78	0.54
	1.50	0.65	82.9	127.54	1.1
	2.0	0.775	76.16	98.27	0.69
	2.0	0.775	79.84	103.02	3.77
	2.5	0.90	61.85	68.72	0.96
	2.5	0.90	67.08	74.53	0.62

TABLE 4.3

SUMMARY OF MASS TRANSFER RESULTS WITH HEAVIER SPHERICAL PARTICLES

$$d_p = 0.038 \text{ m}; \quad \rho_p = 148 \text{ kg m}^{-3}; \quad H_s = 0.24 \text{ m}$$

U_l m s^{-1}	U_g m s^{-1}	H m	A' $\text{m}^2 \text{ m}^{-2}$	a_B $\text{m}^2 \text{ m}^{-3}$	$S (\times 10^{-4})$ s^{-1}
0.022	0.5	0.265	61.64	232.60	0
	1.25	0.41	42.20	102.90	0
	1.50	0.425	37.58	88.42	0
	2.0	0.625	40.13	64.20	0
	2.5	0.71	37.42	52.7	0
	2.5	0.71	45.27	63.76	0
	2.75	0.80	36.5	45.75	1.42
0.033	0.5	0.30	44.16	147.20	0
	1.25	0.46	44.93	97.67	0
	2.00	0.625	33.73	53.96	0
	2.00	0.625	40.21	64.33	0
	2.50	0.75	38.48	51.30	0
	2.50	0.75	35.22	46.96	0
0.0411	0.5	0.34	44.17	129.91	0
	1.25	0.51	39.68	77.8	0
	2.00	0.65	32.404	49.85	4.38
	2.50	0.775	32.53	41.97	0
	2.50	0.775	30.545	39.41	8×10^4

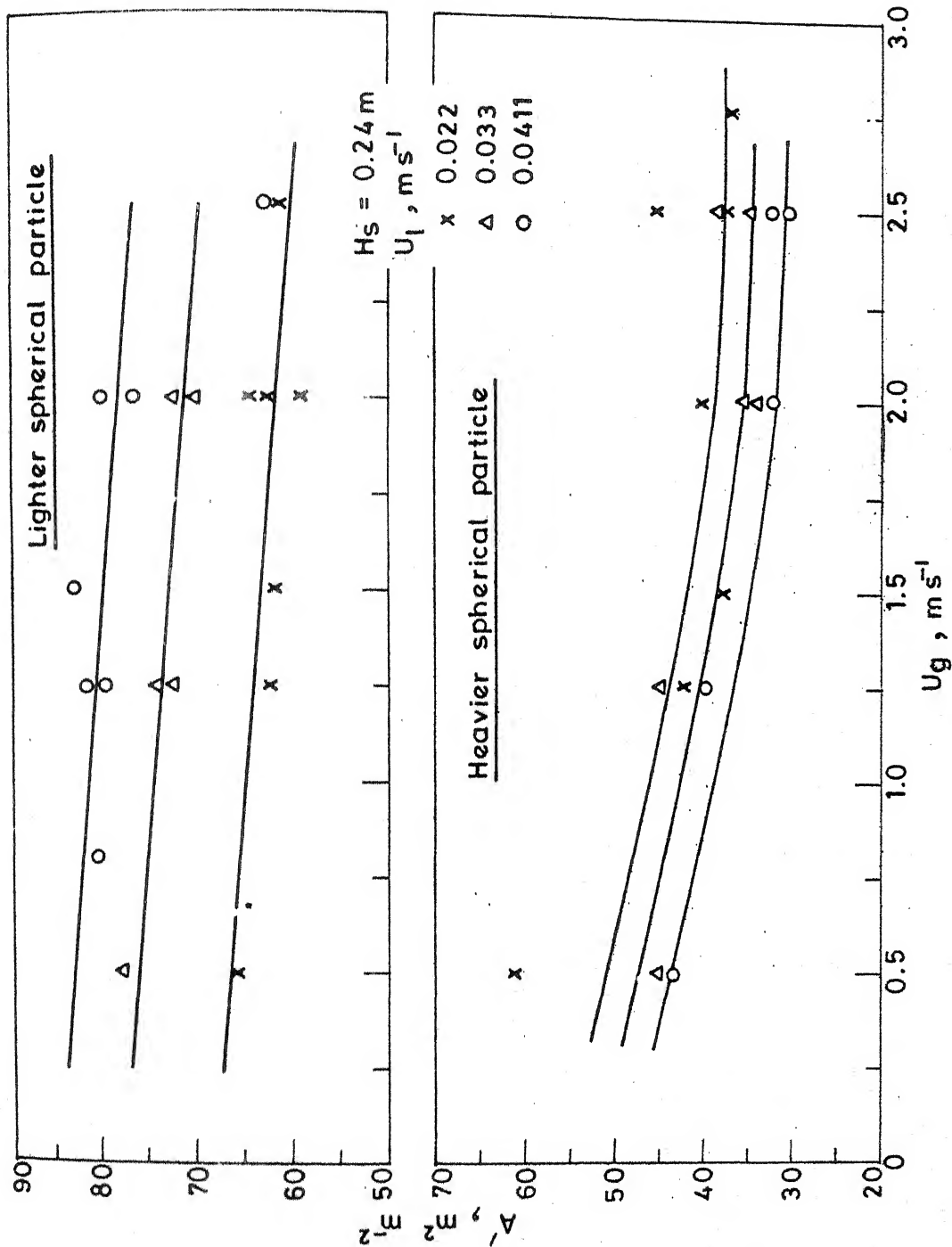


Fig. 4.32 Interfacial area per unit cross-sectional area of the contactor versus gas velocity for lighter and heavier spherical particles.

The interfacial area in the case of heavier particles is considerably lower as compared to those observed with lighter particles. Since several investigators have reported a_B , the plots of a_B versus gas velocity are also shown in Figures 4.33 and 4.34 for these two particles. As can be seen from these figures, a_B was found to decrease with increase in gas velocity for both the particles. There was insignificant effect of liquid velocity on a_B in the case of lighter particles while a_B decreased with liquid velocity for the bed with heavier particles.

The visual observations of the bed with lighter particles indicated that there was a smooth fluidization characterized by the vigorous movement of the individual particles. The liquid was seen to be dispersed in droplets throughout the bed and it appeared opaque when seen from the side. But, the slugging motion of the bed was observed for the bed with the heavier particles. It was seen that the particles were temporarily forming a bridge with the wall and breaking up. The liquid was seen draining from the upper particles to lower particles in rivulets and the bed was transparent in patches as viewed from the side. Since the liquid was dispersed in droplets form in the bed with lighter particles, the interfacial area as well as

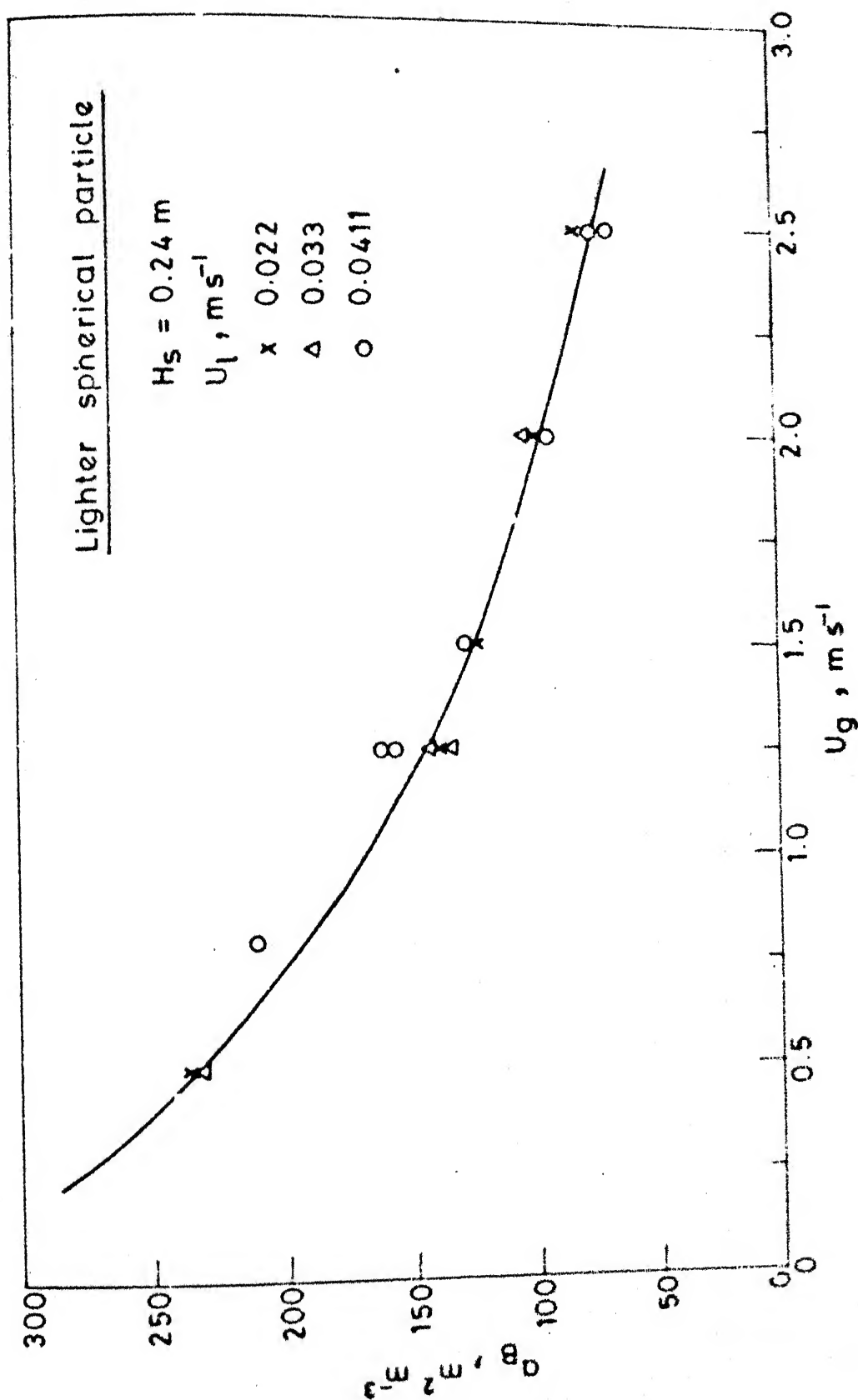


Fig. 4.33 Interfacial area per unit volume of the expanded bed versus gas velocity for lighter spherical particles.

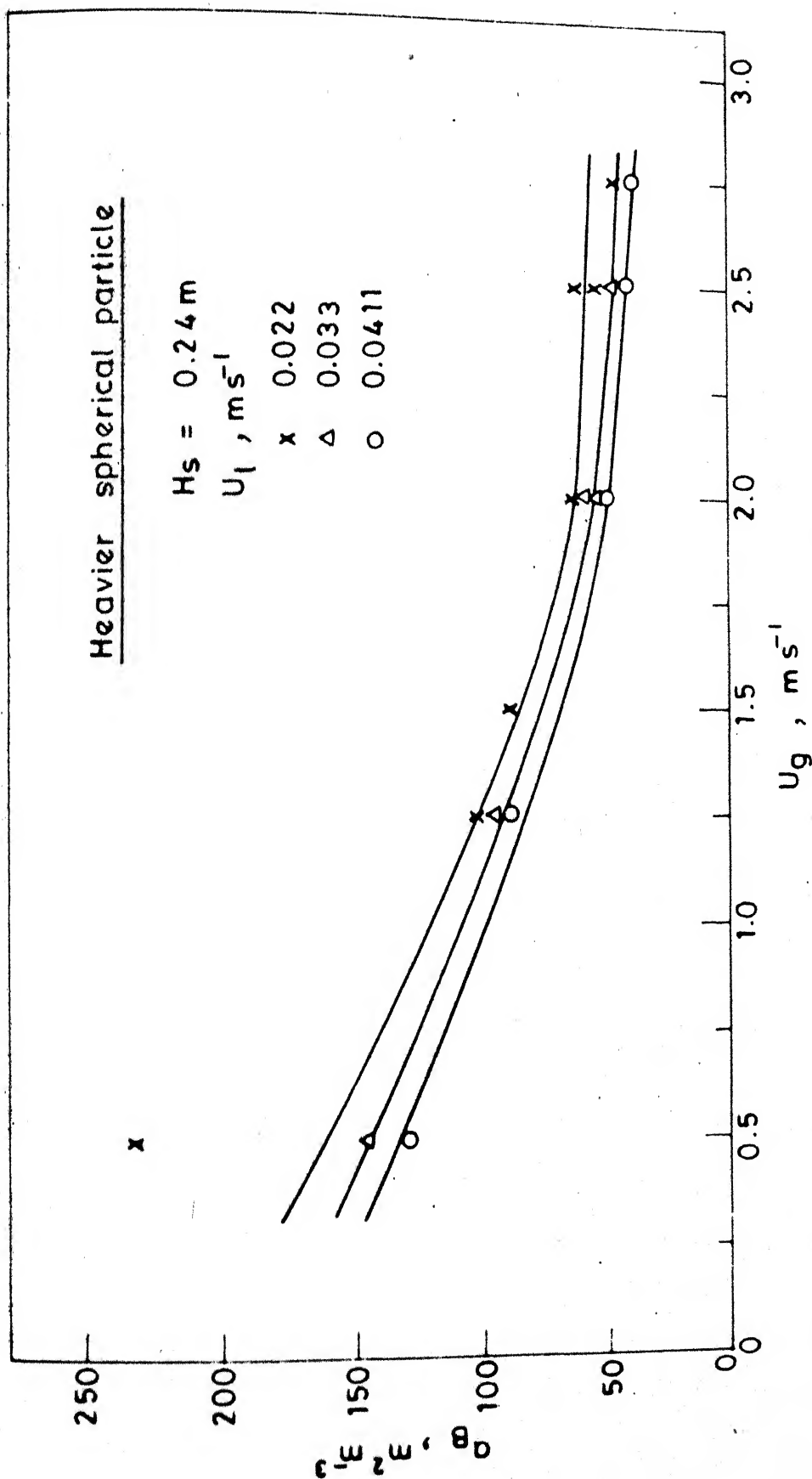


Fig. 4.34 Interfacial area per unit volume of the expanded bed versus gas velocity for heavier spherical particles.

the surface-renewal rate (and hence k_1) were found to be higher than those obtained in the bed with heavier particles. Since the liquid drained in the form of rivulets from one particle layer to another, increase in liquid velocity merely increased the size of these rivulets instead of increasing the interfacial area. On the other hand, in the case of bed with lighter particles, the increase in liquid velocity increased the dispersion contributing to higher interfacial area and surface-renewal rate.

The values of interfacial area in mobile bed contactors reported in literature are summarized in Table 4.4 (experimental details of mass transfer studies reported in literature are already presented in Table 2.4). All these data (except those of Groeneveld, 1967) have been obtained with particles of densities greater than 200 kg m^{-3} . Gel'perin et al. (1972), Wozniak and Østergaard (1973), Wozniak (1977) have reported an increase in interfacial area with gas and liquid velocities. Kito et al. (1976a) who evaluated interfacial area in a mobile bed contactor with 'stagnant' liquid flow, have reported that interfacial area remains constant with gas velocity. On the otherhand, Strumillo and Kudra (1977) observed that the interfacial area first

TABLE 4.4

SUMMARY OF RANGES OF INTERFACIAL AREAS REPORTED IN LITERATURE

Reference	d_p cm	ρ_p kg m ⁻³	H_s m	$U_1(10^2)$ m s ⁻¹	U_g m s ⁻¹	a_T m ²	A m ²	a_B m ²	a_{st} m ²
Groeneveld (1967)	3.73	170	0.25	0.2	2 - 5.5	10-20	-	-	-
			0.34	0.2	2 - 5.5	10-20	-	-	-
			0.43	0.2	2 - 5.5	8-16	-	-	-
			0.25	0.1-0.2	7.0	33-65	-	-	-
			0.25	0.1-0.2	4.4	12-18	-	-	-
Gel'perin et al.(1972)	1.55	470	0.00	1.11	1.5-3.5	-	40-80	-	-
			0.045	1.11	1.5-3.5	-	50-95	-	-
			0.090	1.11	1.5-3.5	-	60-110	-	-
			0.135	1.11	1.5-3.5	-	80-120	-	-
Kito et al. (1976a)	1.10	1000	0.15	Stagnant	0.1-2.0	-	-	300-500	-
Wozniak and Østergaard (1973)	1.0	388	0.22	2-6	0.70	-	-	-	500-1000

Cont...130-B/

Table 4.4 Continued.

Reference	d_p cm	ρ_p kg m ⁻³	H_s m	$U_1(10^2)$ m s ⁻¹	U_g m s ⁻¹	a_T m ²	A m ²	a_B m ²	a_{st} m ²
Wozniak (1977)	1.96	266	0.29	0.8-2.8	1.70	-	-	-	300-650
			0.29	0.8-2.8	2.50	-	-	-	400-750
			0.29	0.8-2.8	3.00	-	-	-	450-800
Rangwala(1973)									
170-450									
Kosev et al. (1971)									
110-250									
Strumillo and Kudra (1977)	1.0	1050	0.08	2.22	1.0-2.8	25-95	-	-	-
Present study	3.80	53	0.24	2.2-4.11	0.5-2.5	1.6-1.2	80-60	240-70	333-250
	3.80	148	0.24	2.2-4.11	0.5-2.5	1.1-0.6	55-30	160-40	229-125

increased and then decreased with gas velocity and it increased with liquid velocity. It should be pointed out that the different investigators have employed different sizes and densities of particles, grids of different free area of openings, and different methods of analysis of the data. Hence no generalized correlations could be obtained. However, the overall trends can be discerned.

The trend in the variation of A' with gas and liquid velocities reported in literature, in contrast to that observed in this work, can be understood from the dependence of the nature of fluidization on the density of particles. O'Neill et al. (1972) have advanced a hypothesis that the fluidization with incipient flooding occurs in beds with particles of densities greater than 233 kg m^{-3} whereas the fluidization without incipient flooding takes place for lighter particles. They have also explained the apparent inconsistencies observed with regard to the variation of minimum fluidization velocity with density of particles. In the beds with lighter particles, used in this work, the liquid was seen to be in dispersed phase and the gas in a continuous phase. In some studies conducted with still heavier

particles ($\rho_p = 500 \text{ kg m}^{-3}$) in this laboratory, large gas bubbles could clearly be seen rising through the emulsion consisting of liquid, particles and small gas bubbles. Perhaps due to this nature of the bed, Gel'perin et al. (1972) have characterised the mobile bed as a bubble column. Further, Kito et al. (1976b, 1976c, 1978, 1981), who studied hydrodynamics with heavier particles, have reported that the liquid holdup is fully supported by the upward flow of the gas; whereas in this work it was observed that only a part of it was supported. This seems to be consistent with the O'Neill et al. (1972) hypothesis. Thus it appears that the magnitude and variation of A' with gas and liquid velocities strongly depend on the density of particles.

The present study and the observation of Strumillo and Kulra (1977) indicate that it is preferable to evaluate interfacial area without a priori assumption of negligible liquid-phase mass-transfer coefficient.

The interphase mass-transfer rate depends on the interfacial area and the individual mass-transfer coefficients. The power expended in the bed is proportional to the pressure drop due to the weight of the

particles and the liquid holdup. The values of interfacial area, as summarized in Table 4.4, and the order of magnitude of surface-renewal rate reported by Strumillo and Kudra (1977) and that observed in the present work suggest that, at least for the system when gas side mass-transfer resistance is not controlling, the low density particles will give higher mass-transfer rates per unit power expended in the bed.

CHAPTER 5

CONCLUSIONS

A comprehensive review of the literature on hydrodynamics, axial mixing and mass transfer in a mobile bed contactor has been presented. The hydrodynamic studies are extensive and reasonably good generalized correlations are available. But there are few studies on axial mixing of the liquid phase and none on the gas phase axial mixing. Although a number of studies have been reported on mass transfer but bulk of the literature is specific in nature and can be applied only to the systems and range of variables investigated.

In the present work, experimental studies have been conducted for the determination of pressure drop, liquid holdup, bed expansion, minimum fluidization velocity, liquid phase axial mixing, mass-transfer coefficient and interfacial area in a 0.15 m ID mobile bed contactor of relatively low density ($53-103 \text{ kg m}^{-3}$) spherical and irregular shaped particles. Air-water system was used for the hydrodynamic and axial mixing studies. The mass-transfer studies were performed using the absorption of CO_2 into NaOH solution.

The total pressure drop was found to be independent of the gas velocity for all the particles, whereas the bed expansion was found to depend on the shape and density of the

particles. It was shown in general that only a part of the liquid held in the bed is supported by the upward flow of gas. The Kito-Tabei-Murata correlation (1978) has been adapted to fit the data of the pressure drop and liquid holdup. The correlations proposed are

$$\frac{h_1}{H_s} = 0.086 + 11 (H_s/d_p)^{-0.4} (fd/D)^{-0.58} (Ga)^{0.09} \times \\ (Fr)_1^{1.66} (Re)_1^{-0.34} (We)_1^{-0.34} \quad (5.1)$$

$$\frac{\Delta P_{LB}}{H_s} = 12.8 (H_s/d_p)^{-0.4} (fd/D)^{-0.58} (Ga)^{0.09} (Fr)_1^{1.66} \times \\ (Re)_1^{-0.34} (We)_1^{-0.34} \quad (5.2)$$

The expansion of the bed with cork particles showed a nature different from the spherical and irregular particles, and hence, two separate empirical correlations have been proposed:

$$\frac{H}{H_s} = 2.132 d_p^{0.12} U_1^{0.31} + 1.02 d_p^{-1.7} \rho_p^{-1.2} U_1^{0.2} U_g \quad (5.3)$$

for the spherical and irregular particles, and

$$\frac{H}{H_s} = -1.07 + 43 U_1 + 1.545 U_g \quad (5.4)$$

for the cork particles.

Since the minimum fluidization velocity was determined from the plots of H/H_s versus U_g by extrapolating the curve to $H/H_s = 1$.

The above two correlations given by Equations (5.3) and (5.4) can also be used for the determination of minimum fluidization velocity by setting $H/H_s = 1$.

It was observed that in some regions the particles congregated at the wall, leaving a particle-free core. The maps depicting these regions have been presented.

The liquid-phase axial mixing was studied using the step-input response technique. The breakthrough curves were interpreted using the single-parameter axial dispersion model. The data of the spherical particles were found in agreement with those of the earlier investigators. The following correlations for the Peclet number and axial dispersion coefficient have been proposed:

$$Pe = 10^{4.49} (Re)_l^{-0.47} (Re)_g^{-0.308} (Ga)^{-0.165} (H_s/d_p)^{0.824} \times (d_p/D)^{1.464} \quad (5.5)$$

$$Pe = 10^{3.25} (\overline{Re})_l^{-0.59} (Re)_g^{0.2} (Ga)^{-0.097} (H_s/d_p)^{0.95} \times (d_p/D)^{1.562} \quad (5.6)$$

and

$$D_L = 10^{-13.85} (\overline{Re})_l^{1.82} (Re)_g^{0.47} (Ga)^{0.27} (H_s/d_p)^{-0.068} \times (d_p/D)^{-2.8} \quad (5.7)$$

It was found that with increase in the static bed height P_e increased and near plug flow condition can be achieved with $H_s/D > 2$. This fact can be utilized for improving the contactor performance provided the congregation of particles at the wall can be avoided.

Mass transfer studies were conducted with 0.038 m diameter spherical particles of densities 53 and 148 kg m⁻³, employing the absorption of CO₂ in NaOH solution. The interfacial area and surface-renewal rate were evaluated constructing Danckwerts' plot. The results indicate that both the interfacial area and surface-renewal rate were higher for the bed with lighter particles than with the heavier ones. The apparent inconsistency in the variation of interfacial area with gas and liquid velocities, reported in literature and those observed in this study, was explained using O'Neill et al (1972) hypothesis of the dependence of the nature of fluidization on the density of particles. The results suggest that it is preferable to evaluate the interfacial area without a priori assumption of negligible liquid-phase mass-transfer coefficient as suggested by Strumillo and Kudra (1977).

Comparing the values of interfacial area with the reported data, it has been shown that the interphase mass transfer rates per unit power expended are high in the bed with low density particles.

Suggestions for future work:-

- (i) This study indicates that a better performance of the mobile bed contactor can be achieved with low density particles; but these particles have a tendency to congregate at the wall. Further studies are necessary to understand this phenomenon, and measures must be found out to prevent the congregation.
- (ii) The hypothesis, advanced by O'Neill et al.(1972), of dependence of the nature of fluidization on the density of particles, seems to offer a promising approach. It should be developed further to understand the nature of mobile bed contactor.
- (iii) To obtain generalised correlations, a systematic investigation need to be undertaken to study the effect of shape, size and density (especially low density) of particles and static bed height on axial mixing, interfacial area, individual interphase heat and mass-transfer coefficients.

REFERENCES

Anon., "New Floating Bed Scrubber would not Plug", Chem. Eng., 66(25), 106 - 8 (1959).

Anon., "High Gas Rates Feature New Absorber", Can. Chem. Processing, 48(10), 66 (1964).

Balabekov, O.S., P.G. Romankov, E.Ya. Tarat and M.F. Mikhalev, "Operating Conditions of Columns with Wetted Moving Spherical Packing", J. Appl. Chem. USSR., 42(7), 1454 - 8 (1969a).

Balabekov, O.S., E. Ya. Tarat, P.G. Romankov and M.F. Mikhalev., "Hydrodynamic Characteristics of Columns with Wetted Fluidized Spherical Packing", J. Appl. Chem. USSR., 42(10), 2128-31 (1969b).

Balabekov, O.S., E.Ya. Tarat, P.G. Romankov and M.F. Mikhalev, J. Appl. Chem. USSR., 44(5), 1061 (1971), cited in reference by Strumillo et al. (1974).

Barile, R.G. and D.W. Meyer, "Turbulent Bed Cooling Tower", Chem. Eng. Progr. Symp. Ser., 67 (119), 134-43 (1971).

Blyakher, I.G., L.Ya. Zhivaikin and N.A. Yurovskaya, "Investigation of Hydrodynamics and Mass Transfer in Equipment with movable packing", Int. Chem. Eng., 7(3), 485-90 (1967).

Brenner, H., "The diffusion Model of Longitudinal Mixing in Beds of Finite Length. Numerical values", Chem. Eng. Sci., 17(4), 229-37 (1962).

Carslaw, H.J. and J.C. Jaeger, "Conduction of Heat in Solids", 2nd ed., Oxford University Press, Oxford, 1959.

Charpentier J.C., " what is New in Absorption with Chemical Reaction?", Review paper, Trans. Instn. Chem. Engrs, 60, 131-56 (1982).

Chen, B.H. and W.J.M. Douglas, "Liquid Holdup and Minimum Fluidization Velocity in a Turbulent Contactor", Can. J. Chem. Eng. 46(4), 245-9 (1968).

Chen, B.H. and W.J.M. Douglas, "Axial Mixing of Liquid in a Turbulent-Bed Contactor", Can. J. Chem. Eng., 47(2), 113-8 (1969).

Danckwerts, P.V., "Gas-Liquid Reaction", McGraw-Hill, New York, 1970.

Danckwerts, P.V. and M.M. Sharma, "The Absorption of Carbon Dioxide into Solutions of Alkalies and Amines (with some Notes on Hydrogen Sulphide and Carbonyl Sulphide)", Review series No.2, The Chemical Engineer, No.22, CE 244-80(1966).

Dianov, E.A., "Absorption of Bromine in an Apparatus with a Fluidized Bed of Spherical Packing", Int. Chem. Eng., 6(2), 264-6 (1966).

Douglas, W.J.M., "Heat and Mass Transfer in a Turbulent Bed Contactor", Chem. Eng. Progr. 50 (7), 66-71 (1964).

Douglas, H.R., I.W.A. Snider and G.H. Tomlinson II, "The Turbulent Contact Absorber", Chem.Eng. Progr. 59(12), 85-9 (1963).

Dunn, E.W., T. Vermeulen, C.R. Wilke and T.T. Word, "Longitudinal Dispersion in Packed Gas-Absorption Columns", Ind. Eng. Chem. Fundam. 16, 116-24 (1977).

Elenkov, D. and A. Kosev, "Mass Transfer in the Liquid Phase in apparatus with Mobile Packing", Theor. Found. Chem.Eng., 4(1), 100-5 (1970).

Epstein, M., et al., Report to EPA by Bechtel Corp., Environmental Protection Technology series, EPA - 650/2-75-047 (June, 1975), cited in reference by Uchida et al.(1977).

Gel'perin, N.I., V.Z. Grishko, V.I. Savchenko and V.M. Shchedro, Khim. i Neftyanoe Mashinostr., No.1, 22(1966), cited in reference by Blyakher et al.(1967).

Gel'perin, N.I., V.I. Savchenko and V.Z. Grishko, Theor. Found. Chem.Eng., 2(1), 65 (1968a), cited in reference by O'Neill et al.(1972).

Gel'perin, N.I., Yu.M. Latyshev and L.I. Blyakham, "Rectification in a Column with Fluidized Beds of spherical Packings", Int. Chem.Eng. 8 (4), 691-3 (1968b).

Gel'perin N.I., V.Z. Grishko and V.A. Mikhailov, Uchenye Zapiski MITKhT im. M.V. Lomonosov, 1(2), 194 (1970), cited in reference by Gel'perin et al.(1972).

Gel'perin, N.I., V.Z. Grishko and V.A. Mikhailov, "Determination of Phase Contact Surface in Mass-Transfer Equipment with Fluidized Spherical Packing", Theor. Found. Chem. Eng., 6(4), 479-83 (1972).

Groeneveld, K.J.W., "A bed of pingpong balls irrigated by water and fluidized by air. Its gas-liquid interfacial area and the residence time distribution in the liquid", Dissertation, Technische Hogeschool, Delft, 1967.

Hartman, M. and G. Standart, "Studies on Distillation, XIX. Diffusion Model of Liquid Mixing on Turbogrid Trays", Collect. Czech. Chem. Commun., 32(3), 1161-81 (1967).

Hitchcock, L.B. and J.S. McIlhenny, "Viscosity and Density of Pure Alkaline Solutions and Their Mixtures", Ind. Eng. Chem. ind. edn., 27(4), 461-6 (1935).

Kafarao, V.V., Theor. Found. Chem. Eng., 2(2), 266 (1968), cited in reference by Koval et al. (1975a).

Kito, M., M. Shimada, R. Iijima, T. Sakai, M. Takata and S. Sugiyama, "Effective Interfacial Area in Mobile Bed Contactors under Liquid Stagnant Flow", Kagaku Kogaku Ronbunshu, 2(1), 16 - 20 (1976a).

Kito, M., M. Shimada, T. Sakai, S. Sugiyama and C.Y. Wen, "Performance of Turbulent Bed Contactor: Gas Holdup and Interfacial Area Under Liquid Stagnant Flow", Fluidization Technology, ed.: - D. Kearns, Vol. 1, part IV, 411-29, Hemisphere Publishing Corp., Washington, 1976a.

Kito, M., Y. Kayama, T. Sakai and S. Sugiyama, "Minimum Fluidization velocity in a Mobile Bed", Kagaku Kogaku Ronbunshu 2(1), 21-4 (1976b).

Kito, M., Y. Kayama, T. Sakai and S. Sugiyama, "Minimum Fluidization velocity in a Mobile Bed", Int. Chem. Eng., 16(4), 710-3 (1976b).

Kito, M., T. Monma, Y. Kayama, T. Sakai and S. Sugiyama, "Pressure Drop and Bed Expansion in a Mobile Bed", Kagaku Kogaku Ronbunshu 2(5), 476-9 (1976c).

Kito, M., Y. Kayama, K. Tsuchiya, T. Sakai and S. Sugiyama, "Performance of a Multi-stage Mobile Bed", Kagaku Kogaku Ronbunshu 3(4), 426-8 (1977).

Kito, M., K. Tabei and K. Murata, "Gas and Liquid Holdups in Mobile Beds under the Countercurrent Flow of Air and Liquid", Ind. Eng. Chem. Process Des. Develop. 17(4), 568-71 (1978).

Kosev, A., G. Peev and D. Elankov., Verfahrenstechnik, 5(8), 340 (1971), cited in reference by Wozniak (1977).

Koval, Zh.A., A.V. Besspalov and O.G. Kuleshov, "Axial Mixing of a Liquid in a Vessel with Mobile Spherical Packing", Theor. Found. Chem. Eng., 9(2), 289-90 (1975a).

Koval, Zh. A., A.V. Besspalov, O.G. Kuleshov and A.P. Zhukov, "Experimental Study of Lengthwise Liquid Mixing in a Column having a Mobile Bed Packing", Theor. Found. Chem. Eng., 9(6), 837-43 (1975b).

Kraiev, N.I., M.I. Niyazov, I.P. Levsh and S.U. Umarov, J. Appl. Chem. USSR., 41, 1961 (1968), cited in reference by Kito et al.(1978).

Kudra, T., G. Bednarek, J. Adamiec and C. Strumillo, "Description of H₂S from Water", I. Chem. Eng. Symp. Ser., No.57 (1978).

Kuroda, M. and K. Tabei, "Theoretical Discussion of the Minimum Fluidization Velocity in a Mobile Bed", Int. Chem. Eng. 21 (2), 219-23 (1981).

Levenspiel, O., "Chemical Reaction Engineering", John Wiley, New York, 1972.

Levsh I.P., N.I. Kraiev and M.I. Niyazov, "Calculation of the Pressure Drop and Heights of Three-Phase Fluidized Beds", Int. Chem. Eng., 8 (2), 311-2 (1968a).

Levsh, I.P., M.I., Niyazov, N.I. Kraiev and F.F. Ganikhanova, "Mass Transfer in Absorbers with Fluidized Packed Beds", Int. Chem. Eng., 8(3), 379-80 (1968b).

Levsh I.P., N.I. Kraiev and M.I. Niyazov, "Hydrodynamic Calculation of Absorbers with Fluidized Beds", Int. Chem. Eng., 8(4), 619-22 (1968c).

McMichael, W.J., L.S. Fan and C.Y. Wen, "Analysis of Sulfur Dioxide Wet Limestone Scrubbing Data from Pilot Plant Spray and TCA Scrubbers", Ind. Eng. Chem. Process Des. Develop., 15(3), 459-67 (1976).

Nijsing, R.A.T.O., R.H. Hendriks and H. Kramers, "Absorption of CO_2 in Jets and Falling Films of Electrolyte Solutions, with and without Chemical Reaction", Chem.Eng. Sci., 10(1), 88-104 (1959).

O'Neill, E.K., D.J. Nicklin, N.J. Morgan and L.S. Leung, "The Hydrodynamics of Gas-Liquid Contacting in Towers with Fluidised Packings", Can. J. Chem. Eng. 50(5), 595-601 (1972).

Otake, T. and E. Kunugita, "Mixing Characteristics of Irrigated Packed Towers", Chem. Eng.(Japan), 22 (3), 144-50 (1958).

Otake, T., E. Kunugita and T. Yamanishi, "Mixing Characteristics of Gas and Liquid Flowing through Gas-Liquid Packed Beds", Chem. Eng.(Japan), 26(7), 800-6 (1962).

Perry, R.H. and C.H. Chilton, "Chemical Engineers' Hand book" 5th ed., McGraw-Hill Kogakusha, Ltd., Tokyo, 1973.

Pinsent, B.R.W., L. Pearson and F.J.W. Roughton, "The Kinetics of Combination of Carbon Dioxide with Hydroxide Ions", Trans. Faraday Soc., 52(11), 1512-20 (1956).

Pohorecki, R., "Applications of the Danckwerts Method to Measurements of Interfacial Area and Liquid - Side Mass-Transfer coefficient on Sieve trays", Int. Chem. Eng., 15(4), 647-57 (1975).

Pohorecki, R., "Mass Transfer with Chemical Reaction During Gas Absorption on a Sieve Plate", Chem. Eng. Sci., 31(6), 637 - 44 (1976).

Porter, K.E., M.B. King and K.C. Varshney, "Interfacial Areas and Liquid-Film Mass-Transfer Coefficients for a 3-ft Diameter Bubble-Cap Plate Derived from Absorption Rates of Carbon Dioxide into Water and Caustic Soda Solutions", Trans.Instn. Chem. Engrs., 44, T274-83 (1966).

Ramm, V.M. and I.A. Gildenblat, "Absorption of Gases", Review paper, Theor. Found. Chem. Eng., 4(1), 17-25 (1970).

Rangwala, H., Dissertation, Dept. Chem.Eng., I.I.T. Bombay, 1973, cited in reference by Wozniak (1977).

Ratcliff, G.A. and J.G. Holdcroft, "Diffusivities of Gases in Aqueous Electrolyte Solutions", Trans. Instn. Chem. Engrs., 41, 315-9 (1963).

Schuesser, W.E. and L. Lapidus, "Further studies of Fluid Flow and Mass Transfer in Trickle Beds", A.I.Chem.Eng.J, 7(1), 163-71 (1961).

Shah, Y.T., "Gas-Liquid-Solid Reactor Design", Mc-Graw-Hill, New York, 1979.

Shah, Y.T., G.J. Stiegel and M.M. Sharma, "Backmixing in Gas-Liquid Reactors", A.I. Chem.Eng. J., 24(3), 369-400 (1978).

Shapiro, S. and Ya. Gurvich, "Analytical Chemistry", Mir Publishers, Moscow, 1972.

Sherwood, T.K., R.L. Pigford and C.R. Wilke, "Mass Transfer", McGraw-Hill Kogakusha Ltd., Tokyo, 1975.

Strumillo, C., J. Adamiec and T. Kudra, "Packed Columns with Expanding Beds", Int. Chem. Eng. 14(4), 652-7 (1974).

Strumillo, C., J. Adamiec and T. Kudra, "The Performance of Turbulent Bed Contactors", paper presented at the second international conference, Institution of Chemical Engineers, University of Salford, April 1976.

Strumillo, C. and T. Kudra, "Interfacial Area in Three-Phase Fluidized Beds", Chem. Eng. Sci., 32(3), 229-32 (1977).

Tichy, J., A. Wong and W.J.M. Douglas, "Pressure Drop in a Mobile-Bed Contactor", Can. J. Chem. Eng. 50(2), 215-20 (1972).

Tichy, J. and W.J.M. Douglas, "Bed Expansion in a Mobile Bed Contactor", Can. J. Chem. Eng. 50(6), 702-7 (1972).

Tichy, J. and W.J.M. Douglas, "Certain Hydrodynamic Characteristics of Mobile - Bed Contactors", Can. J. Chem. Eng., 51(5), 618-20 (1973).

Tomony, J.P., "Turbulent Contact Absorber", Pulp and Paper, June 15 (1964).

Uchida, S., C.S. Chang and C.Y. Wen, "Mechanics of a Turbulent Contact Absorber", Can. J. Chem. Eng. 55(4), 392-6 (1977).

Uchida, S., T. Suzuki and H. Maejima, "The Flooding condition of a Turbulent Contact Absorber", Can. J. Chem. Eng., 58(3), 406 - 8 (1980).

van der Laan, E. Th., "Notes on the Diffusion-Type Model for the Longitudinal Mixing in Flow (O. Levenspiel and W.K. Smith)", Chem. Eng. Sci., 7(3), 187-91 (1956).

Vogel, A.I., "A Text-Book of Quantitative Inorganic Analysis", 3rd ed., The English Language Book Society, 1961.

Vukovic, D.V., F.K. Zdanski, G.V. Vunjak, Z.B. Grbavcic and H.Littman, "Pressure Drop, Bed Expansion and Liquid Holdup in a Three Phase Spouted Bed Contactor", Can. J. Chem. Eng. 52(2), 180-4 (1974).

Wen, C.Y. and C.S. Chang, "Absorption of SO_2 in Lime and Limestone Slurry: Pressure Drop Effect on Turbulent Contact Absorber Performance", Environ. Sci. Tech., 12(6), 703-7 (1978).

Wozniak, M., "Pressure Drop and Effective Interfacial Area in a column with a Mobile Bed", Int. Chem. Eng., 17(3), 553-9 (1977).

Wozniak, M. and K. Østergaard, "A Report on Mass Transfer Investigations in a Turbulent Bed Contactor", Technical University of Denmark, Department of Chemical Engineering, Lyngby, Denmark 1972.

Wozniak, M. and K. Østergaard, "An Investigation of Mass Transfer in a Countercurrent Three-Phase Fluidized Bed", Chem.Eng. Sci., 28(1), 167-71 (1973).

Yagi, S. and T. Miyauchi, "On the Residence Time Curves of the Continuous Reactors", Chem. Eng. (Japan), 17(10), 382-6 (1953).

Zhukov, A.P., Zh. A. Koval, A.V. Bespalov and O.G. Kuleshov, "Investigation of Mass Transfer Limited by the Resistance of the Liquid Phase in Absorbers with Moving Spherical Packing", Theor. Found. Chem. Eng., 10(1), 114-7 (1976).

Appendix A

Carbon dioxide Analyzer

In the mass transfer studies, the composition of CO_2 in the air- CO_2 mixture was analyzed with the aid of specially constructed Orsat-type gas analyzer. A schematic diagram of the analyzer is shown in Figure A-1. It consisted of a glass gas sampler and a glass equalizing bottle for holding NaOH solution. The sampler had an absorption bulb (A) of 330 cc volume with a long graduated glass stem (B) of volume 20 cc. It was fitted with an one-way teflon stop-cock (SC-1) at the top and a two-way teflon stop-cock (SC-2) at the bottom. The sampler was connected to the equalizing bottle (C) by a flexible polyethylene tube as shown in figure. The gas sampler was fixed on to a wooden board. The gas sample was analyzed as follows.

The gas, streaming out through the gas sampling point SG (as shown in Figure 3.1), was passed through the gas sampler (keeping stop-cock SC-2 open to atmosphere) continuously for a period not less than 5 min. At a predetermined time, stop-cock SC-1 was closed and the trapped gas sample was allowed to equalize with the ambient pressure. Then stop-cock SC-2 was opened to let about 75 cc of NaOH solution enter the sampler.

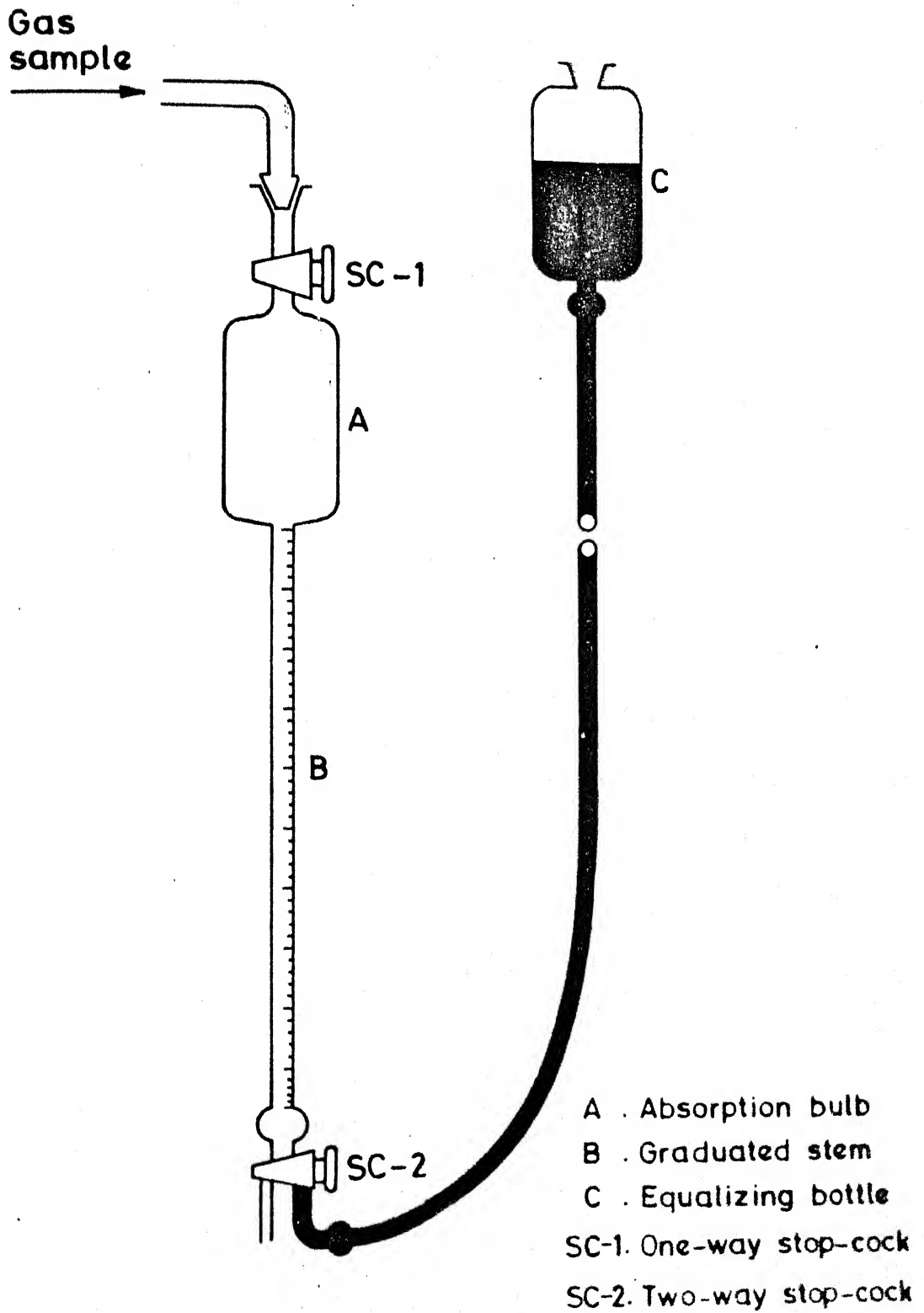


Fig. A-1 Schematic diagram of the Orsat-type carbon dioxide analyzer.

Then stop-cock SC-2 was closed and the sampler was vigorously shaken for about 3 min to ensure complete absorption of CO_2 into the solution. The stop-cock SC-2 was again opened and the sampler was held high such that the solution interfaces in the graduated stem and in the equalizing bottle were at the same level. This ensured that the gas pressure in the sampler was at the ambient pressure. At this stage, the volume of CO_2 in the gas sample was determined from the solution level in the graduated stem.

The accuracy of the analysis was checked using gas samples of known compositions. The gas mixture containing 2 to 6 % of CO_2 by volume could be analyzed with an accuracy of 0.05 % of CO_2 .

To prevent absorption of water vapor into NaOH solution, a part of the solution which was prepared for the mass-transfer run was used for the analysis. It was observed that the temperature of the gas sample was different from that of solution during a run. On vigorous shaking with the solution, the gas temperature fell resulting in decrease in volume of the gas sample. As the run progressed the gas came in equilibrium with the solution in which part of NaOH was converted to Na_2CO_3 . As a result there was a minor variation in the amount of water vapor in the gas stream. To take these effects into account

blank analysis of CO_2 -free air that was circulated through the bed for long enough time, before and after each run was made. The blank analysis gave volume contraction of about 2.5 cc to 4.0 cc in 350 cc. The difference between blank analyse is before and after the run was about 0.5 cc to 1.0 cc. The temperature of the gas sample and that of the solution in the equalizing bottle was monitored periodically throughout a run, and temperature difference was found to vary by 2 to 3 °C. The correction was applied assuming that the blank analysis varied linearly during the period of a run.

Appendix B

Physico-Chemical Properties

In the evaluation of interfacial area, estimation of a number of physico-chemical properties is required. In literature, some of these properties are available either in a graphical form or in a tabular form. To facilitate computer calculations the available data were correlated in the form of empirical relations in the case of those properties for which no analytical relations are available. The accuracy of these empirical relations was better than 1 %. The required physico-chemical properties and the relations used are presented here.

(i) Diffusion Coefficient of CO_2 in water, D_w

Based on the data presented by Ratcliff and Holdcroft (1963), the following relations were obtained for D_w (in $\text{cm}^2 \text{s}^{-1}$):-

$$D_w = (0.042 T + 0.87) \times 10^{-5} \quad ; \text{ for } 15^\circ\text{C} < T < 25^\circ\text{C} \quad (\text{B-1})$$

$$D_w = (0.051 T + 0.645) \times 10^{-5} \quad ; \text{ for } 25^\circ\text{C} < T < 35^\circ\text{C} \quad (\text{B-2})$$

$$D_w = (0.06 T + 0.33) \times 10^{-5} \quad ; \text{ for } 35^\circ\text{C} < T < 50^\circ\text{C} \quad (\text{B-3})$$

(ii) Solubility of CO_2 in Water, H_w

The solubility of CO_2 in water H_w (in $\text{gmol l}^{-1} \text{atm}^{-1}$) was evaluated using the following expression given

by Danckwerts and Sharma (1966):-

$$\log_{10} \mu_w = \frac{1140}{(273 + T)} - 5.3 \quad (\text{B-4})$$

where T is in °C.

(iii) Viscosity of water, μ_w

From the monograph presented in Chemical Engineers' Handbook (Perry and Chilton, 1973) the following relation was obtained for μ_w (in centipoise):-

$$\mu_w = 1.34 - 0.016 T ; \text{ for } 15^\circ\text{C} < T < 50^\circ\text{C} \quad (\text{B-5})$$

(iv) Viscosity of Solution Containing NaOH and Na_2CO_3 , μ_s

Hitchcock and McIlhenny (1935) have presented the data of viscosity and density of solutions of NaOH and Na_2CO_3 , and their mixtures upto a concentration of 8N (NaOH) in the temperature range of 20 to 40°C. From the viscosity data the following correlations were obtained for μ_s (in centipoise)

$$\mu_s = (1 + 0.2 (N-2)) * \exp (-6.67 \ln (T + 273) + 38.414 - \dots) \quad \text{for } N \leq 2 \quad (\text{B-6})$$

$$\mu_s = (1 + 0.3(N-2)) * \exp (-6.67 \ln (T+273) + 38.414 - \dots) \quad \text{for } N > 2 \quad (\text{B-7})$$

where $N = [\text{NaOH}] + 2 [\text{Na}_2\text{CO}_3]$

$f = [\text{NaOH}] / N$

and T is in $^{\circ}\text{C}$.

(v) Diffusion Coefficient of CO_2 in Solution Containing NaOH and Na_2CO_3 , D_{CO_2}

The relations proposed by Ratcliff and Holdcroft (1963) and Nijssing et al. (1959) for D_{CO_2} have been widely used. The correlation proposed by Ratcliff and Holdcroft has been obtained by analyzing the data of a number of electrolytes like NaCl, NaNO_3 , Na_2SO_4 , MgCl_2 , $\text{Mg}(\text{NO}_3)_2$ etc., hence their correlation

$$D_{\text{CO}_2} = D_w \left(\frac{\mu_s}{\mu_w} \right)^{-0.637} \quad (\text{B-8})$$

was used for the evaluation of D_{CO_2} (in $\text{cm}^2 \text{s}^{-1}$).

(vi) Ionic Strength of the Solution, I

The ionic strength was calculated from the following relation (Danckwerts, 1970):-

$$I = \frac{1}{2} \sum c_i z_i^2 \quad (\text{B-9})$$

where c_i = concentration of the i th ion

z_i = the charge of the i th ion

(vii) Solubility of CO_2 in Solution Containing NaOH
and Na_2CO_3 , H_2CO_3

The following relation (Danckwerts, 1970) was used for H_2CO_3 (in $\text{gmol l}^{-1} \text{ atm}^{-1}$)

$$\log_{10} \frac{H_{\text{CO}_2}}{H_w} = - h_{\text{NaOH}} I_{\text{NaOH}} - h_{\text{Na}_2\text{CO}_3} I_{\text{Na}_2\text{CO}_3} \quad (\text{B-10})$$

where

$$h_{\text{NaOH}} = h_{\text{Na}^+} + h_{\text{OH}^-} + h_g$$

$$h_{\text{Na}_2\text{CO}_3} = h_{\text{Na}^+} + h_{\text{CO}_3^{2-}} + h_g$$

here h_{Na^+} , h_{OH^-} , $h_{\text{CO}_3^{2-}}$ and h_g are contributions

of positive ion, negative ions and gas to solubility factors h_{NaOH} and $h_{\text{Na}_2\text{CO}_3}$.

Based on the data presented by Danckwerts (1970)

the following relations were obtained:-

$$h_g = - 0.0009 T + 0.0035 \quad ; \quad \text{for } 15^\circ\text{C} < T < 25^\circ\text{C} \quad (\text{B-11})$$

$$h_g = - 0.00055 T - 0.00525 \quad ; \quad \text{for } 25^\circ\text{C} < T < 35^\circ\text{C} \quad (\text{B-12})$$

$$h_g = - 0.003 T - 0.14 \quad ; \quad \text{for } 35^\circ\text{C} < T < 50^\circ\text{C} \quad (\text{B-13})$$

$$h_{\text{NaOH}} = 0.091 + 0.066 + h_g \quad (\text{B-14})$$

and

$$h_{\text{Na}_2\text{CO}_3} = 0.091 + 0.021 + h_g \quad (\text{B-15})$$

(viii) Second-order Rate-Constant for Reaction of CO₂ with Sodium Hydroxide Solution, k₂

The second-order rate constant k₂ (l gmol⁻¹ s⁻¹) was evaluated using the following relations which were obtained based on the data and relations available in literature (Danckwerts and Sharma, 1966; Pinsent et al., 1956; Sherwood et al., 1975):-

$$k_2 = k_{OH} * 10^{(0.135 \times I)} \quad (B-16)$$

where k_{OH} is the reaction rate constant at infinite dilution and is given by the relation (Danckwerts and Sharma, 1966)

$$k_{OH} = 10^{(13.365 - 2895/(T + 273))} \quad (B-17)$$

where T is in °C.